X-724-67-87

NASA TM X- 55770

AIMP (IMP-D)
TECHNICAL SUMMARY DESCRIPTION

GPO PRICE $ _____

CFSTI PRICE(S) $ _____

Hard copy (HC) $3.00

Microfiche (MF) .65

ff 653 July 65

MARCH 1967

GODDARD SPACE FLIGHT CENTER

GREENBELT, MARYLAND

X-724-67-87

AIMP (IMP-D)
TECHNICAL SUMMARY DESCRIPTION

March 1967

Goddard Space Flight Center
Greenbelt, Maryland

AIMP (IMP-D)
TECHNICAL SUMMARY DESCRIPTION

FOREWORD

This document describes the AIMP-D satellite, which was launched from Kennedy Space Center July 1, 1966 into a highly elliptical orbit which carries it well beyond the moon each orbit. The structure, experiments, telemetry, power system, and instruments of the spacecraft are described.

CONTENTS

Page

FOREWORD iii

INTRODUCTION 1

EXPERIMENTS

University of California Ionizing Radiation Experiment 1

Purpose 1
Description 2
Theory of Operation 4
Telemetry 6

Thermal Ion Electron 7

Purpose 7
Description 8
Theory of Operation 8

The Ion Mode 9
The Electron Mode 9

Telemetry 10

University of Iowa Energetic Particle Experiment 11

Purpose 11
Description 11

MIT Plasma Probe Experiment 17

Purpose 17
Description 18
Theory of Operation 20

Integral Measurements 20
Differential Measurements 23
Calibration and Performance Measurements 24

Telemetry 25

Ames Magnetometer Experiment 25

Purpose 25
Description 25
Theory of Operation 27
Telemetry 34

CONTENTS (Continued)

	Page
GSFC Magnetometer Experiment	34
Purpose	34
Description	35
Theory of Operation	35
Telemetry	38
Solar Cell Damage Experiment	38
Purpose	38
Description	39
Passive Experiments	39
SPACECRAFT AND SUBSYSTEMS	
AIMP-D Structure	40
Stabilization	46
Retromotor	46
Motor Case	46
Propellant	46
Nozzle	48
Igniter Subsystem	49
Retromotor Adapter	50
Thermal Control	50
Telemetry Data System	51
Encoder	51
Encoder Operation	54
Analog Experiment Data	56
Digital Data	56
Crystal Oscillator Binary Countdown and Sync Pulse Generator	58
Satellite Clock (Sequence Counter)	58
In-Flight Calibration	58
Encoder Accumulation	59
Optical Aspect Parity Check	59
Use of Metal Oxide Silicon Field Effect Transistors	59
Performance Parameters	59

CONTENTS (Continued)

	Page
Spacecraft RF System	61
Telemetry Transmitter	63
Command Subsystem	63
Range	64
Range Rate	66
AIMP Antenna System	66
Power Systems	67
AIMP Solar Array	67
AIMP Solar Array Regulator	72
AIMP Prime Converter	72
AIMP Encoder Converter	75
AIMP-D Optical Aspect Converter	76
AIMP Battery	77
Spacecraft Programmers	81
Undervoltage System	81
Fourth Stage Ignition and Separation Timer	83
Flipper Control and Fourth Stage Performance Parameter	84
Flipper Control	84
Fourth Stage Performance Parameters	84
Optical Aspect System	85
Digital Sensors and Their Functions	86
Moon-Earth System	88
Miscellaneous	90
Fuses	90
Four Volt Standard	90
Accelerometer	90

ILLUSTRATIONS

Figure		Page
1	Ion Chamber	3
2	"S" - "T" Accumulator	5
3	Time Between Pulses	5
4	Time Measurement System	6

ILLUSTRATIONS (Continued)

Figure		Page
5	Retarding Potential Analyzer	8
6	Block Diagram of Thermal Ion Electron	10
7	Experiment View Angles	13
8	Block Diagram - University of Iowa	15
9	University of Iowa Telemetry Format	16
10	University of Iowa Data Timing Diagram	17
11	Faraday Cup	18
12	Method of Measurement	19
13	Plasma Integral Measurement	21
14	Grid Arrangement	21
15	Differential Measurement Effect	23
16	MIT Measurement Sequence	25
17	MIT Plasma Probe Telemetry Format	26
18	Ames Magnetometer Experiment Block Diagram	28
19	Ames Magnetometer Sensor Block Diagram	29
20	Ames Timing Diagram	31
20A	Ames Flip/Calibrate Timing Diagram	33
21	GSFC Magnetometer Experiment Block Diagram	36
22	GSFC Triaxal Fluxgate	36
23	GSFC Telemetry Format	38
24	AIMP Structure (isometric)	42
25	AIMP Spacecraft - Side View	43
26	AIMP Structure - Top View	44
27	Launch Configuration	45
28	TE-M-458 Retromotor	47
29	Encoder Operation	53
30	AIMP Encoder Format	55
31	Performance Parameter Block Diagram	60
32	Simplified Block Diagram - Range and Range Rate System	62
33	Command Sequence	64
34	Range and Range Rate Transmitter Modulation	65
35	Antenna Pattern	68
36	Antenna Pattern (0 = 90°)	69
37	Solar Paddle Construction	70
38	Solar Array Regulator Block Diagram	73
39	Voltage Regulator	73
40	Encoder Converter Block Diagram	76
41	Optical Aspect Converter Block Diagram	77
42	Battery Discharge Characteristics	78

ILLUSTRATIONS (Continued)

Figure		Page
43	Battery Charge Sequence	79
44	Undervoltage Block Diagram	80
45	Fourth Stage Ignition and Separation Timer	82
46	Solar Aspect Sensor	87
47	Moon-Earth Telescope	89

TABLES

Table No.		Page
1	Thermal Ion Experiment Format	12
2	Physical and Mechanical Properties of the Inert and Live Propellants	47
3	Motor Performance Data	48
4	TE-P-462 Igniter Data	49
5	Composition of AIMP Encoder Modules	52
6	AIMP-D Performance Parameter Assignments	57
7	AIMP Power Allotment	74
8	Output Voltage of Encoder Converter	75

AIMP (IMP-D)
TECHNICAL SUMMARY DESCRIPTION

INTRODUCTION

This document gives a functional description of the major subsystems on the AIMP-D spacecraft (Explorer XXXIII) which was launched on 1 July 1966. This document has been prepared by the AIMP project staff with the cooperation of the experimenters and GSFC technical personnel.

Explorer XXXIII is in an elliptical orbit about the earth in which the orbital parameters, due to lunar perturbation, vary rapidly. In general, the orbital parameters remain within the following bounds:

Perigee : 32,000 to 200,000 km

Apogee : 400,000 to 600,000 kms

Inclination: 5 to 50 degrees

EXPERIMENTS

The AIMP-D spacecraft carried seven active experiments. They are described below.

University of California Ionizing Radiation Experiment

Purpose — This experiment has five major scientific objectives. They are:

- A search for low-energy solar electrons in interplanetary space. Fluxes as small as about 3 cm^{-2} sr^{-1} sec^{-1} are detectable. The main interest here is with electron fluxes inside gas clouds which produce magnetic storms. If this aspect of the experiment is negative, at least a very small lower limit will have been set.

- Detection of low-energy protons, and the relation of these to storm producing solar plasma to complement the electron measurement.

- Monitoring of the flux of terrestrial electrons and protons sluffed off the magnetosphere which appear near the moon. The frequency of appearance and intensity of energetic electrons in the geomagnetic tail can be monitored 90 R_E, from the earth.

- A precise and sensitive monitor of changes in the galactic cosmic ray intensity of all time scales down to 6 minutes or so by use of the ion chamber.

- A time history of solar cosmic ray events provided by the counters over three integral energy regions:

  GM 1 $\geq$ 50 kev

  Ion Chamber $\geq$ 15 Mev

  GM 2 $\geq$ 0.5 Mev

- Spectral changes appear as changes in the ratios of the three integral rates.

Description — The experiment consists of three sensors capable of measuring different energy level electrons and protons. The electronic circuits associated with the sensors measure the rates or number of energetic particles sensed in a given period of time. Two GM tubes are used to measure low energy electrons (greater than 20 Kev) and protons (greater than 400 Kev), while an ion chamber of the Neher type (spherical) is used to measure high energy electrons (greater than 1 Mev) and protons (greater than 15 Mev).

The only difference between the two GM sensors is the use of a backscatter technique on one of them in order to prevent protons from entering the GM tube. Thus GM1 will, with the backscatter adaption, be sensitive to only electrons of energies greater than 40 Kev while GM2 will be sensitive to electrons greater than 20 Kev and protons with energies greater than 400 Kev. By taking the difference in count rates between the two, the low energy proton count is obtained. The low energy counters are Lionel Type 205HT GM tubes.

The GM tubes are directional at the energy levels they measure, while the ion chamber is omnidirectional. The backscatter GM sensor is so mounted within the experiment that its aperture is a 61° cone normal to the spin axis but displaced 27° from the normal to the outside facet. The other GM tube has a 45° conical aperture perpendicular to the spacecraft spin axis. The ion chamber is mounted on top of the experiment, and when the experiment is placed in the spacecraft, the ion chamber protrudes about halfway above the top outside skin of the spacecraft.

The ion chamber is a .030" thick aluminum sphere pressurized to approximately 100 psi with pure Argon gas. Figure 1 is a schematic interpretation of the ion chamber.

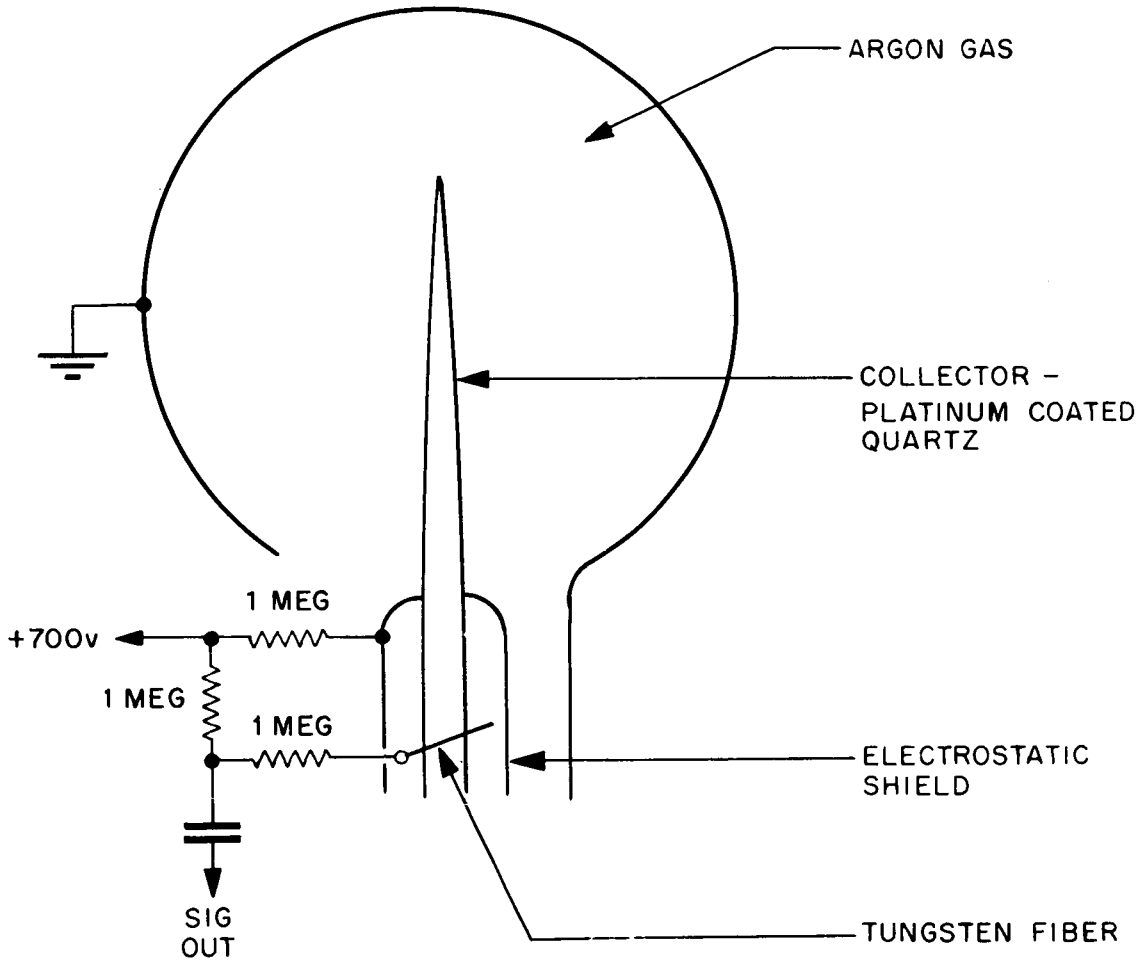

Figure 1–Ion Chamber

Before the ion chamber is energized, the tungsten fiber is not touching the collector and it is uncharged. When the +700V is applied, the fiber is charged to this potential. The charge then existing between the collector and fiber attracts the fiber and charges the collector to +700V which then repels the tungsten fiber, thus opening the contact between the fiber and the coated collector rod. Its action is similar to that of a gold leaf galvanometer. Protons and electrons entering the chamber ionize the gas, resulting in a partial discharge of the collector potential. Continued bombardment of the chamber reduces the collector charge to a point (approximately +600V) where the tungsten fiber again

makes contact with the collector, which is then electrically connected to the 700V source and is recharged to +700V. The charge current causes a "signal output" which is amplified and counted. In general then, the ion chamber acts as an integrator where the output is proportional to the rate at which the electrons and protons bombard the chamber. The maximum output rate of the chamber is about 100 pps.

Theory of Operation — The data from the sensors is fed to four 16-bit accumulators in the digital data processor of the encoder after appropriate amplification, shaping and timing. All accumulators are re-set after read out, so that only period counts are made.

The two GM tubes feed accumulators directly after pulse shaping and amplification. These accumulators are the "S-T" type which will count signal pulses (S) up to the maximum of the accumulator and will then count clock pulses (T) for the rest of the accumulation period.

The purpose of this device is to allow for an overflow situation, where more pulses occur than can be counted during the time period. For each GM tube read-out, a 16-bit accumulator, 5a and 6a respectively, is used. If the 16th bit is "O" then the readout is the number of pulses acquired in the accumulation period. If the 16th bit is "1", then the first 15 bits of the accumulator give the number of clock pulses acquired after the overflow.

From Figure 2(a), it can be seen that the last bit of the "S-T" accumulator is used for the control to switch over and count the clock instead of signal inputs. The clock frequency selected is such that the accumulator would not overflow if the clock were counted for the entire accumulation period. Therefore, as seen in Figure 2(b), determination of the rate at which the signal inputs were counted, up to the point where the accumulator overflowed, is made by using the equation

$$\frac{2^{15}}{T_2 - T_1}$$

where T_1 is the count telemetered in the "T" mode and T_2 is a nominal accumulation time of 39.68 second.

For the ion chamber, one 12-bit and one 16-bit accumulator is used (5b and 6b); one determines the total chamber count during the accumulation period and the other measures either the time between the first pair of pulses (if 2 or more

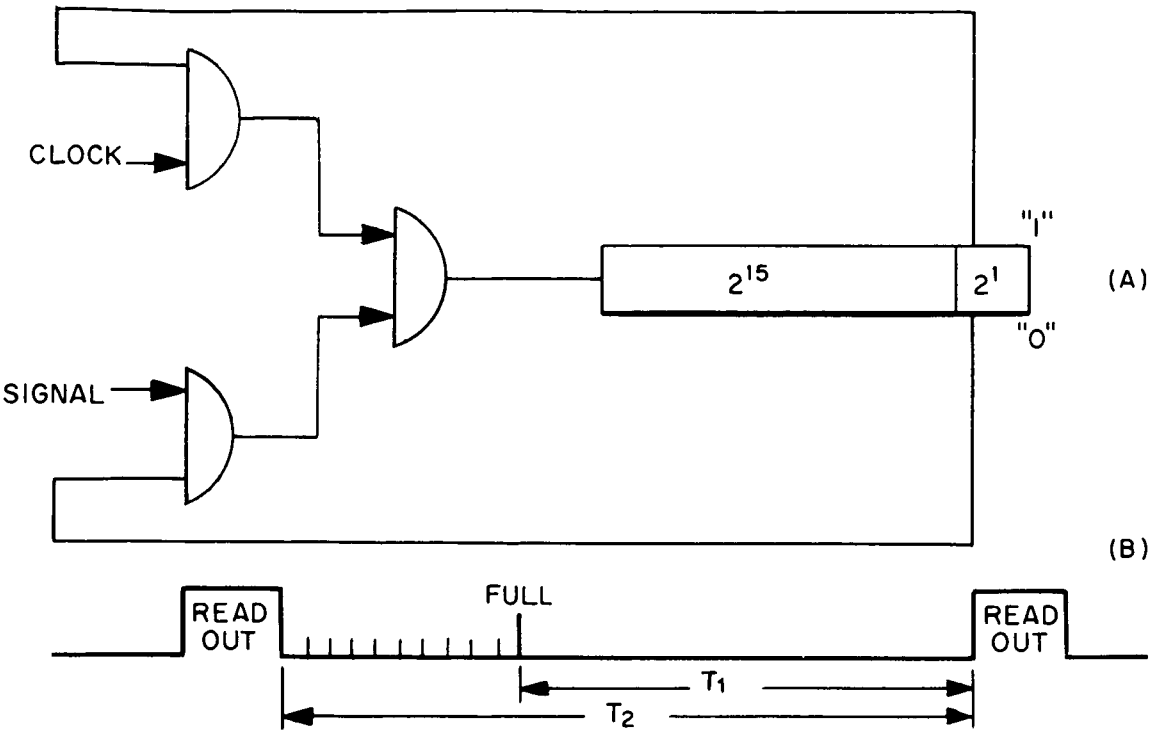

Figure 2–"S" – "T" Accumulator

occur in the accumulation period) or the time from a pulse to the next readout (freeze) time.

The 6B accumulator is used to measure total ion chamber counts. The signal from the ion chamber is amplified and triggers a one-shot multivibrator which is used to drive the accumulator input.

For the time between pulses, the 5b accumulator is used as described by Figure 3.

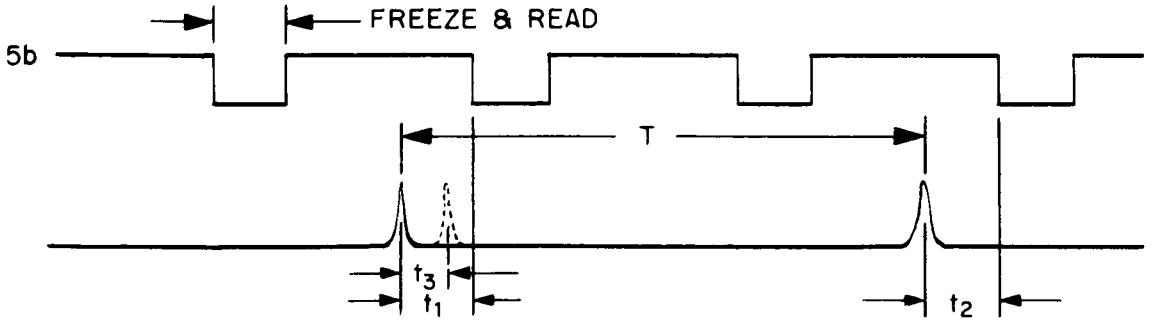

Figure 3–Time Between Pulses

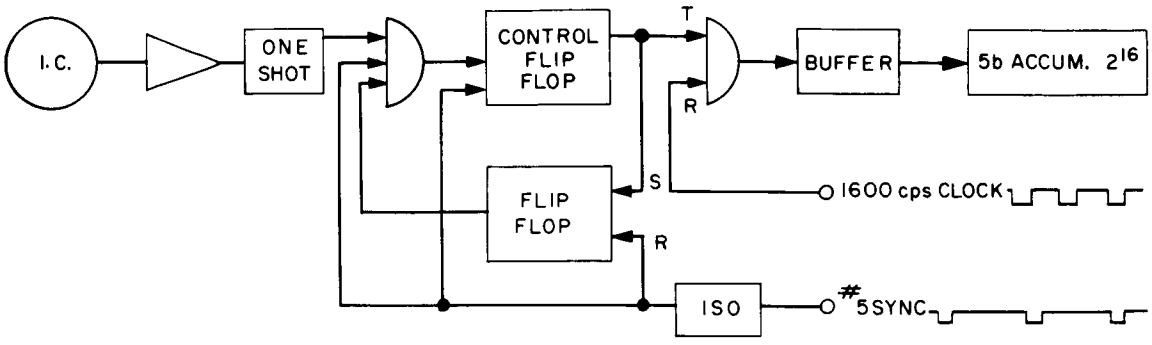

Figure 4–Time Measurement System

Figure 4 shows the logic circuit which permits the measurements of t_1, t_2, and t_3. The ion chamber output, after shaping by a one-shot multivibrator, triggers a flip-flop which gates the 1600 cps clock into the 5b accumulator. If there are no other ion chamber outputs before the accumulation period ends, then the clock count is stopped by the resetting of the control flip-flop with the #5 sync (accumulator freeze). The stored count in the accumulator is t_1 (Figure 3). This same process is repeated every time there is only one ion chamber pulse per accumulation period. For very low bit rates, the total time "T" between bits is calculated as shown by Figure 3 with t_1 and t_2 determined by identical processes. If there is more than one pulse per accumulation then the second pulse returns the control flip-flop to its original state, which in turn sets another flip-flop (see Figure 4), to block the input gate such that further bits during this same accumulation period do not start the clock count again. The 1600 cps count in the accumulator then defines t_3 (Figure 3). Thus both large and small ion chamber count rates can be measured. Extremely high count rates are not expected, therefore an "S" - "T" type accumulator is not used for the ion chamber direct count (accumulator 6b).

Both flip-flops are re-set during the #5 accumulator freeze and readout.

Telemetry — The University of California Ionizing Radiation experiment uses three 16-bit accumulators and one 12-bit accumulator to store data, with a periodic readout and reset of each twice every sequence. An additional 4-bits are used for a redundancy check on the 6a accumulator.

The format for the readout of each accumulator is shown on the following page.

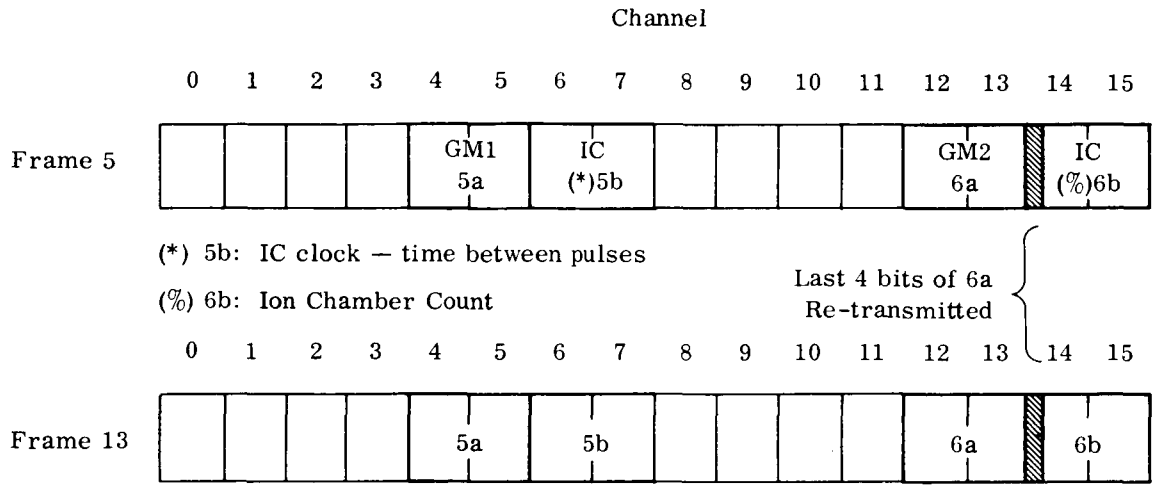

Frames 5 and 13 were allocated so that the accumulation time for each accumulator read-in would be the same.

The four most significant bits of accumulator 6a are repeated as shown below.

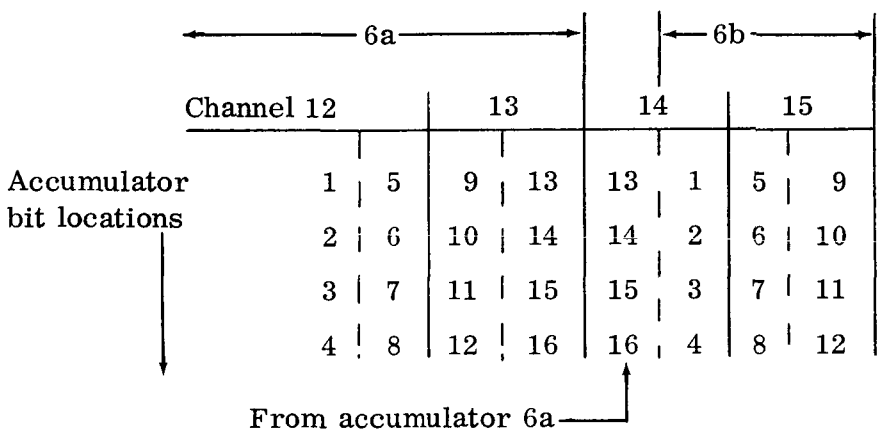

Thermal Ion Electron Experiment

Purpose — The Thermal Ion Electron experiment is designed to measure low energy electrons and ions of the plasma flow in free space.

In particular, the experiment is designed to measure the number, density, and temperature of ions and electrons in the energy levels below 45 eV.

Description — A three-grid Faraday cup is used to measure first ion and then electron currents as a function of various retarding potentials within the cup.

Electron currents are analyzed according to

$$(ie)_0 = \frac{1}{4}\left[e(\alpha_e N_e \bar{C}_e A)\right]$$

where $(ie)_0$ is the collector current, A is the area of the collector, α_e is the electrical transparency, and $\bar{C}_e$ is the mean electron velocity computed from the measured electron temperature. Temperatures are computed from the slope of the volt-ampere characteristic according to

$$T_e = \frac{e\,(\Delta\Phi)}{k\,(\ln(i_1/i_2))}$$

where e is the electronic charge, k is Boltzmann's constant, and $\Delta\Phi$ is the change in retarding voltage between measured collector current and i_1 and i_2.

Theory of Operation — A diagram of the retarding potential trap is shown in Figure 5. The trap is a three-inch Faraday cup, covered by a plate which

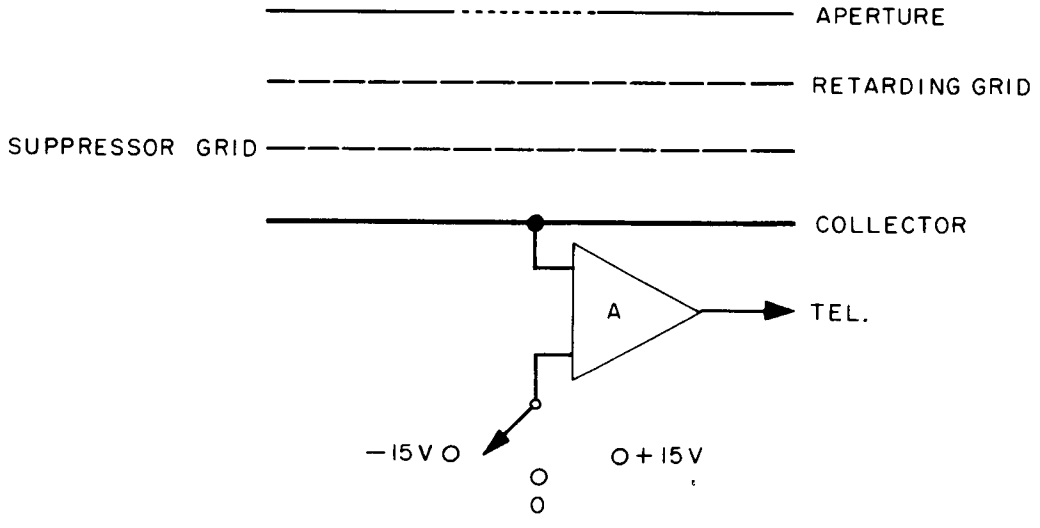

Figure 5–Retarding Potential Analyzer

acts as a guard ring. The cover has a circular aperture one inch in diameter. The aperture is covered by a tungsten wire mesh whose transparency to both electrons and ions is calibrated. The cover of the trap and the aperture are held at a constant voltage to exclude the particles of "like" polarity and to accelerate the "oppositely" charged particles. The aperture is made small so that the admittance angle is more nearly perpendicular to the trap.

The second grid is used to retard the particles which have entered the trap. A third grid is employed to suppress photoemission from the collector. The collector is connected to an electrometer which measures the currents as a function of the retarding potentials.

The Ion Mode — The outside and aperture grid are maintained at -45 volts DC; thus, electrons of energies below 45 eV are excluded from the trap and all ions are accelerated inward. The ions after entering the aperture are retarded by the potential present on the second, or retarding grid. A programmer steps the voltage, on this grid, in 15 equal increments from 0 to +45 volts. The retarding voltage steps are synchronized with the telemetry read-out rate, so that during each telemetry read-out, currents have essentially a steady value. A potential of -15 volts in respect to ground is applied to the collector in order to insure collection of all ions which have passed through the retarding grid. Photoelectrons emitted from the collector will be returned to the collector by a potential of -40 volts on the third grid. This mode of ion current measurement is followed by a similar mode in which the retarding voltages are stepped from 0 to +15 volts in 15 equal increments. This mode of operation will offer improved resolution for less energetic or thermal particles.

The Electron Mode — The voltage polarities for the electron mode are made opposite to the ion mode polarities, thereby excluding the ions and measuring the electron current as a function of retarding potentials. In the electron mode the collector is made 15 volts positive in respect to spacecraft, so that photoelectrons emitted during this mode are returned to the collector and their effect on the measured current is suppressed.

Figure 6 is a block diagram of the experiment showing the major components. A Faraday cup sensor, a logarithmic amplifier where sensitivity to either positive or negative current ranges from 10^{-11} to 10^{-7} amperes, an analog to digital converter that converts the electrometer voltage output to a 4-bit digital word. An electronic programmer generates the sensor voltages and the commands for polarity reversal and electrometer calibration.

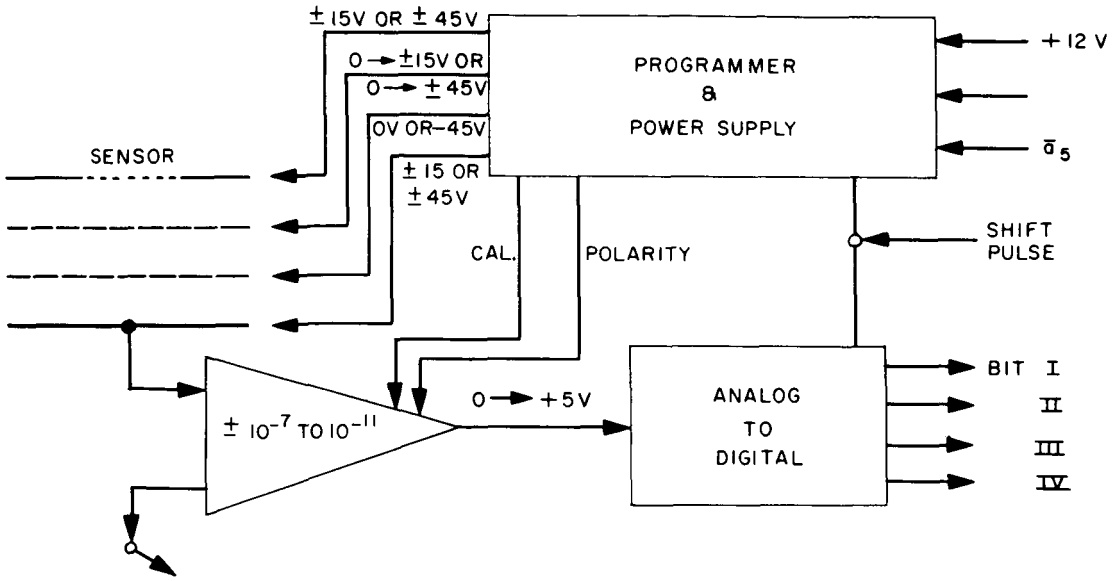

Figure 6–Block Diagram of Thermal Ion Electron

During each 100 microseconds following a shift pulse, the programmer commands the changes in the trap voltage format and in addition the stored digital word is transferred into the buffer. Each retarding potential measurement is then made for the following 80 milliseconds and the program is thus advanced at the rate of the shift pulse.

Telemetry — The thermal ion electron experiment functions during channels 5, 6 and 7 of frame 7 and 15. In each sequence, 12 digital four-bit words are read out to telemetry.

Internal to the experiment, the format consists of 90 four-bit words; words 1 through 45 constitute the ion retardation and calibration measurement; and words 46 through 90 constitute the electron measurement.

To maintain synchronism with telemetry, the experiment's internal program is reset to either step 1 or step 46 once every 32 sequences (A_5) or at the rate of once every 384 words. During each 384 word reset, the internal program will cycle the ion-electron measurements 4.26 times, and then the program is reset to either step 1 or step 46. The step chosen is not predictable.

In order to check the function of the experiment, the calibration words are observed. The ion calibration words are 37 and 38 (digital output 13, 13); words 39 and 40 (digital output 7, 7); and words 41 and 42 (digital output 3, 3).

For electron calibration the words and output are 82 and 83 (digital output 14, 14); 84 and 85 (digital output 8, 8); and 86 and 87 (digital output 3,3).

Table 1 depicts the internal experimental program and the location of the calibrations in that array. The observed changes in the calibrates with temperature are shown also.

The digital word in steps 1 to 35 and 46 to 81 are in general at values below 4, but this value is dependent upon the amount of background noise present in the sensor. The calibrates are only used to observe that the experiment is in synchronism and working properly.

University of Iowa Energetic Particle Experiment

Purpose — The primary scientific objective of this experiment is the measurement of the spatial, temporal, and angular distributions of electrons of energy exceeding 40 Kev in the magnetospheric wake of the earth at $\sim$60 earth radii. In addition, a search for electrons exceeding 40 Kev in the wake of the moon will be made with detailed studies of the distributions as above. Further, studies of the incidence and intensity vs. time profile of low energy solar cosmic rays (protons and alpha particles separately) in interplanetary space and their energy spectra and angular distribution.

Solar X-rays in the 0-14A° range will also be measured.

Description — The experiment consists of four sensors, three Geiger-Mueller (GM) tubes and a PN junction semiconductor. The sensors are located as shown in Figure 7 such that GM1 and the PN junction collimator axes are parallel but canted 22.5° from the normal to the spacecraft facet.

GM1 is an EON type 6213 mica window tube. The collimator forms a fan-shaped view angle of 120° in a meridian plane and 30° in the equatorial plane, with the center line in the equatorial plane. The threshold energy of the detector is 0.5 Mev for protons, 2 Mev for alpha particles, and 40 Kev for electrons. This detector is also sensitive to photons in the wave length range 0 to 14A°. The maximum output rate of pulses from the detector-circuit combination is about 22,000/sec. Calibration procedures are utilized to extend the dynamic range to 10^7 true counts/sec.

GM2 is identical with GM1 except that the collimator provides a 50° conical view with its axis parallel to the spacecraft spin axis.

TABLE 1
THERMAL ION-ELECTRON EXPERIMENT FORMAT

Ion Program

High Retardation	1/3	2/3	3/3	4/3	5/3	6/3	7/3	8/3	9/3	10/3	11/3	12/3	13/3	14/3	15/3
Low Retardation	16/3	17/3	18/3	19/3	20/3	21/3	22/3	23/3	24/3	25/3	26/3	27/3	28/3	29/3	30/3
Calibrate	31/3	32/3	33/3	34/3	35/3	36/3	37/13	38/13	39/7	40/7	41/3	42/3	43/0	44/0	45/0

Electron Program

High Retardation	46/4	47/3	48/2	49/1	50/	51/	52/	53/	54/3	55/	56/	57/	58/	59/3	60/
Low Retardation	61/3	62/2	63/3	64/	65/	66/	67/	68/	69/3	70/	71/	72/	73/3	74/	75/
Calibrate	76/3	77/	78/	79/2	80/	81/3	82/14	83/14	84/8	85/8	86/3	87/3	88/1	89/1	90/0

	Channel 5a	Channel 5b	Channel 6a	Channel 6b	Channel 7a	Channel 7b
FRAME 7 →						

Temperature Drifts

Ion Calibrations	+50°C	+25°C	+12°C	O°C	-10°C	-15°C
	12	13	14	15	15	15
	6	7	8	9	11	11
	2	3	4	5	5	6

Electron Calibrations	+50°C	+25°C	+12°C	O°C	-10°C	-15°C
	13	14	15	15	15	15
	7	8	9	10	10	10
	2	3	4	5	6	6

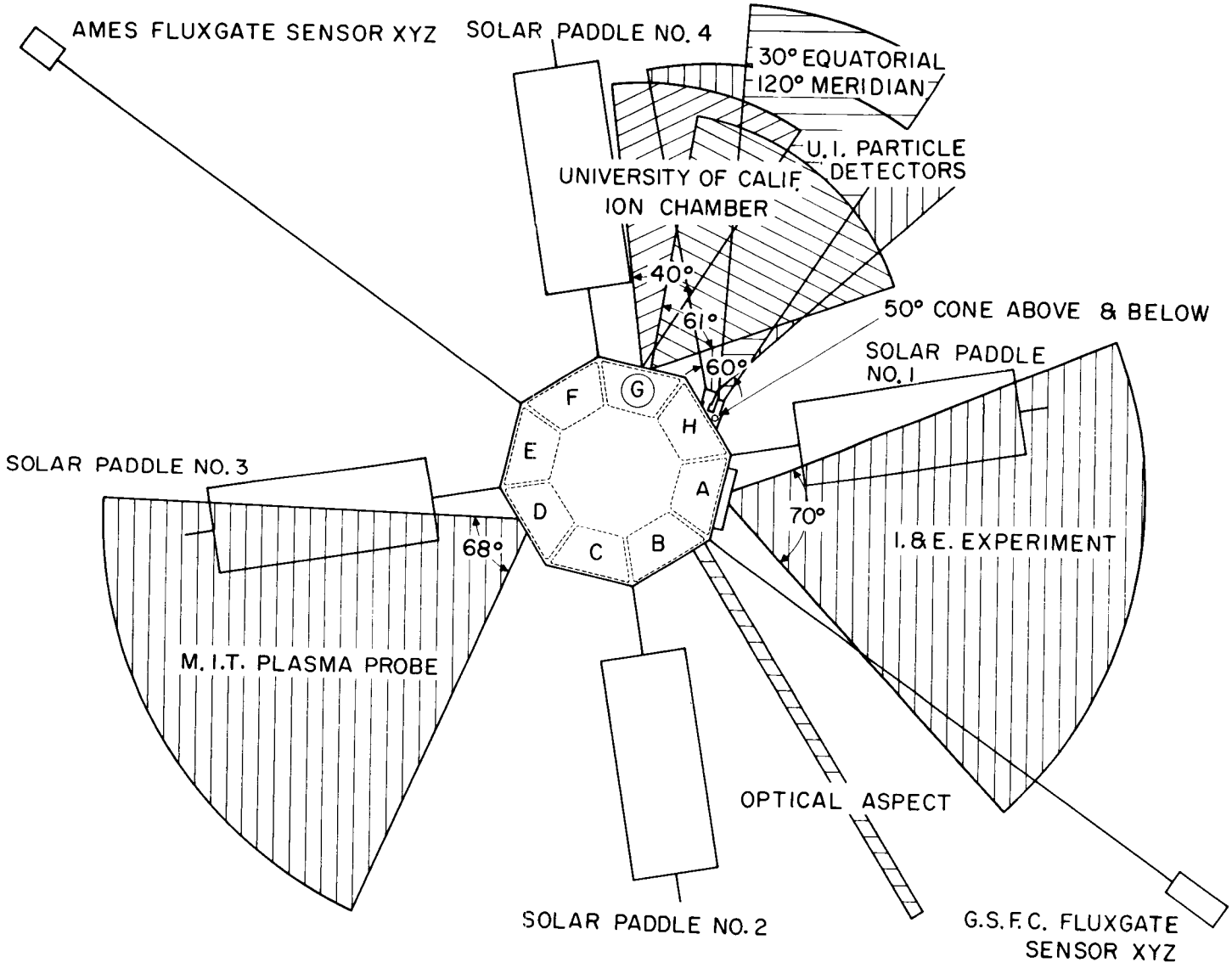

Figure 7–Experiment View Angles

GM3 is identical with GM2 except that the axis of its collimator is oriented 180° to that of GM2.

The PN junction is a thin, totally depleted, surface barrier silicon detector having a thickness of about 25 microns. The collimator has its axis in the equatorial plane of the spacecraft passing through the rotational axis, and parallel to that of GM1 with a 60° conical view angle. The detector is shielded by a foil and is insensitive to the electromagnetic spectrum of the sun. It is also insensitive to electrons of any energy, up to intensity levels far above those previously found to exist in interplanetary space. Four pulse-height discriminator levels are provided with the thresholds set for the following energy ranges of protons and alpha particles.

Level 1 protons	$0.25 \leq E_p \leq 20$	Mev
alpha	$0.40 \leq E_\alpha \leq 200$	Mev
Level 2 protons	$0.50 \leq E_p \leq 3.6$	Mev
alpha	$0.85 \leq E_\alpha \leq 100$	Mev
Level 3 protons	$0.90 \leq E_p \leq 1.9$	Mev
alpha	$1.20 \leq E_\alpha \leq 40$	Mev
Level 4 alpha only	$2.10 \leq E_\alpha \leq 15.0$	Mev

The maximum output rate is limited to 25,000 counts/sec. A very weak source (Am^{241}) is permanently mounted in the collimator to provide alpha particles of ~5 Mev with a count rate of ~0.1 counts/sec so that alpha counts on all levels from 5 Mev to 200 Mev will be provided.

In order to obtain more data within the telemetry constraints and to apply meaning to the data collected by the sensors, their outputs are commutated in terms of time and spacecraft spin orientation, as shown in the block diagram of Figure 8.

The GM tubes as shown in Figure 8 all feed identical amplifiers which provide a saturated output. These outputs are then commutated or time-shared as shown prior to being sent to accumulators in the encoder. In addition, the GM1 output is also divided into four quadrants with respect to the spin axis and the sun direction (i.e., the sun line to the spacecraft is used as the reference).

The PN junction detector senses the various energy level protons and alpha particles by amplitude comparison. The higher the energy of the particle the larger the pulse amplitude from the detector. The various energy levels are

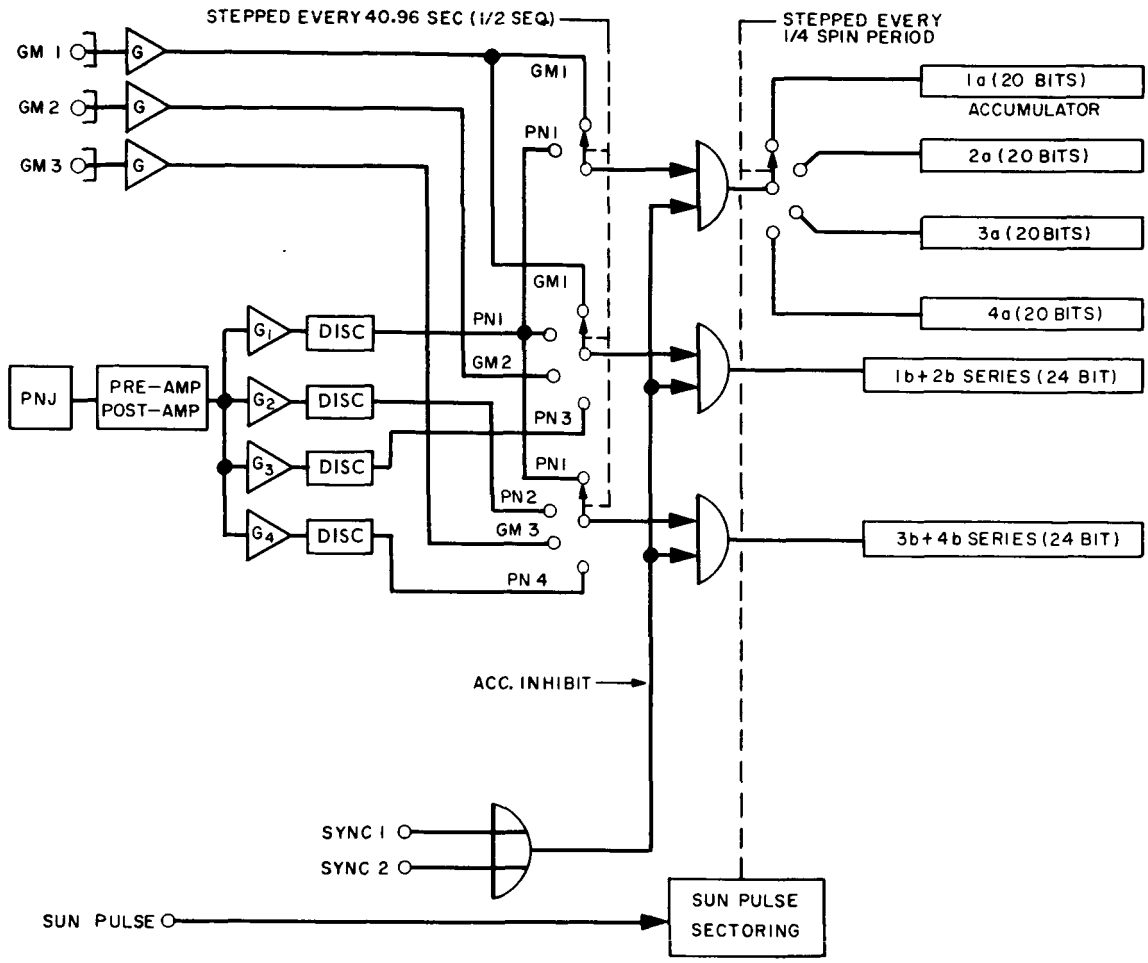

Figure 8–Block Diagram – University of Iowa

segregated by having four amplifiers of different gains in parallel, each feeding a peak discriminator. Each discriminator is set for the same d.c. threshold level and the different gains in the amplifier provide the telemetry system with the different detector output levels. The four output levels are commutated and sent to accumulators.

The sync signals used to inhibit the data inputs to the accumulators provide equal accumulation times for all data. Thus there is no input to the accumulators for Frames 1, 2, 3, and 9, 10, 11, leaving five frames for accumulating data between each read-out sequence. This system can be better understood by reference to Figure 9.

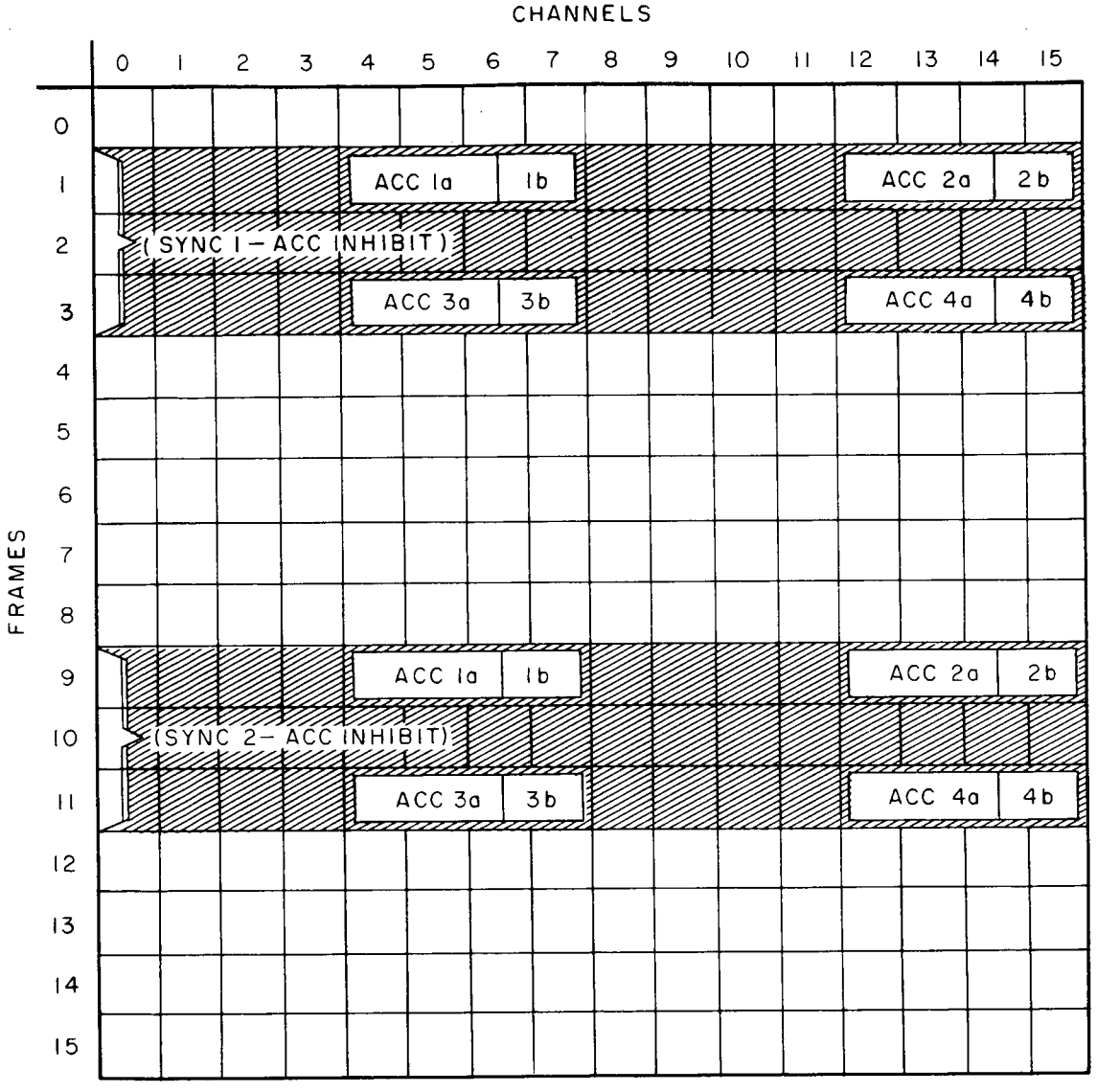

Figure 9–University of Iowa Telemetry Format

These same sync signals are used to provide the half-sequence commutating rate for the sensor sampling as shown in Figure 8. Thus it takes two sequences to sample all the data. There are no calibration sequences, but the onboard Am^{241} source provides a continuous reference level which can be evaluated during quiet periods.

Figure 10 is a timing diagram showing the various relationships described above.

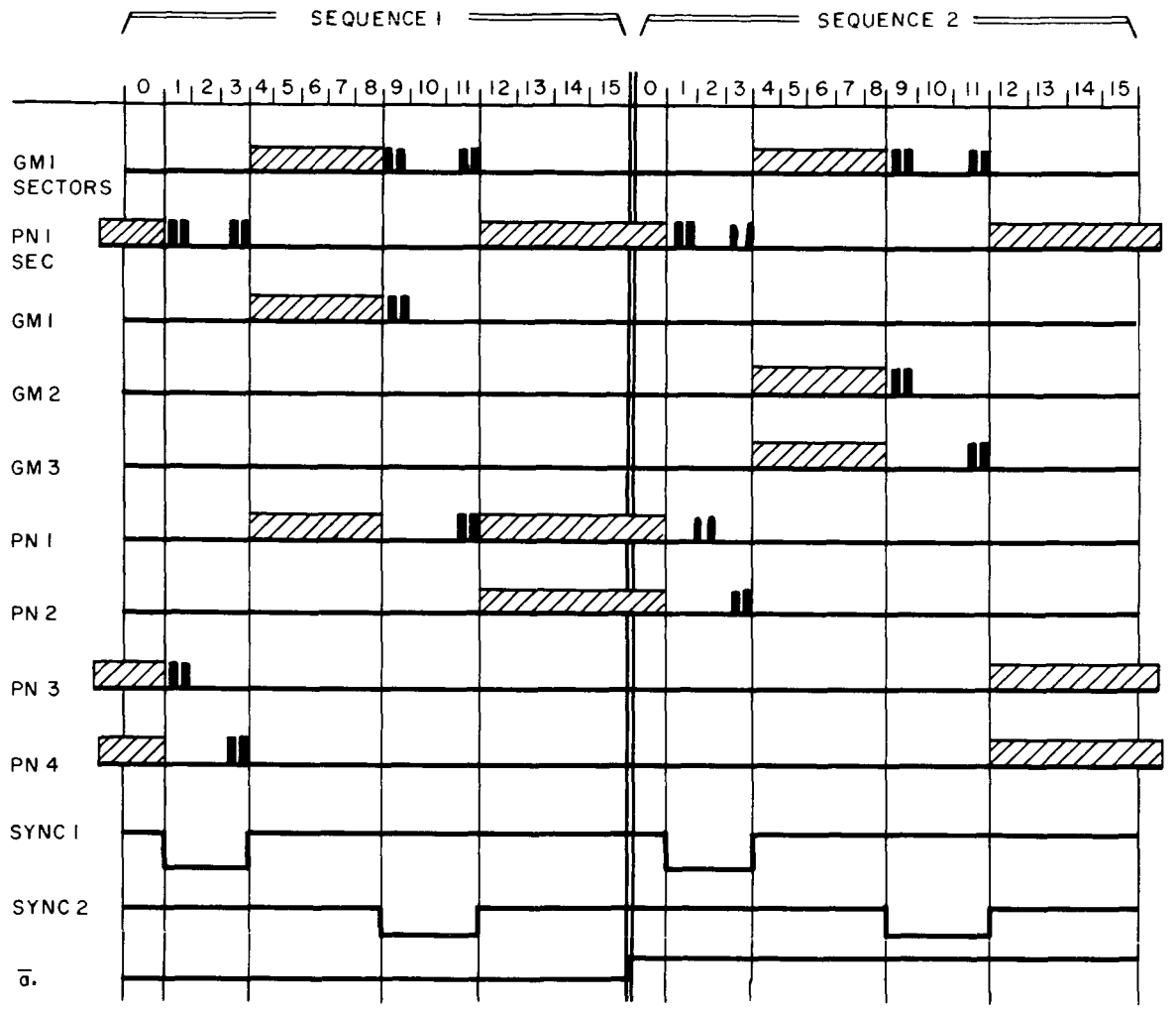

Figure 10–University of Iowa Data Timing Diagram

MIT Plasma Probe Experiment

Purpose — The "Plasma Probe" is designed to measure the properties of the plasma flow in free space. The lunar orbit for the AIMP D&E series will provide a satellite which for the most part is anchored in space beyond the influence of the local environment of the earth. Thus, general properties of the plasma in the vicinity of the earth being monitored by other satellites and space probes which are in orbit simultaneously can be compared with those from AIMP. In this way information concerning spatial and temporal changes in the plasma properties can be obtained.

In particular, measurements of the energy spectrum and angular distribution of the proton and electron flux of the plasma will be made over the range

of 50 eV to 5 KeV (typical values of 300 eV to 1 KeV). The following discrete properties will be measured:

- Angular distribution of the total proton flux in the equatorial plane of the spacecraft.
- Angular distribution of the total proton flux in the meridian plane of the spacecraft.
- Energy distribution of the proton flux at or near the same angle as the peak of the total proton flux.
- Angular distribution of the electron flux in the equatorial plane of the spacecraft.
- Angular distribution of the electron flux in the meridian plane of the spacecraft.
- Energy distribution of the electron flux at approximately 90° to the sun-satellite line.

Description — The technique used to measure these properties utilizes a Faraday cup. A collector and grid arrangement is used to establish a current flow based on the number of charged particles "collected" (Figure 11). For the sensor area of this experiment, currents of 10^{-12} to 10^{-7} amps are typical.

The grid (Figure 11) is used to determine the energy level of the protons or electrons that are to be measured. The grid is charged with a "like" potential relative to the charge of the particles being measured. Thus for the configuration of Figure 11, positive ions with energies less than +V will not be collected and those above +V will be collected.

In this experiment, two basic measurements are made: (1) an integral measurement is made of all the protons (or electrons) of energies up to a given

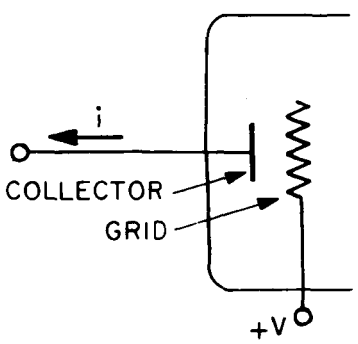

$i = A e \phi$

WHERE A = AREA OF COLLECTOR

e = ELECTRONIC CHARGE OF PARTICLE

ϕ = FLUX OF PARTICLE ($n\bar{v}$) I.E., NUMBER (DENSITY) n AND VELOCITY $\bar{v}$.

Figure 11–Faraday Cup

maximum value and, (2) a differential measurement is made of various energy levels. From this information, the flux density and energy spectrum can be obtained.

In order to obtain angular or directional information about the plasma flow relative to the spacecraft and sun, the sensor is located with its viewing axis normal to the spin axis of the spacecraft. Since the "cup" has a view angle of ±15° in the equatorial plane and ±45° in the meridian plane, the angular distribution of positive ions (or electrons) in the spacecraft equatorial plane is obtained when the sun to spin axis is 90 ±30°. This measurement alone does not give the discrete direction of the plasma flow relative to all space; a measurement in an orthogonal plane containing the spin axis and cup normal (spacecraft meridian plane) is required. This latter measurement is accomplished by dividing the collector symmetrically with respect to the spacecraft equatorial plane with two outputs as shown in Figure 12. By this means the direction of a uni-directional beam can be determined to within ±5°.

The MIT Experiment is contained within three module frames. The electronics are contained within two frames, each 1.25 inches high; the sensor completely occupies the third frame, which is 6.28 inches high. The criteria for locating the experiment in the spacecraft are the following:

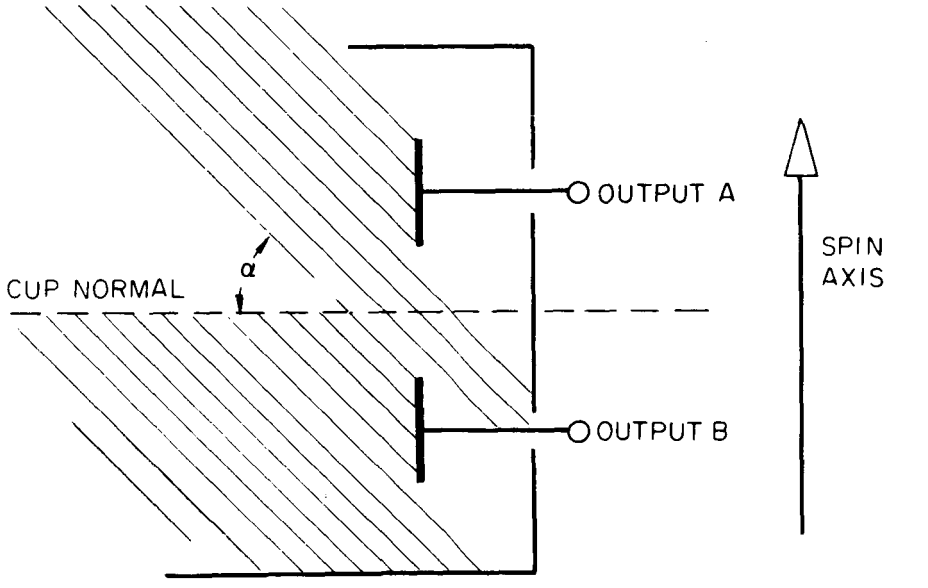

Figure 12–Method of Measurement

- The sensor must be provided an unobstructed field of view for a 68° solid cone angle, with the axis of the cone normal to the payload spin axis.
- The sensor should be located in the facet providing the best thermal stability.
- The electronics should be located as near as possible to the sensor so as to minimize the high-voltage cable lengths.

These requirements, along with static balance considerations, resulted in the MIT sensor being located in Facet D with the electronics adjacent in Facet C. Facet D is located midway between the two largest heat sensors and is optimum for thermal stability. The sensor requires a cutout in the honeycomb cover, approximately 5 to 6" in diameter.

Theory of Operation — In general, it is desirable to take detailed measurements every time the plasma is viewed, but the low telemetry rate makes this impossible unless on-board data reduction is used. On-board data reduction is impractical. For the low bit rate AIMP telemetry, the following methods are used.

Integral Measurements (Angular Distribution) — The first sun pulse after the beginning of Frame 6 of the telemetry format initiates the integral measurement. The sensor is energized (640 ms prior to the beginning of F6 to insure adequate time for the modulating voltage to rise to the desired amplitude) and an analog signal is obtained which represents the total energy of the plasma versus angular position (of the spin-stabilized spacecraft) as is represented in Figure 13. At the spacecraft spin rate, when the plasma is radially directed from the sun, the peak will always occur approximately 0.6 seconds after the sun pulse since the cup is located 90° behind (counter to spin direction) the optical aspect sensor.

The analog voltage resulting from this measurement is transmitted during Frame 6 as a real-time measurement.

The analog signal for the integral proton measurement could be obtained by using the sensor shown in Figure 11 and measuring the proton current developed. However, a true measurement of the plasma cannot be made in this manner when the "cup" faces the sun (the direction of maximum plasma) because photoelectric currents are emitted from the collector. Although this photocurrent can be suppressed by placing another grid in front of the collector with the appropriate bias level, there still remains a photocurrent produced by light reflected from the collector onto this suppressor grid. Distinguishing between

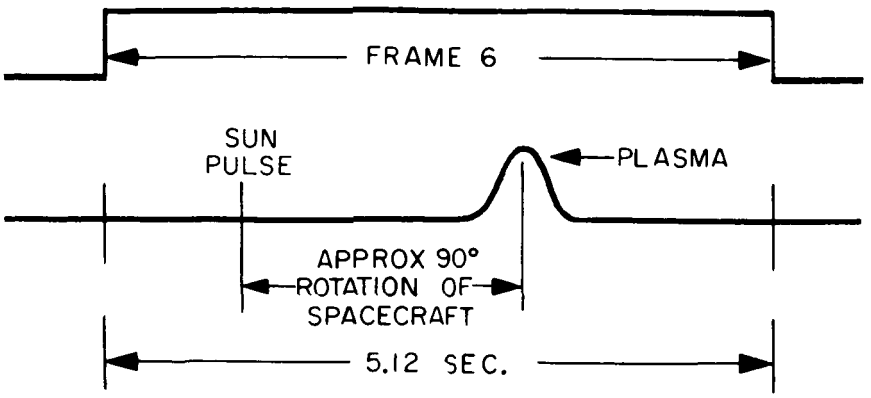

Figure 13–Plasma Integral Measurement

this current and the plasma is made possible by modulating the plasma current without, at the same time, modulating the reverse photoelectric current. Figure 14 illustrates the grid requirements for a modulated output.

Grid 4 is at ground potential (potential of the spacecraft skin); grid 3 serves to modulate the incoming protons by means of a square-wave voltage. Grid 2, also at ground potential, serves as a shield between the modulation grid and the collector. Grid 1 is maintained negative to eliminate electron currents. During the part of the modulation signal when the voltage on grid 3 is zero, protons and electrons flow into the cup. The electrons are repelled by grid 1, but the protons reach the collector. When the modulation voltage is positive, and equal to or greater than the energy of the incoming protons, the protons cannot pass grid 3 and thus there is no collector current. Thus there is an a.c. signal at the collector caused by the alternate arrival and non-arrival of the

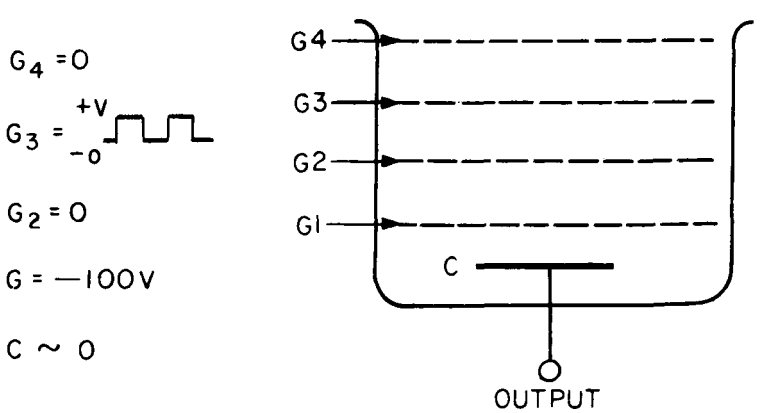

Figure 14–Grid Arrangement

plasma protons. The photo-electrons from the collector and grid 1 are shielded from the modulating voltage by grid 2, and therefore the photo-current gives a d.c. but no a.c. signal.

For the integral (or total flux) measurement, the logic circuit within the experiment electronics turns on the 1 Kc 50 V to 3 Kv square wave modulation just prior to the start of Frame 6 and it remains on until the end of Frame 6. The 3 Kv peak of the modulation is selected to be higher than the highest expected energy in the spectrum thus when the modulation cycle is zero all particles are collected. The resultant 1 Kc signal is amplified, filtered, detected, and gated to the telemetry encoder during Frame 6.

During Sequence 1 (collection mode A-B) the sensor output represents the difference between the plasma illuminating each half of the collector. The normal sampling circuits in the experiment can only amplitude discriminate this signal (cannot determine whether A > B or vice versa). In order to make this distinction the amplitude is synchronously detected during the peak of the integral measurement in Frame 6. This information is presented to the telemetry during Sequence 1, Frame 14(1b).

During the integral measurement period, means are also provided to determine the peak or point of maximum total energy collected during the Frame 6 interval. This peak amplitude is stored and displayed to TLM during Frame 6 (15a). This peak then defines the center of the plasma. If the time the peak occurs is measured relative to a spacecraft parameter associated with the spin rate — the optical aspect sensor or "sun pulse" for instance — then regardless of the spinning characteristics of the spacecraft, detailed measurements can be made of a specific point in the plasma. (This only holds true however, as long as the plasma is quiet relative to the measurement time).

The "time to peak" measurement is made by utilizing a peak detector and comparison circuit such that each sample taken at 50 cps rate is compared with the stored amplitude of the previous 1 Kc pulse. If the previous sample is less, then the new amplitude is stored. This process is continued for the duration of Frame 6 (the integral measurement period). The time measurement is accomplished by counting the 50 cps encoder clock signal beginning with the first sun pulse of Frame 6 and transferring the count each time the comparator senses a larger signal than that stored. The final count registered before the end of Frame 6 (or the next sun pulse) represents the "time to peak." This time is stored in a register for use in the differential measurements as well as displayed to Telemetry on Frame 14 (13).

Differential Measurements (Energy Spectrum) — After the integral measurement of the plasma is made in real time, an energy distribution measurement is performed. For such a measurement it would be desirable to sample the entire energy distribution of the plasma versus angle or direction. Again, due to the low bit rate of the AIMP telemetry, this is impractical. Therefore, the energy spectrum only at the center of the plasma is measured. However, in order to get some measure of the energy distribution at points other than the center of the plasma, means are provided to determine if a maximum (for each energy window) exists between the sun pulse and the measured center of the plasma where the actual distribution measurement is being made.

The mechanization for making the differential measurements is similar to that used for the integral measurement except that a relatively narrow biased a.c. energy window is applied to the grid with the 1 Kc modulation such as shown in Figure 15.

Thus only that energy differential represented by ΔE_1 is collected. Eight discrete but not necessarily equal steps are used to cover the spectrum up to the maximum measured during the integral measurement.

In order to measure the energy spectrum at the plasma center, the stored "time to peak" is compared with a count of the 50 cps clock; when they are equal the sensor output is sampled, and the data is stored for readout in Frame 14. To obtain a degree of confidence whether this point just measured was at the center of the plasma or whether the plasma energy distribution is double peaked, the modulator is turned on for a full revolution of the spacecraft while the differential measurement is made as described above. The peak detector is operated for the same time the modulator is on and records the peak observed during this time up to the time the sensor is sampled for the differential measurement. The peak detector output and the differential measurement are compared, thereby answering the question "was there a higher peak

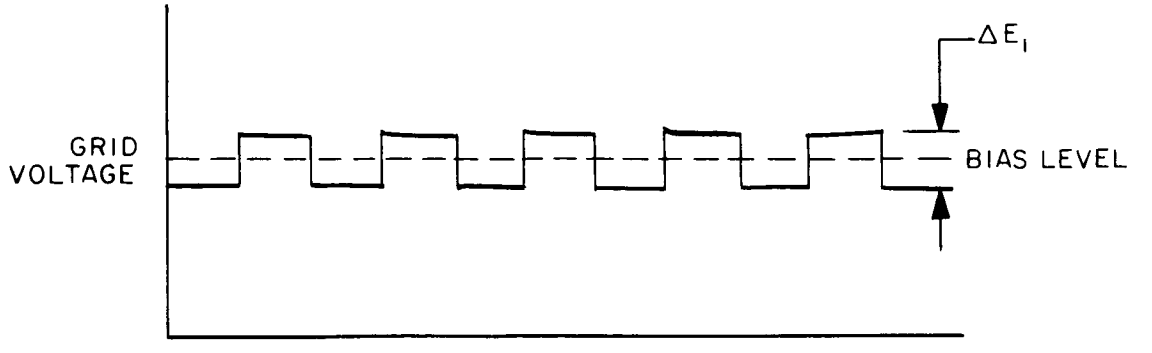

Figure 15–Differential Measurement Effect

than the differential peak just measured?". The answer is stored as one bit of an eight-bit register; with the remaining seven bits of the register reserved for the answer to this same question for the balance of the seven differential measurements in the sequence. This eight-bit word is displayed to telemetry during Frame 14(12).

After a differential measurement, the modulator is indexed to the next energy level in the spectrum. The process continues until eight consecutive measurements have been made, which will be completed prior to the start of Frame 14. When Frame 14 comes up, the capacitor-stored analog voltage for each differential flux value is digitized sequentially and displayed to Telemetry during Frame 14 (2-9).

The measurements described for Frame 6 through Frame 14 constitute one sequence. The end of Frame 14 indexes the system so that the first sun pulse after the next Frame 6 beginning initiates the same circuit operation except for the appropriate addition or subtraction of the A&B collector outputs. Thus with four sequences, a complete set of experimental data is obtained as follows:

Sequence	Type Measurement	Description
0	Proton	Sum (A+B) of collector outputs
1	Proton	Difference (A+B) collector outputs
2	Proton	Sum (A+B) of collector outputs
3	Electron	Sum (A+B) of collector outputs

For the electron measurements, the polarity of the modulating voltage is reversed.

When the system switches to a pseudo sun pulse there is one "sun pulse" missed. When this condition exists, the integral measurement only will be made starting with the beginning of Frame 6 instead of the sun pulse. No differential measurements will be made then for that particular sequence.

Calibration and Performance Measurements — In Frame 6 (14b), which is directly after the real time integral measurement is completed, the cup high voltage is monitored and gated to telemetry. During Frame 6 (15b) a calibration of the sensor amplifier chain is made. Four input levels are employed to provide calibration over the 4 decade range of the system in successive sequences. Once every 16 sequences a calibration sequence is substituted for the first sequence to provide a calibration of the differential measurement chain

during Frame 14 (2-9). All else in this calibrate sequence is the same as the first sequence. In order to identify the sequences Frame 14 (1a) is utilized. During Frame 14 (10 and 11) the temperature thermistors in the two electronics packages are monitored.

A typical timing diagram for the measurement sequence of this experiment is as shown in Figure 16.

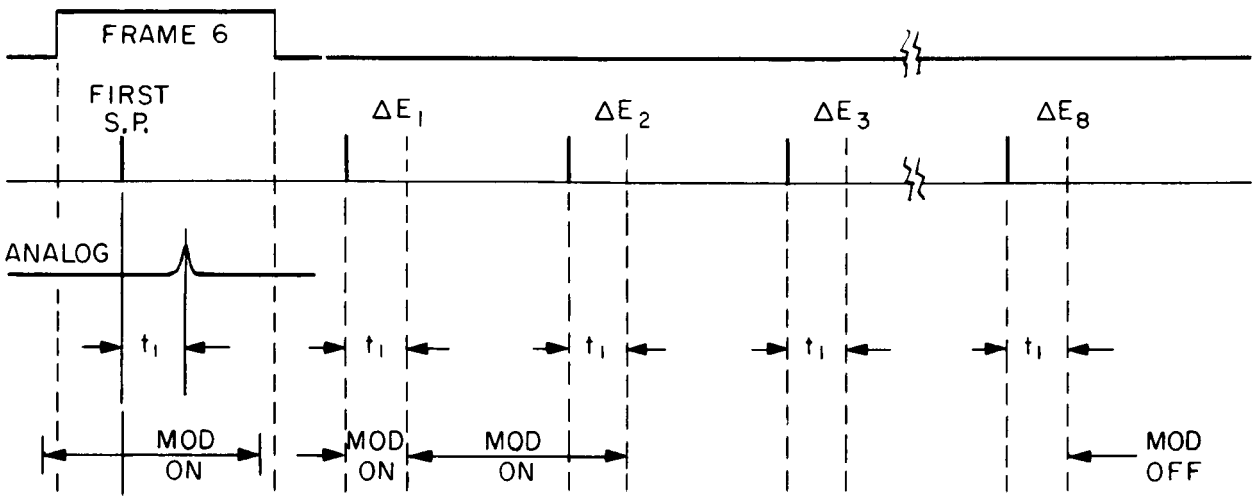

Figure 16–MIT Measurement Sequence

Telemetry — The telemetry format is shown in Figure 17. As noted previously, four complete sequences are required to cover all the measurements. However, to provide for calibration of the differential measurement circuit, a special sequence is substituted for the first sequence every sixteenth sequence.

The input to the encoder for Frame 6 is an analog, while that for Frame 14 is digital (eight bits per channel).

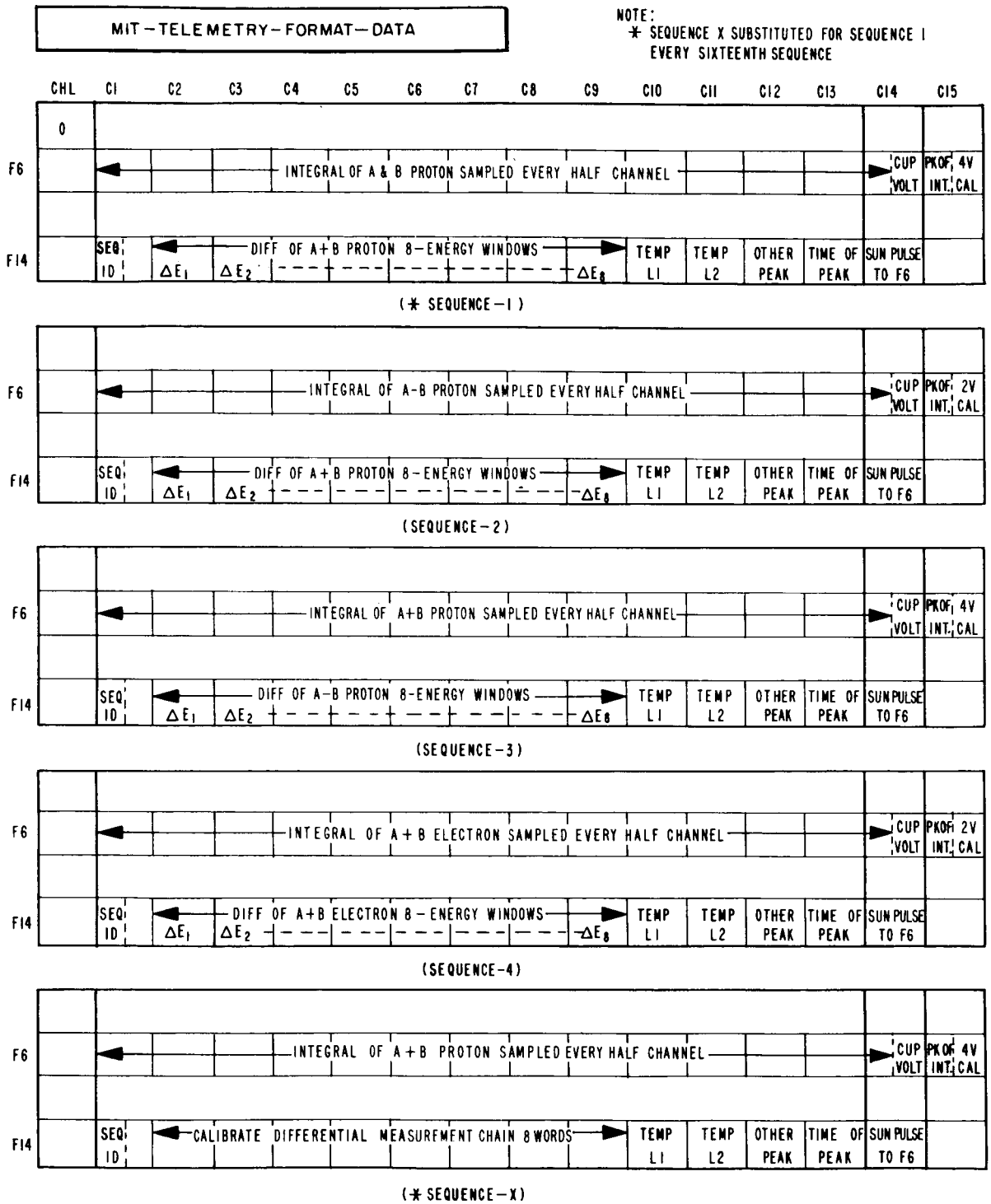

Figure 17–MIT Plasma Probe Telemetry Format

Ames Magnetometer Experiment

Purpose — The Ames Magnetometer Experiment for AIMP was designed to measure the magnitude, direction, and spatial and temporal variations of the magnetic field in interplanetary space as the spacecraft orbits the moon. The magnitude of the field is generally expected to be very low (approximately two gamma) with occasional high levels (up to 200 gamma) caused by sources such as solar disturbances. The direction of the field is expected to change rapidly and unpredictably.

Description — The magnetometer system includes two separate assemblies, a sensor package, which is mounted at the end of a boom; and an electronic package, which is mounted within the spacecraft main structure. Figure 18 is a block diagram of the system.

The sensor package includes three fluxgate sensors, a flipper mechanism, and flipper position indicators. Each sensor has the directional response of a free space dipole, and the three sensors are positioned along three mutually perpendicular axes with two of them mounted orthogonally on the flipper mechanism. One of these latter two lies along the spacecraft Y-axis and the other along the Z-axis.

The flipper mechanism, which is powered by two bimetal motors, one for clockwise and the other for counter-clockwise rotation, rotates each sensor by 90°. The heater power is controlled by the spacecraft encoder thru the Flipper Control card.

The electronics card has a ranging system where three gain conditions are selected sequentially providing full scale outputs of 20, 60, and 200 gamma.

Theory of Operation — The fluxgate sensors are driven to saturation by a 5.65 Kc oscillator. In the presence of an external magnetic field, the core flux of the sensor is unbalanced, and a second harmonic signal at 11.3 Kc appears in the output winding. The output is then a linear function of the external applied magnetic field.

Each sensor has its own signal amplifier tuned to 11.3 Kc. This signal is demodulated, resulting in a d.c. output. This d.c. output varies at the spin rate of the spacecraft as it rotates through the magnetic field. A block diagram of the sensor system is shown in Figure 19.

A phase-locked loop is used to synchronize the spacecraft spin with the reference signals for the spin demodulation system. The phase-locked loop produces two separate frequencies with their difference frequency locked in phase with the sun pulse furnished by the spacecraft. A reference frequency (ω_r) of 95 cps is generated from a fixed frequency oscillator. A variable frequency oscillator (VCO) operates such that a frequency equal to $\omega_r + \omega_s$ is obtained, where ω_s is the spacecraft spin (0.33 to 0.5 cps).

The spin demodulation process consists of modulating the signal amplifier outputs (varying d.c.) with the reference frequency, ω_r, and demodulating the resulting

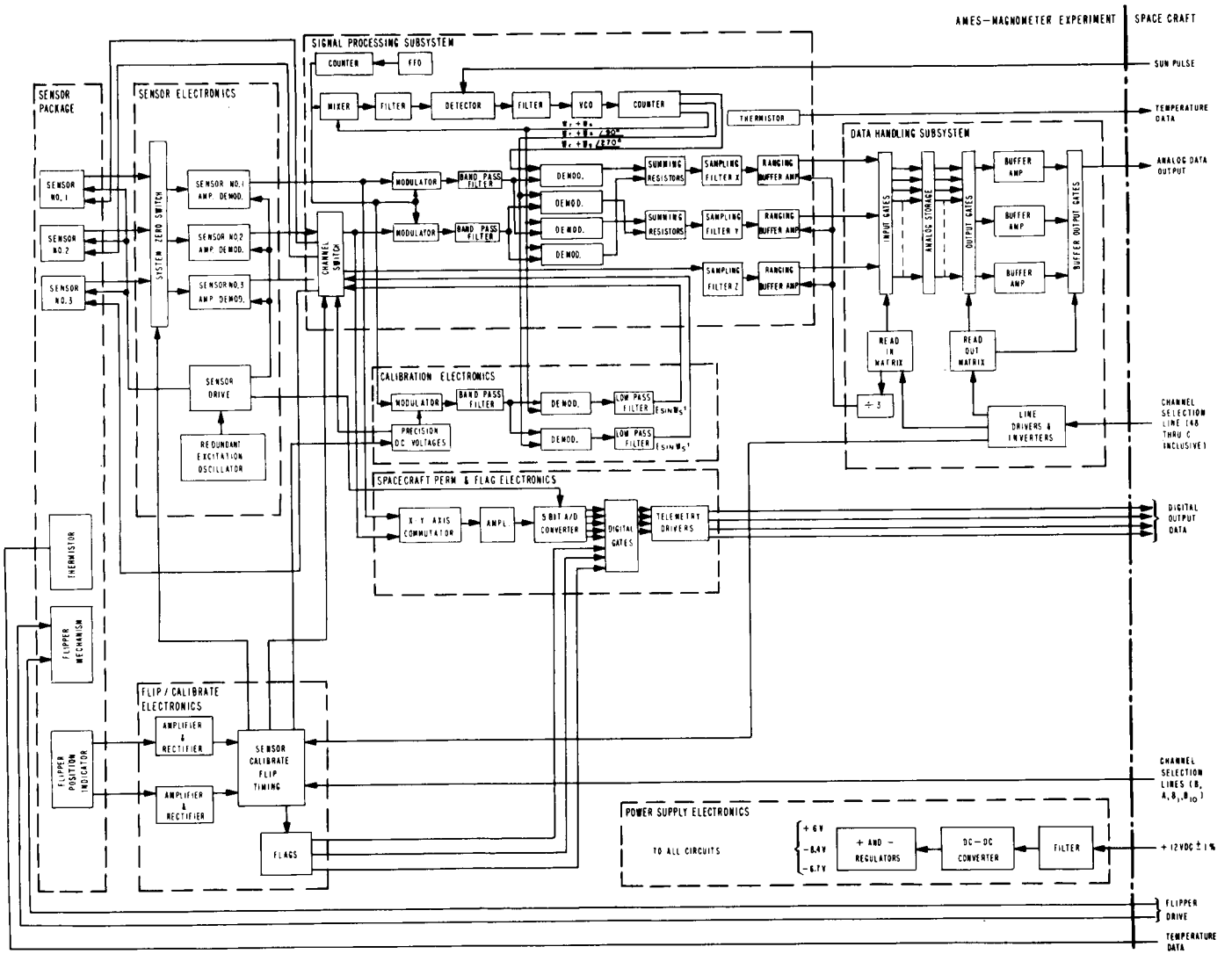

Figure 18–Ames Magnetometer Experiment Block Diagram

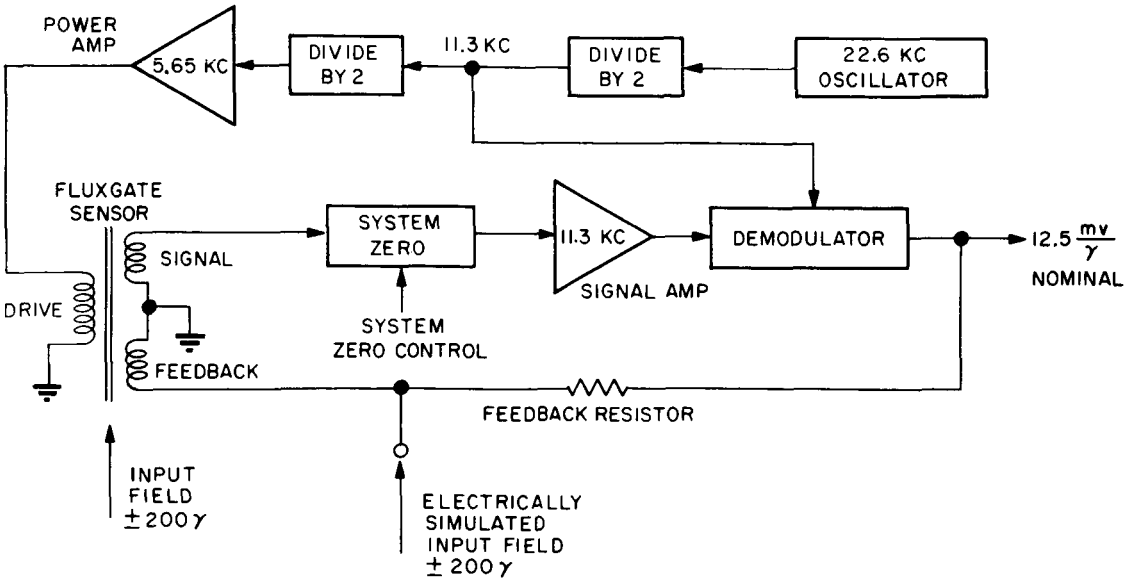

Figure 19–Ames Magnetometer Sensor Block Diagram

signal by mixing with $\omega_r + \omega_s$. Four outputs are obtained from this mixing process at different phases. These outputs are appropriately combined to cancel the unwanted sidebands. The output of the experiment represents the resultant magnetic field vector in the two spin modulated axes.

The output of the sensor located on the Z-axis (spin axis) is not spin demodulated but goes directly to the sampling filters. These filters are the same for all three axes and provide for a low pass characteristic 0 to 0.05 cps which eliminates unwanted high frequencies which could cause aliasing errors during the subsequent sampling and data storage process.

Since Y-axis signals are spin-modulated and Z-axis signals are not, signal processing electronics must be interchanged whenever the sensors are flipped. This is accomplished by an electronic four-pole, double-throw switching circuit.

The spacecraft telemetry system will accept data samples from the Ames magnetometer only at certain times. However, to obtain maximum information from the magnetometer, the data must be sampled periodically. The data handling subsystem provides the interface between the periodic sampling and readout to telemetry.

The data handling subsystem simultaneously samples the magnetic field intensity of the X, Y and Z-axes once approximately every two seconds, stores the data and amplifies and sends the information to the telemetry system once every 20.48 seconds. The timing of the system is obtained from a series of binary clock signals received from the spacecraft.

Analog data is stored by thirty capacitors which hold voltages over the storage interval. The capacitors are charged and read out (input and output

gates respectively) through series field effect transistors which are controlled by the spacecraft clock signals. The data handling buffer amplifiers provide a gain of 1.25 so that the output signal is biased at +2.5 vdc and varies between zero and +5.0 vdc.

Figure 20 shows the timing for data sampling and readout to telemetry. Data samples are stored during the channels indicated for three-axis measurement. The actual time provided for storing the signal is one-eighth of a channel, and this one-eighth channel period is placed within the channel so that the sampling rate is very nearly periodic. The sampling period is 2.04 seconds except that starting with the third period in a sequence (Channel 12, Frame 0 to Channel 3, Frame 1) every fifth period occurs at 2.08 seconds.

The stored data is read out to telemetry in Frames 0, 4, 8 and 12, and all thirty storage capacitors are read during each frame. The actual time provided for readout is one-half channel with the first half designated sub-channel A and the second sub-channel B.

An additional function of the data handling subsystem is to provide a signal for changing the gain of the ranging amplifiers. A divide-by-three counter is connected to the input stages so that the counter changes state after a data sample is taken. Counter outputs are combined to control the gain of the ranging amplifiers so that full-scale system ranges of 20, 60, and 200 gamma are provided, always in that order. The three ranging amplifiers are always on the same range within a single sequence.

The magnetometer system includes a flip and calibrate procedure which provides certain checks on the system performance during the flight of the instrument. The proper use of information supplied during the flip/calibrate cycle will indicate any changes in scale factors, offsets, spacecraft perm, etc. The following four types of events occur during flip/calibrate:

- Calibration — A magnetic field signal is simulated in the fluxgate sensors by applying an electrical calibration current to the sensor feedback winding. Field levels of +50, +16, -16, and -50 gamma are applied. Spin-modulated calibration signals are applied to the signal channels which pass through the spin demodulator. A flag indicates when calibration signals are being applied to the sensors.
- Flip — Two of the fluxgate sensors are mounted on a flipper mechanism and a flag indicates its position.
- Channel Switch — Since Y-axis signals are spin-modulated and Z-axis signals are not, signal processing electronics must be interchanged

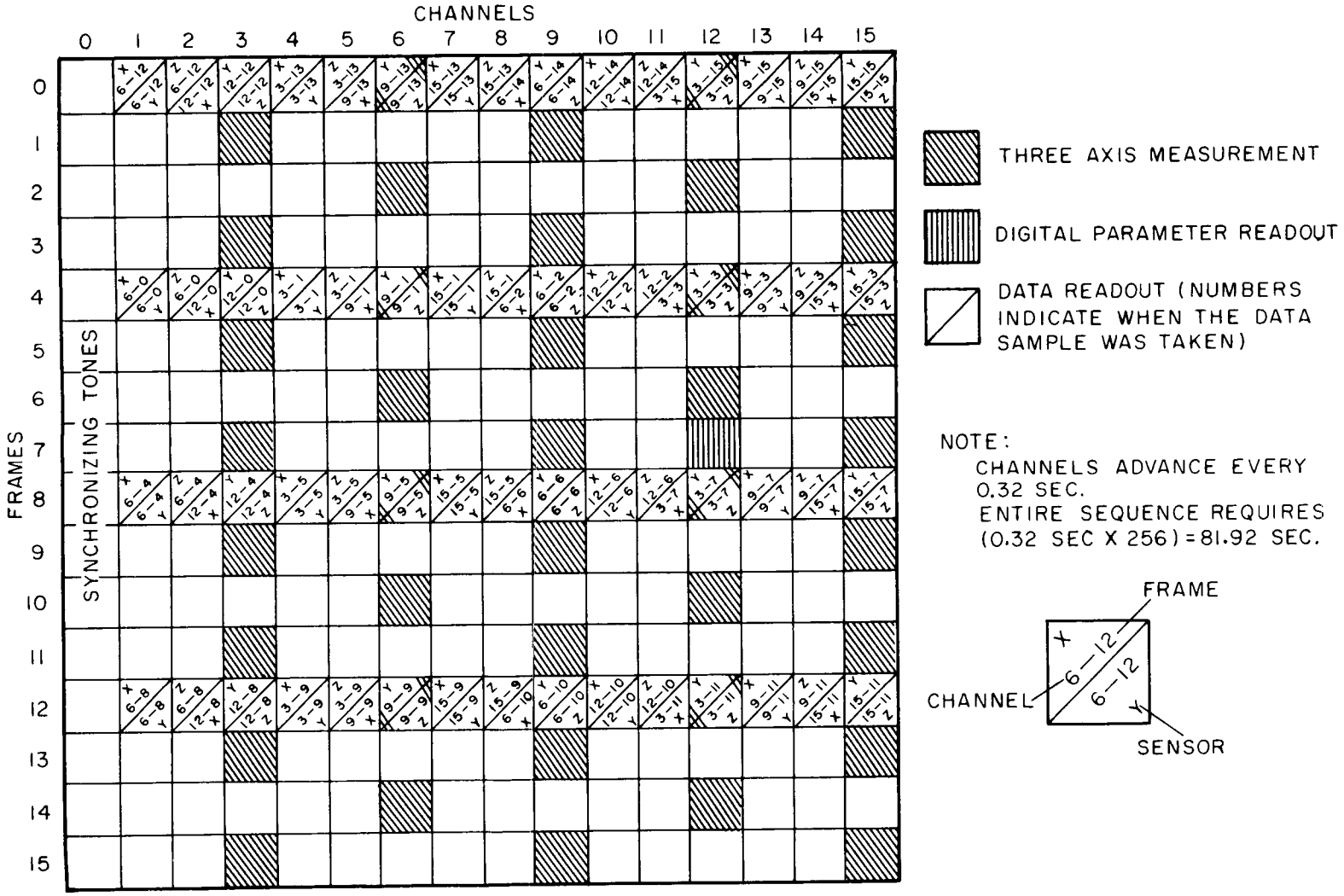

Figure 20–Ames Timing Diagram

whenever the sensors are flipped. This is accomplished by a channel switch and a flag indicates the position of the channel switch.

- System Zero — In order to estimate system zero offsets, the sensor electronics input can be shorted to ground, in all three axes simultaneously.

The flip/calibrate cycle is initiated when the spacecraft channel selection line a_{10} goes negative. This occurs every 1024 telemetry sequences or approximately every 23.3 hours. Once the cycle has been started, the order of events is:

a. Calibrate/System Zero

b. Flipper Actuation

c. Calibrate/System Zero

d. Channel Switch Actuation

e. Calibrate/System Zero

Note that three separate calibrations occur during the complete cycle. These calibrations are all the same, but the magnetometer system is in a different state regarding flipper position or channel switch position during each calibration time. Also, because the flipper and channel switch can each assume two different positions, succeeding flip/calibrate cycles will be different depending on the positions at the start of the cycle.

The detailed timing of a complete flip/calibrate cycle (even) is shown in Figure 20A.

When spacecraft channel selection line a_{10} goes negative, a calibration signal of +50 gamma is applied to the feedback windings of all three sensors, and the calibrate flag goes high (one). Also, power is applied to the flipper drive motor. The +50 gamma signal lasts for one-half sequence, and then calibration signals of +16, -16, and -50 gamma are applied in that order, each lasting for one-half sequence.

After two full sequences the calibration signals cease, the calibration flag goes off (zero) and system zero is applied to all three sensor channels. The system zero remains applied for one full sequence.

Flipper motor power is applied for eight sequences (approximately 10.9 minutes). However, flipper actuation can occur at any time less than 10.9 minutes but more than approximately three minutes. Actual flip time will vary depending on the voltage level applied to the flipper motor and the thermal conditions which exist around the flipper motor.

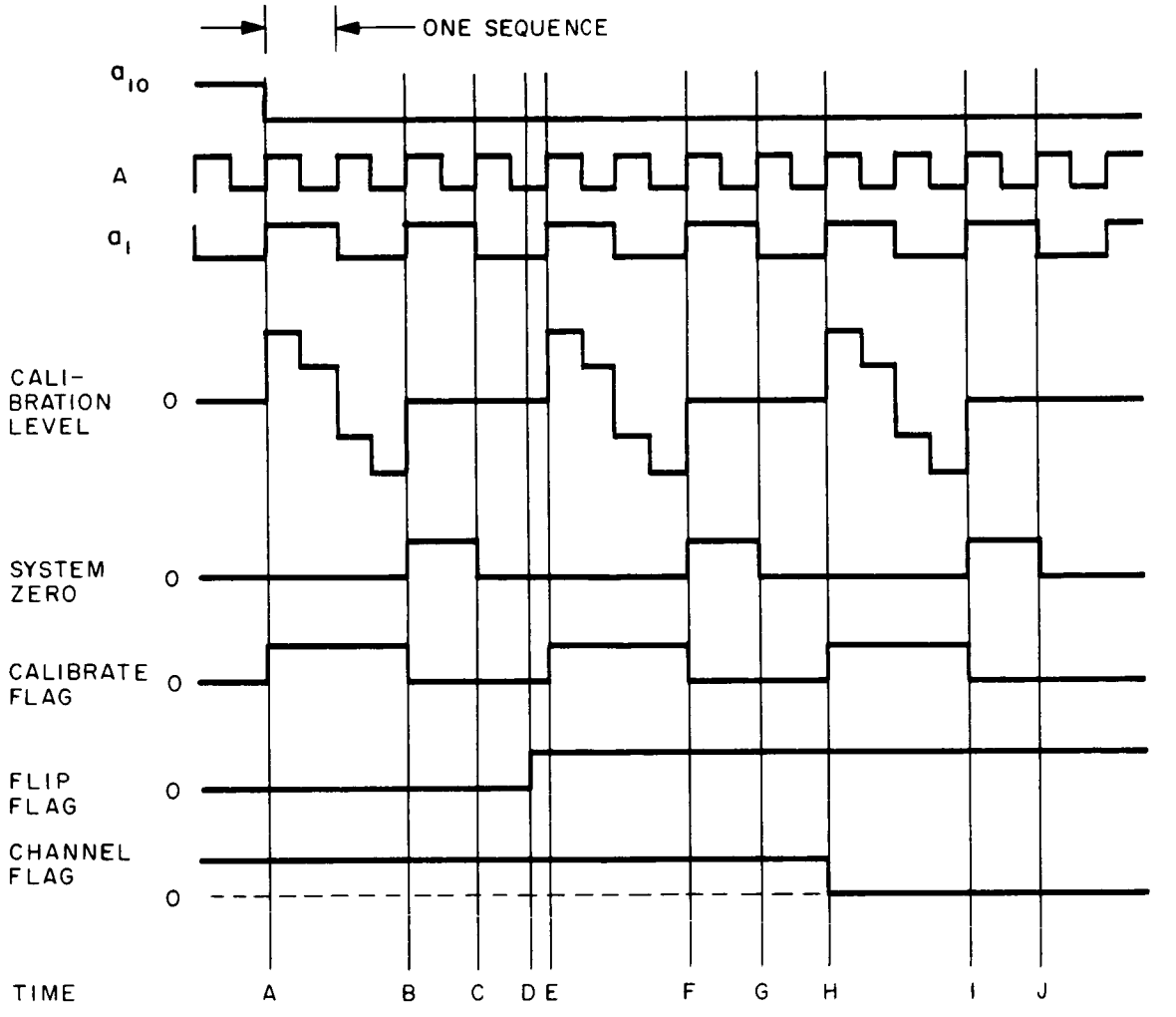

Figure 20A–Ames Flip/Calibrate Timing Diagram

The intermediate calibration period will normally start at the beginning of either the fifth, seventh or ninth sequence after a_{10} goes negative, and it will start at the first of these three opportunities after flip occurs. However, if flip occurs during the first half of the fifth or seventh sequence, calibration will start immediately. In this latter case, the first (+50 gamma) calibration level will not be applied for a time long enough for the sampling filters to respond, so it will not be an accurate calibration.

The intermediate and final calibration periods are the same as the initial calibration in that +50, +16, -16, and -50 gamma levels are applied each for one-half sequence during which the calibration flag is on. System zero is then

applied for one full sequence. The channel switch is actuated at the start of the final calibration period (time H).

Note that during the third, fourth, eighth, tenth and all subsequent sequences, there is no calibration or system zero, so the magnetometer functions normally in measuring external magnetic fields.

The spacecraft perm or bypass channel is provided to measure the d.c. component of the X and Y axis sensor electronics outputs, so that spacecraft perm and sensor offsets can be determined. This d.c. component normally is not passed by the spin demodulator and sampling filter in the signal processing subsystem. A secondary objective is to provide a limited measure of the interplanetary magnetic field as a back-up for the main data channels.

The output of this channel is provided by a 5-bit A/D converter and is sent on telemetry as part of the Ames flag word.

Telemetry — As shown in Figure 20, the data is sent on telemetry in Frames 0, 4, 8, and 12 and is an analog input to the encoding system. Each frame starts in the sequence of X axis, Y axis, Z axis, X axis, etc. However, since there are three signal ranges, the ranges are not a commutation of the binary sequence format of the encoder. Thus, each sequence will start with the X, Y, Z read-ins each from a different range but always in the sequence of 20, 60, 200, 20 etc. There are no flags indicating which range the system is operating in, so that the ground data processing requires a synchronizing program to determine this.

The sensor data is all analog, while the flag words are digital inputs to the encoder.

GSFC Magnetometer Experiment

Purpose — The experiment is designed to yield the precise vector magnetic field data from the spin-stabilized spacecraft. The information to be collected is of significance in the development of theories on the origin of the solar system, its present physical state and the dynamical behavior of the interplanetary medium. There are three subjects for investigation in this experiment:

- The interplanetary magnetic field.
- The lunar magnetic field, and
- The interaction effects associated with the streaming solar plasma and the moon.

Description — Magnetic contamination due to spacecraft fields makes it mandatory to place the magnetometer sensors as remote from the satellite as possible. To achieve this, the sensor unit is mounted in a canister at the extremity of one of two booms, which will be diametrically opposite each other with respect to the spin axis to balance the spacecraft.

The instrument is a three-orthogonal component (triaxial) fluxgate magnetometer with a flipper mechanism included to rotate the sensor parallel to the spin axis and one of the sensors perpendicular to the spin axis by an angle of 90°. This achieves the same effect as rotating by 180° to provide a means of calibrating.

The sensors have a sensitivity of ±1/4 gamma each with a dynamic range of ±64 gamma. This leads to a quantization error, with the 8-bit A/D conversion for telemetry, equal to the sensitivity.

The electronics, consisting of the fluxgate sensor drive, signal amplifier, and demodulator as well as the A/D converter, are located within the main spacecraft structure.

For purposes of RF shielding, the cabling in the boom to the sensor and the sensor assembly are enclosed within a continuous metal shield which forms part of the RF skin of the spacecraft.

Theory of Operation — The instrument measures the relative magnetic field intensity along three mutually orthogonal axes essentially simultaneously. The three axial fluxgate sensors are assembled together as a single physical unit. Each sensor is cyclically saturated at approximately 10 Kc, and the second harmonic content is generated by the presence of a magnetic field component along the axis of the element. In other words, the sensor output is a function of its angular position relative to the magnetic field flux lines. The voltage output from the system is then calibrated to yield the vector magnetic field component. A block diagram of the system is shown in Figure 21. Figure 22 shows the sensor drive and demodulator circuitry.

The frequency response of the sensor is compatible with the spin rate of the spacecraft, since the sensor solenoids must respond to field changes produced by the spin of the spacecraft. Hence the band-pass of the electronics is chosen so that only 0 to 5 cycles per second are passed without attenuation.

The three axes are sampled, digitized and buffer stored in less than 10 milliseconds (which corresponds to about 1° of spacecraft rotation for a spin period of about 3 seconds). These stored values (24 bits for all three axes) are

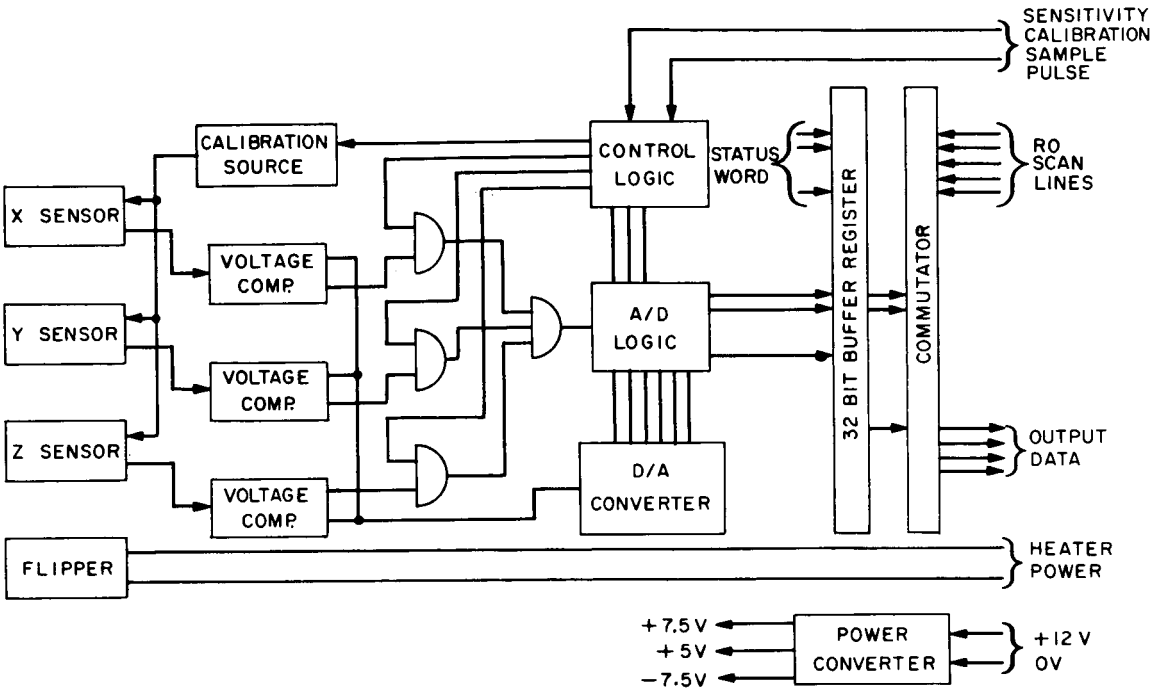

Figure 21–GSFC Magnetometer Experiment Block Diagram

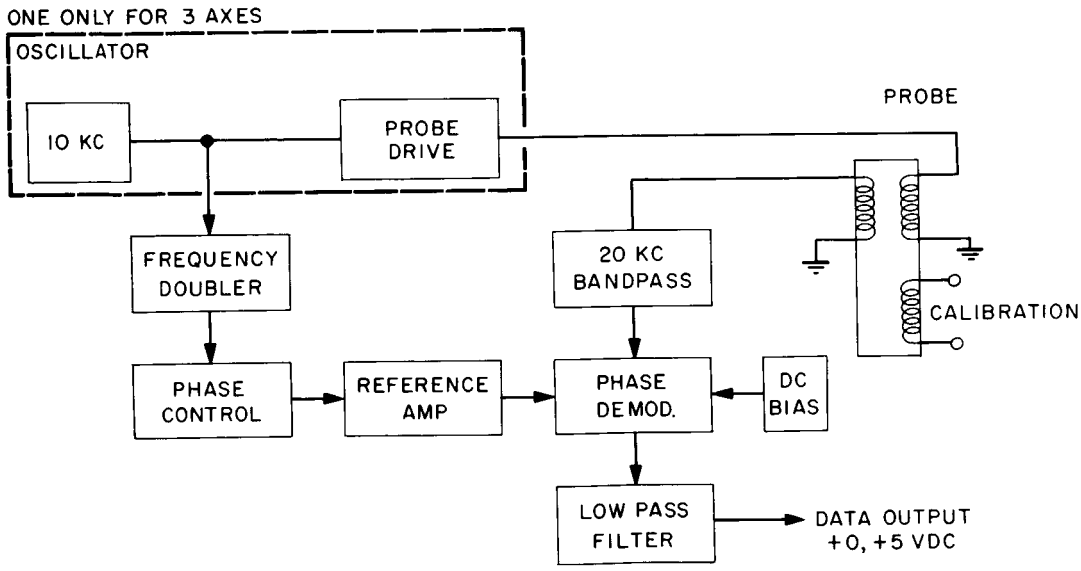

Figure 22–GSFC Triaxial Fluxgate

then read out by the spacecraft telemetry data system four bits at a time twice every other frame, whereas the sampling of the field is done once every frame (a rate of once every 5.28 seconds). For obvious reasons of format simplification, the sampling was chosen to be synchronous with the telemetry rate rather than with the spin rate of the spacecraft.

Calibration of the system takes two forms, (1) a check of the zero point offsets due to sensor drift, and, (2) the sensitivity of each axis due to sensor changes with life.

The zero drift is determined in-flight by effectively reversing its directional sense by 180° while the ambient field is constant. The spin stabilization of the spacecraft is used to advantage for this check by mounting two of the sensors perpendicular to the spin axis as well as perpendicular to each other. Thus the basic rotation of the spacecraft reorients the sensors by 180° (when telemetry samples the field at times which are equivalent to 180° separation, which is possible since the telemetry is asynchronous with the spin rate) and thereby calibrates the zeros for two of the three axes. To check the zero of the sensor parallel to the spin axis, a flipper mechanism is provided which rotates the orthogonal sensor assembly 90° about an axis through one of the perpendicular sensors such that the other two sensor positions are interchanged relative to the spin axis. The zero of the spin axis sensor, since it is now perpendicular to the spin axis, is checked in the same manner as the others were.

The sensitivity of the sensors is checked in flight by the addition of a known field parallel to the sensor by a special solenoidal coil mounted as an integral part of the sensor and supplied with a known current from the experiment electronics.

The signals to initiate the flip and the calibrate functions are obtained from the encoder. The flip signal is a 10.4 minute "on" signal processed thru the flipper control electronics card. The "flip" is repeated once a day (23.3 hrs.). The calibrate signal duration is only one telemetry sequence and is repeated twice a day but is removed in time from the "flip" signal by 5.8 hours.

The heater power for the flipper mechanism is interlocked such that heater power is only applied after the 4th stage retro-motor is separated from the spacecraft.

The sync pulses supplied from the encoder are as follows:

Channel 1 and 9, of every odd frame

Channel 2 and 10, of every odd frame

Channel 3 and 11, of every odd frame

Channel 4 of every frame

Channel 12, Frame 15

$\overline{S}$

$\overline{A}$

A_9

Telemetry — The experiment provides for a digital output of 32 bits, 24 bits for the three sensor outputs and 8 bits for housekeeping data. This is formatted as shown in Figure 23.

The experiment receives read out pulses for the magnetic field data at the odd frames on Channels 1-3 and 9-11. The data is sampled every frame at the start of Channel 4. The data is read out thru a matrix thereby eliminating shifting data from a buffer storage register and the problems associated with shift-pulse generation and noise on the shift lines.

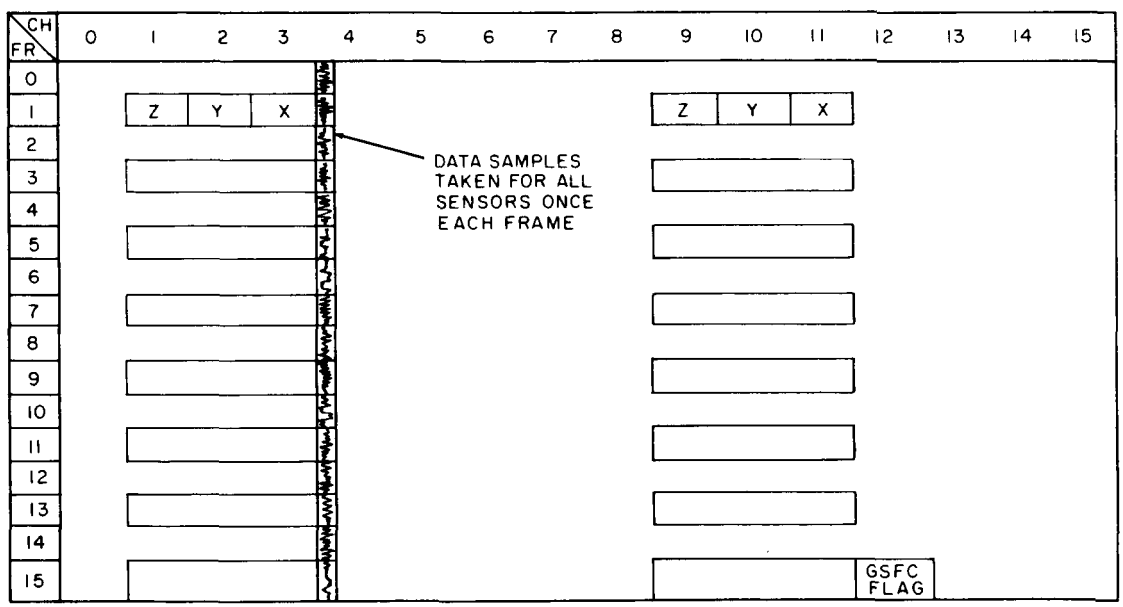

Figure 23–GSFC Telemetry Format

Solar Cell Damage Experiment

Purpose — The solar-cell damage experiment is a GSFC-engineering experiment which will provide information on integral radiation damage to solar

cells and solar-cell cover glass of varying thicknesses and composition, as well as on the protection afforded solar cells by each type of cover glass.

Description — To accomplish the solar cell damage experiment, one facet of the spacecraft carries a panel of four groups of sixteen 1-cm × 2-cm n-on-p silicon solar cells with a nominal base resistivity of 10 ohms/cm. Mounting the panel on a facet permits cell exposure that will provide meaningful data on most spin-axis/sun line orientations. One group of cells will be unshielded; the second will have an integral 25-micron cover glass; the third, a 6-mil fused silica cover glass; and the fourth, a 6-mil micro-sheet cover.

The sixteen solar cells composing each group are series-connected and independently loaded with a precision resistor to produce a 4.0 to 4.5-volt output under space conditions with normal incident illumination. These solar cells are typical production cells of a type which have undergone extensive laboratory testing to determine electron-irradiation and proton-irradiation effects. Therefore, output variations among solar-cell groups can be related to solar-cell or solar-cell-cover-glass damage. The solar cell temperature is monitored with a thermistor which is imbedded within the solar cell panel just under the cells.

To assure experiment accuracy, the cell groups were calibrated for illumination, angle of incidence, and temperature effect, both after environmental testing and before flight. The weight of the panel is approximately 100 grams.

Passive Experiments

Two passive experiments, using telemetry and range and range rate signal variations, were planned for the AIMP satellites. But both of these require a lunar orbiting spacecraft and were, therefore, not possible with IMP-D.

A. M. Peterson (Stanford University) will study the spacecraft telemetry signal to determine the effects of the lunar ionosphere on radio-wave propagation.

W. M. Kaula (University of California, Los Angeles) will analyze variations in the range and range-rate tracking data to obtain selenodetic information.

SPACECRAFT AND SUBSYSTEMS

AIMP-D Structure

The satellite structure as presently constituted is the product of planning and experimentation some of which began soon after the orbiting of IMP-A into a high elliptical orbit (197,000 Km apogee and 192 Km perigee) in November, 1963.

The basic mission objectives translated into spacecraft hardware resulted in some interesting structural design and material selection problems. Where the previous structures had only to survive the launch environment and appendage erection loads and then proceed to act as platforms for the experiments, this structure also had to withstand the launch environment and appendage erection loads and then withstand retromotor deceleration and vibration with appendages extended.

The materials employed in the structure to maintain the structural weight within the weight limit and to meet the magnetic cleanliness of the spacecraft included aluminum, magnesium, nylon, delrin, fiberglass, and aluminum honeycomb, all of which afford comparable low weight to strength ratios.

The following design features were successfully incorporated into the structural design:

- Thermal Balance:

  Compatible passive coatings

  Optimization of internal conduction and radiation

  Optimum placement of high heat dissipating components

- Electrical Restraints:

  Proximity of associated electronics

  R-F shielding providing antenna ground plane and internal circuit shields and complete spacecraft ground plane.

- Stability requirements:

  Dynamic and static balance

  Inertia Ratios

- Modular Concept
- Accessibility for rework and/or replacement
- Non-magnetic hardware (complete structure was less than 1/2 gamma at 36 inches)
- Low weight (high strength to weight ratio)

A mathematical analysis of all structural components was made using the following design parameters:

- Launch vehicle acceleration and vibration levels
- 3rd stage spin-up (angular acceleration) 0 rpm to 165 rpm in 0.6 sec.
- Sustained 3rd stage/spacecraft rotation at 188 rpm (150 × 1.25) 3rd stage thrust
- Yo-Yo despin deceleration 150 rpm to 78 rpm in 0.5 sec.
- Solar cell paddle erection at 78 rpm and despin to 41 rpm
- Magnetometer sensor boom erection at 41 rpm and despin to 27.5 rpm
- Retromotor thrust and vibration with appendages extended.

The actual weight of the AIMP-D structure did not increase over that for IMP-A. IMP-A's structural weight was 22 percent of the total weight and AIMP-D was only 15 percent of the total weight at launch.

In the course of qualification testing, the structure survived all the tests with minor changes and modifications.

The AIMP structure, shown in isometric in Figure 24 and in side and top views in Figures 25 and 26, is basically a two-piece magnesium axial-thrust cylinder with a third-stage attach flange on one end and a fourth-stage retromotor attach flange on the other end. This cylinder provides attachment flanges for the eight aluminum radial struts which attach at the cylinder and at brackets on the periphery of the octagonal aluminum-honeycomb platform. The brackets between the eight struts and the platform also serve as hinge joints for the four solar-cell paddles and the two fluxgate magnetometer experiments. These magnetometers are mounted on fiberglass tubes which are folded during launch and erected after injection into orbit.

The periphery of the platform and a flange near the top of the center tube support an aluminum-honeycomb top cover which provides RF shielding and a surface for the passive thermal control coatings.

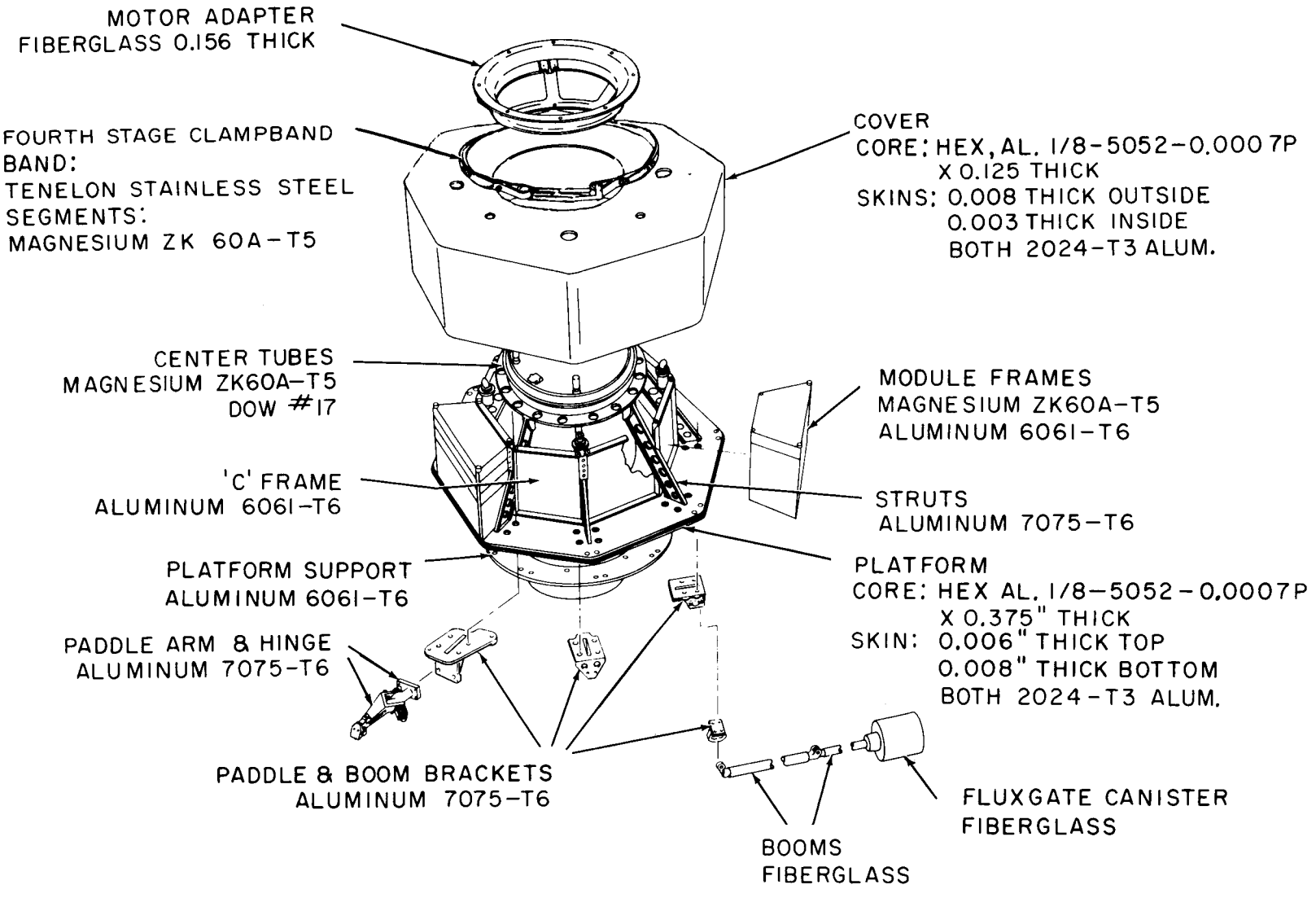

Figure 24–AIMP Structure (isometric)

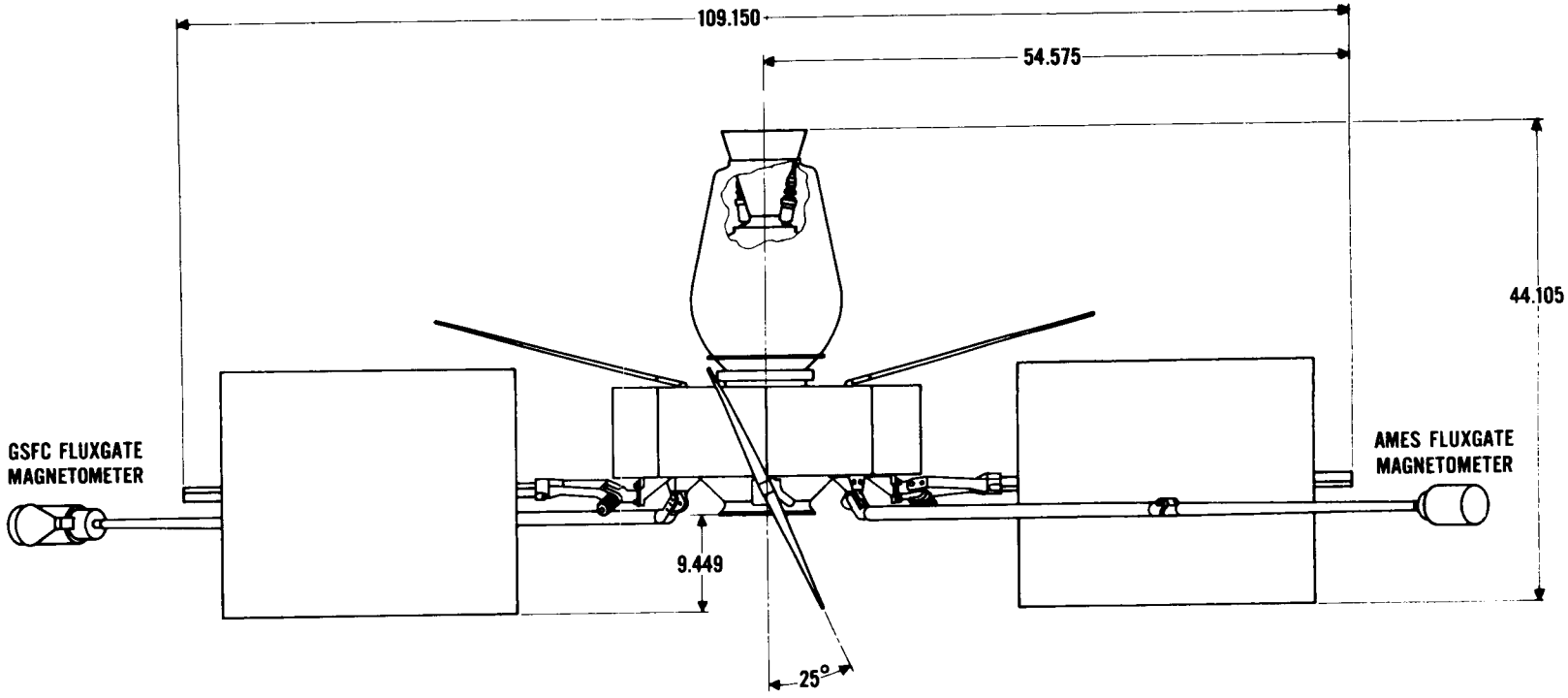

Figure 25–AIMP Spacecraft - Side View

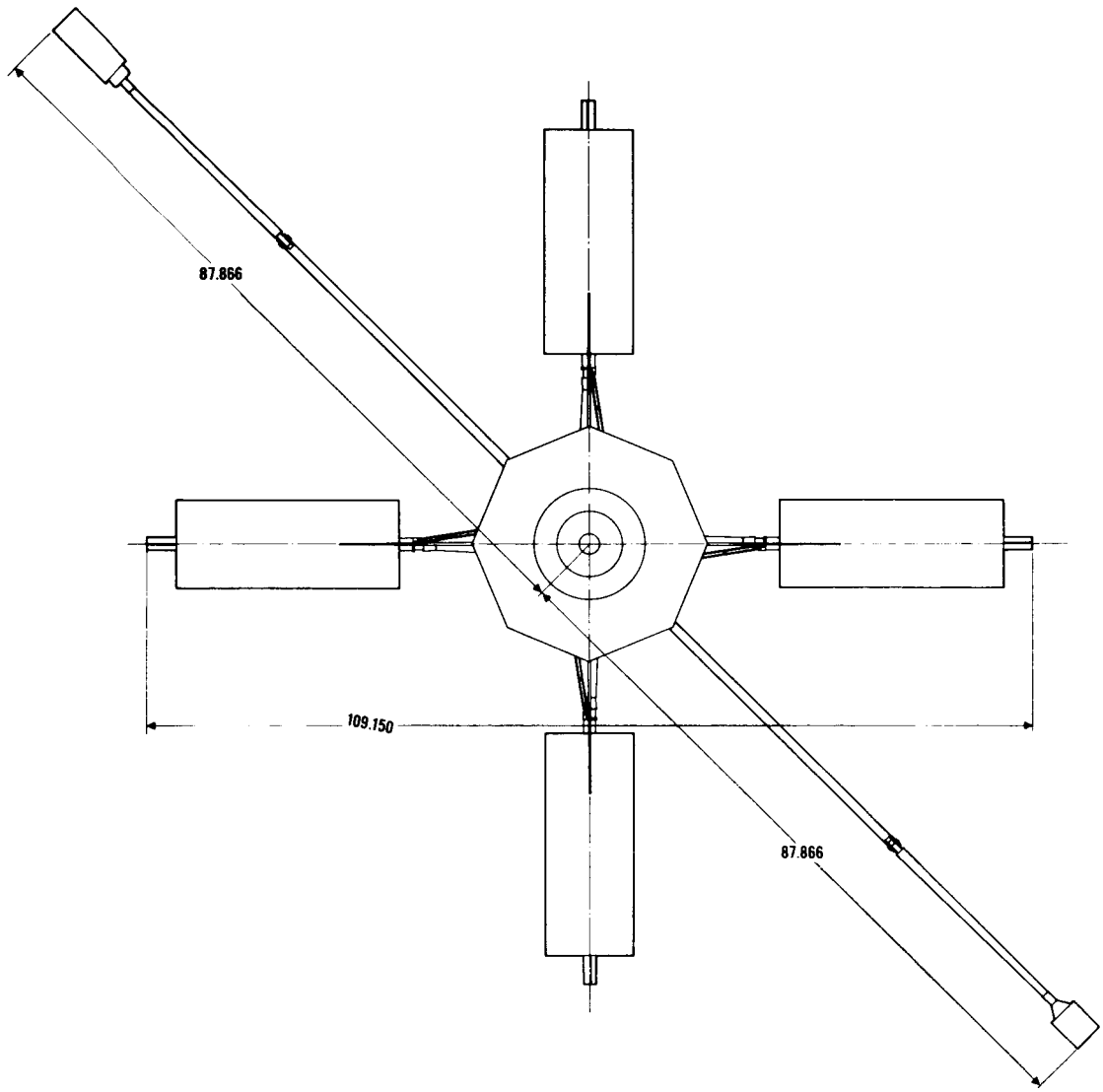

Figure 26–AIMP Structure - Top View

All experiments and instruments are packaged in standardized module frames and are mounted on the periphery of the platform for easy accessibility, rework, or replacement.

The retromotor is bolted to an epoxy-fiberglass adapter which serves as a thermal insulator between the retromotor and spacecraft and provides low vibrational transmissibility. The retromotor and adapter are separated by employing a marmon clamp with bolt guillotines at the center tube interface after fourth-stage burnout to increase the magnetic cleanliness and the moment-of-inertia stability ratio.

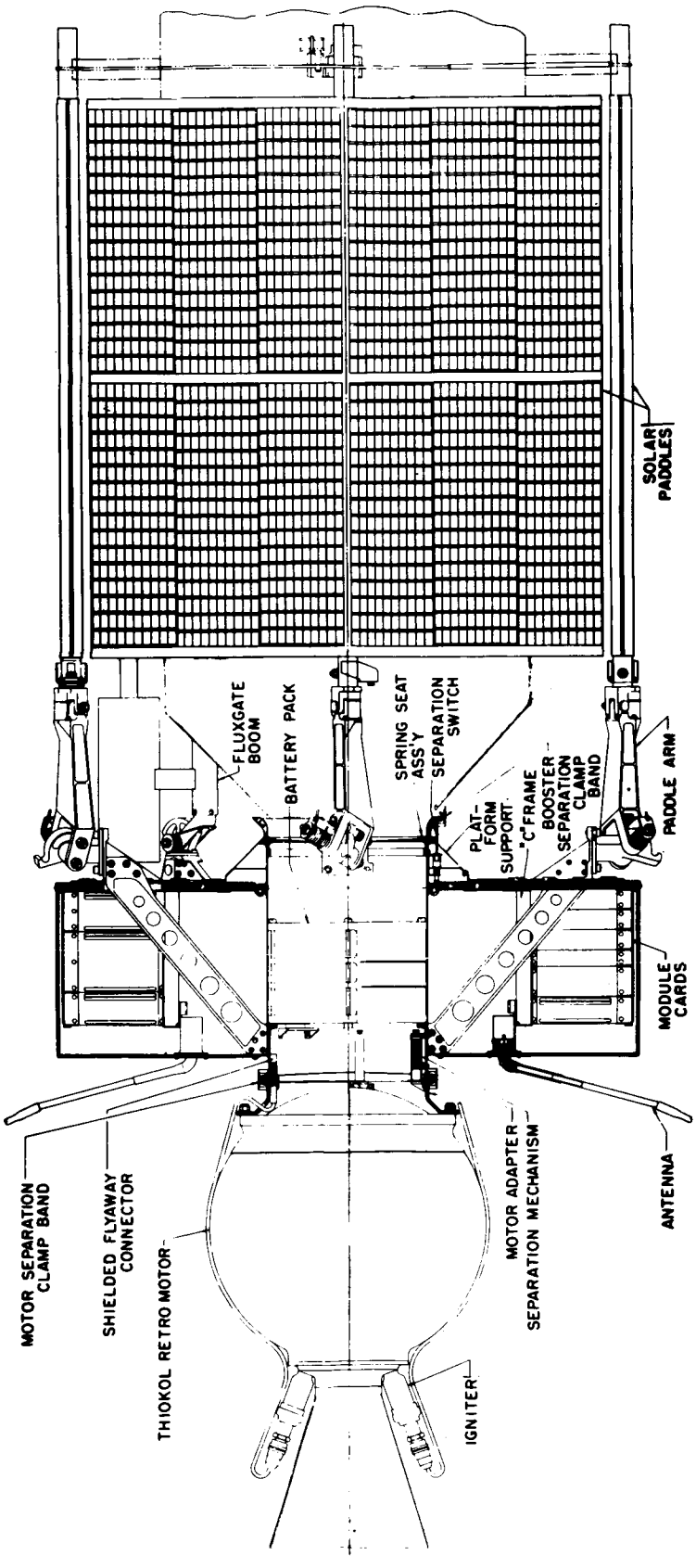

Figure 27–Launch Configuration

Figure 27 shows the spacecraft in launch configuration.

Stabilization

The launch-vehicle guidance system provided stabilization through first- and second-stage burn and the coast-phase pitch program. At the end of the coast-phase pitch program, spin rockets located on a spin-table connection between the second and third-stage spin the spacecraft/third-stage package to a nominal 150 rpm. The expended second-stage motor was jettisoned after spin-up. After third-stage burnout, a yo-yo despin mechanism reduced the spin rate to approximately 100 rpm. Erection of the solar paddles and the fluxgate booms further reduced the spin rate to 27 rpm ±2 rpm. After spacecraft/third-stage separation, the spacecraft-retromotor combination had roll/pitch moment-of inertia ratio compatible with the spin rate for adequate spin-stabilization for the transfer trajectory coast period.

At the end of the transfer period, the retromotor was fired by direct command. After retromotor burnout and separation, the spacecraft had a favorable moment-of-inertia ratio.

Retromotor

Motor Case — The AIMP motor cases were forged in two hemispheres of 6 Al-4V titanium with the attachment ring being an integral part of one hemisphere. After machining, the two hemispheres were TIG-welded and heat-treated. The external surfaces of the cases were then polished to a mirror-finish to reduce thermal radiation from the motor. The aft-end hemisphere of the motor case is internally insulated with Genguard V44, a Buna-N composition of the General Tire and Rubber Company. The insulator contains an integral separation boot to relieve thermally-induced strains in the propellant grain. Varying in thickness from 0.100 to 0.140 inches, the insulator is pre-formed on a mandrel and then pressure-molded into the case. Figure 28 shows the retromotor in cutaway.

Propellant — The propellant for the AIMP retromotor is an ammonium perchlorate polyurethane composite with an aluminum additive. The vacuum specific impulse of the propellant is 275 seconds. The propellant grain design for the AIMP motor is a head-end, eight-point star. The igniters are located with their centerlines directed into the propellant valleys. Automatic ignition conditions for the propellant are 400°F for one hour, or 300° for eight hours.

The various tooling is attached to the case and the liner is brushed over the interior surfaces of the case and then cured for 12 hours at 170°F. The weight of the liner is 0.17 pounds. The liner improves adhesion between the case and

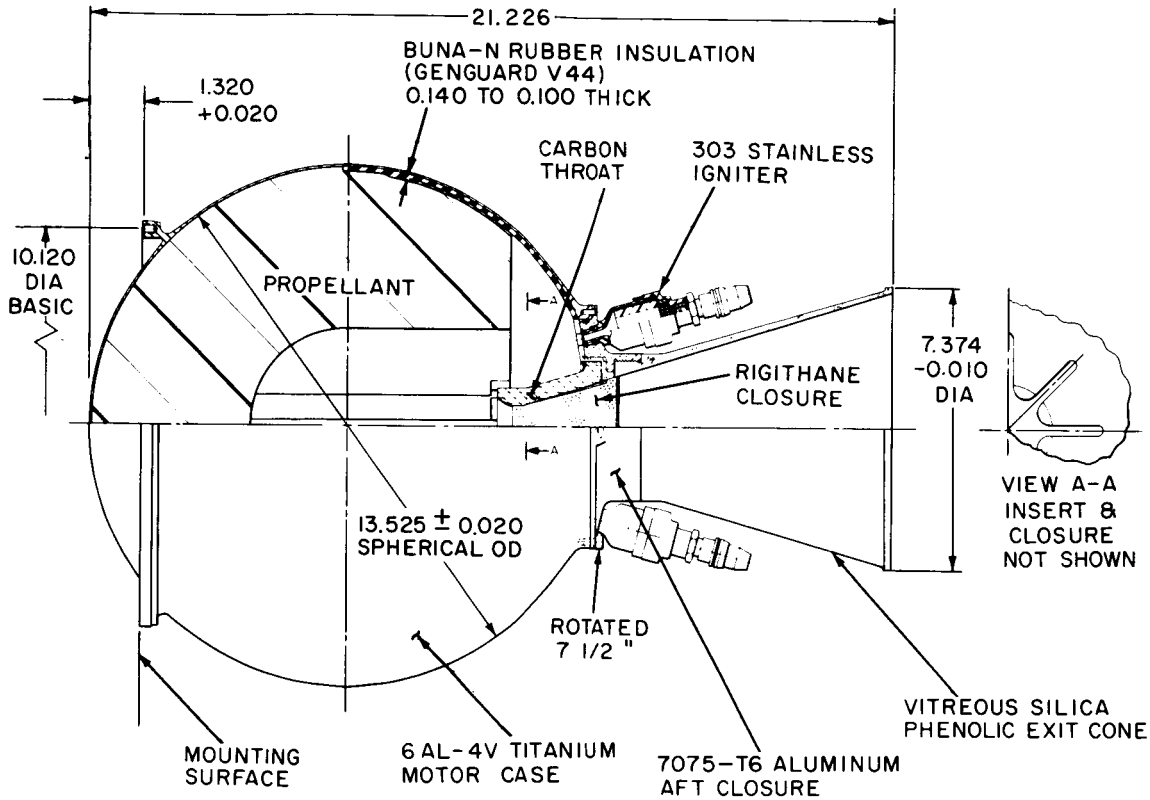

Figure 28–TE-M-458 Retromotor

TABLE 2
Physical and Mechanical Properties of the
Inert and Live Propellants*

Parameter	Inert	Live
Density, lb/in.^{3}	0.0616	0.0614
Specific Heat, Btu/lb°F	0.266**	0.30**
Thermal Conductivity, Btu/hr-ft-°F	0.3	0.242**
Modulus, psi	600	545
Stress, psi	100	94
Strain, in./in.	0.29	0.29

*Temperature sensitive characteristics are specified for 80° F.

**These values as actually measured by Naval Propellant Plant, Indian Head, Maryland.

the propellant. Table 2 contains propellant data, and Table 3 summarizes motor performance.

Nozzle — The nozzle consists of an aft closure, throat, and exit cone. The AIMP retromotor uses as a fixed-aft closure an aluminum-machined part with an integral lip to retain the graphite throat, two tapped holes for mounting the igniters, 24 holes through which the closure is bolted to the motor case, and a larger internal thread for attaching the exit cone. The internal surfaces are

TABLE 3
Motor Performance Data

Parameter	Motor Conditioned Firing Temperature		
	0°F	+60°F	+120°F
Pressure and Time (calculated nominal)			
Maximum Chamber Pressure (psia)	514	550	585
Average Chamber Pressure (psia)	468	500	535
Burn Time (sec)	23.2	21.8	20.4
Action Time (sec)	24.0	22.4	21.0
Ignition Delay Time (sec)	0.070	0.060	0.055
Ignition Rise Time (sec)	0.030	0.020	0.015
Ignition Time (sec)	0.100	0.080	0.070
Thrust and Impulse (calculated nominal)			
Maximum Thrust (lbf)	855	916	976
Burn Time, Average Thrust (lbf)	795	850	910
Total Impulse (lbf-sec)	18,000	18,800	18,800
Propellant Specific Impulse (lbf-sec/lbm)	275	275	275

thermally insulated by covering with a vitreous silicaphenolic insulation varying in thickness from 0.120 to 0.160 inches. The high density graphite throat is bonded to the aft closure with Epon VIII adhesive and the throat diameter is then machined relative to the aft closure diameter. The pressure seal between the motor case and aft closure is obtained by the use of an O-ring. The exit cone is a high pressure molding of vitreous silicaphenolic averaging 0.18 inches in thickness. The exit cones are covered inside and outside with vapor deposited aluminum before assembly into the aft closure. The exit cone is threaded into the aft closure with Epon 913 adhesive as a locking compound.

The nozzle assembly (consisting of the exit cone, aft closure, and a throat) is a 17-degree cone with an area expansion ratio of 41.7:1.

Igniter Subsystem — The motor is ignited by using redundant TE-P-462 igniter assemblies located external to the motor case, 180 degrees apart, and screwed into the aft closure with an O-ring seal. The igniter consists of a case and head cap made from 302 stainless steel, a tube of propellant, a Holex number

TABLE 4
TE-P-462 Igniter Data

Characteristic	Requirement
Quantity Per Motor	Two igniters 180 degrees apart, single bridgewire each
Squib Specification	Thiokol Spec. SE - 225
Bridgewire Resistance	$1.0^{+0.2}_{-0.0}$ ohms
Recommended All Fire Current	4 ±0.5 amps
No Fire Current	Meets ETR 1 amp, or 1 watt for 5 minutes, no fire requirement
Insulation Resistance	Greater than 100 megohms at 500 vdc (pin to pin, or pin to case)
Resistance After Firing	1000 ohms minimum (pin to pin, or pin to case)
Temperature Limits	-60°F to +190°F

4497 squib (1-ampere, 1-watt no-fire, single bridgewire squib), a boron-pellet booster charge, and a silica phenolic nozzle throat section. Each assembly weights 0.34 pounds, burns for 0.2 seconds, and weighs 0.30 pounds after firing. Should one igniter fail to ignite, it would "cook-off" (ignite) during motor burning. Table 4 summarizes igniter characteristics.

Retromotor Adapter — Although the magnetic properties of the titanium retromotor case were such that separation was not mandatory, the original AIMP design, using retromotor separation, had advantages which made its retention advisable. The motor adapter is a short cylindrical section with the retromotor bolted to one end and the other end secured to the spacecraft via a marmon clamp. Separation is accomplished by cutting the two bolts holding the marmon clamp together. All electrical leads for motor ignition, marmon clamp separation, and motor thermistors pass through fly-away connectors located inside the cylinder at the separation plane. Four compression springs, located 90-degrees apart at the separation plane, separate the retromotor and adapter from the spacecraft with a relative velocity of 4.5 feet per second.

The high motor case temperatures experienced during thermal soak-back following motor ignition dictated that the motor adapter have a high-thermal resistance in order to protect the spacecraft battery (located just below the adapter) from excessive temperatures. In addition, to minimize the energy amplification into the motor from vibrational inputs from the launch vehicle, the adapter had to be fairly rigid. It was decided that fiberglass offered the best solution to these two requirements. The following constituents were used in the motor adapter:

- Fabric — Style 181 glass cloth pre-impregnated with Epon 828, approximately 0.009 inches thick.
- Resin — Epon 828, 100 parts by weight.
- Catalyst — Nadic Methyl Anhydride, 90 parts by weight per 100 parts of resin.
- Hardener — BDMA (Benzyldimethylamine), 1 part by weight per 100 parts of resin.

The cloth and resin were laid up on a mandrel, cured, and post-cured at 400°F for one hour, and then critical-dimensions machined. For proper thermal balance and grounding continuity, the surfaces of the adapter were coated with vapor-deposited aluminum. The average thickness of the adapter is 0.156 inches.

Thermal Control — Thermal control is achieved through a passive system of surface coatings, insulation, and structural conduction-path design which will

maintain temperature gradients and excursions within acceptable limits at the selected solar aspect angles and orbital conditions.

The final thermal control design consists of two blankets, each one a multi-layered construction of alternating sheets of aluminized Kapton (H-Film) and tissue glass. The main blanket is conical and open at both ends. The blanket is slipped over the retromotor and fastened to the mounting flange of the retromotor with 16 number 6-32 stainless steel screws into threaded holes provided on the vertical face of the retromotor mounting flange. All pleats and openings at the bottom edge are taped shut using aluminized Kapton tape and the top of the blanket is secured to the exit cone with Kapton tape. Venting slits are left in the blanket in the area of the exit cone.

Telemetry Data System

The telemetry data system is composed of the encoder and the performance parameter systems. The two fundamental functions of the encoder are (1) to furnish the experiments and instruments sync pulses to determine sample times and/or reference frequencies, and (2) to convert the received input voltages to a frequency which is used to modulate the RF carrier. The performance parameter system's primary purpose is to convert the input voltages or currents from various performance and temperature sensors into a voltage input to the encoder. The other functions performed by each system are covered in the detailed descriptions given below.

Encoder — The encoder is housed in an aluminum breakaway AIMP-type frame which is 3.375 inches high. A shield of .031-inch aluminum is attached top and bottom to the frame. One twenty-five pin, one fifty pin, and two thirty-seven pin male Cannon connectors are arranged vertically on the rear of the housing. The encoder weighs 2034 grams.

The encoder consists of a number of cordwood construction welded circuit modules, each of which is a subsystem. These modules are individually tested and potted separately before being mounted on a circuit board. After total system checkout all voids within the housing are filled with a foam potting. The five major encoder modules which are: (1) UI encoder module, (2) California encoder module (3) odd frame processor, (4) encoder module, and (5) the analog processor. Table 5 gives the content of each module.

Following the basic philosophy used in the construction of small spacecraft to eliminate as many interface problems as possible and to provide as much support as practicable to the experiment, the functions of the encoder have been extended to include many diverse areas (see Figure 29). The functions provided by the AIMP encoder are:

TABLE 5
Composition of AIMP Encoder Modules

Encoder Module	Analog Processor Module	Odd Frame Processor
Binary countdown	Analog oscillator	Sequence counter
Frequency synthesizer	Commutation Analog PP's	Optical aspect parity check
Video conditioner	Commutation analog experiment	Sync pulses for:
Sync pulses for:	inputs, Ames and MIT	GSFC Magnetometer
Optical Aspect	In-flight oscillator	Thermal Ion
MIT	calibration	Performance parameter
Ames		8 bit accumulator

California Module	UI Module
California Accumulators	UI Accumulators
Two "S-T" 16 bit acc.	Four "S" 20 bit acc.
One "S" 16 bit acc.	Sync pulses for
One "S" 12 bit acc.	UI
Sync pulses for	
California	

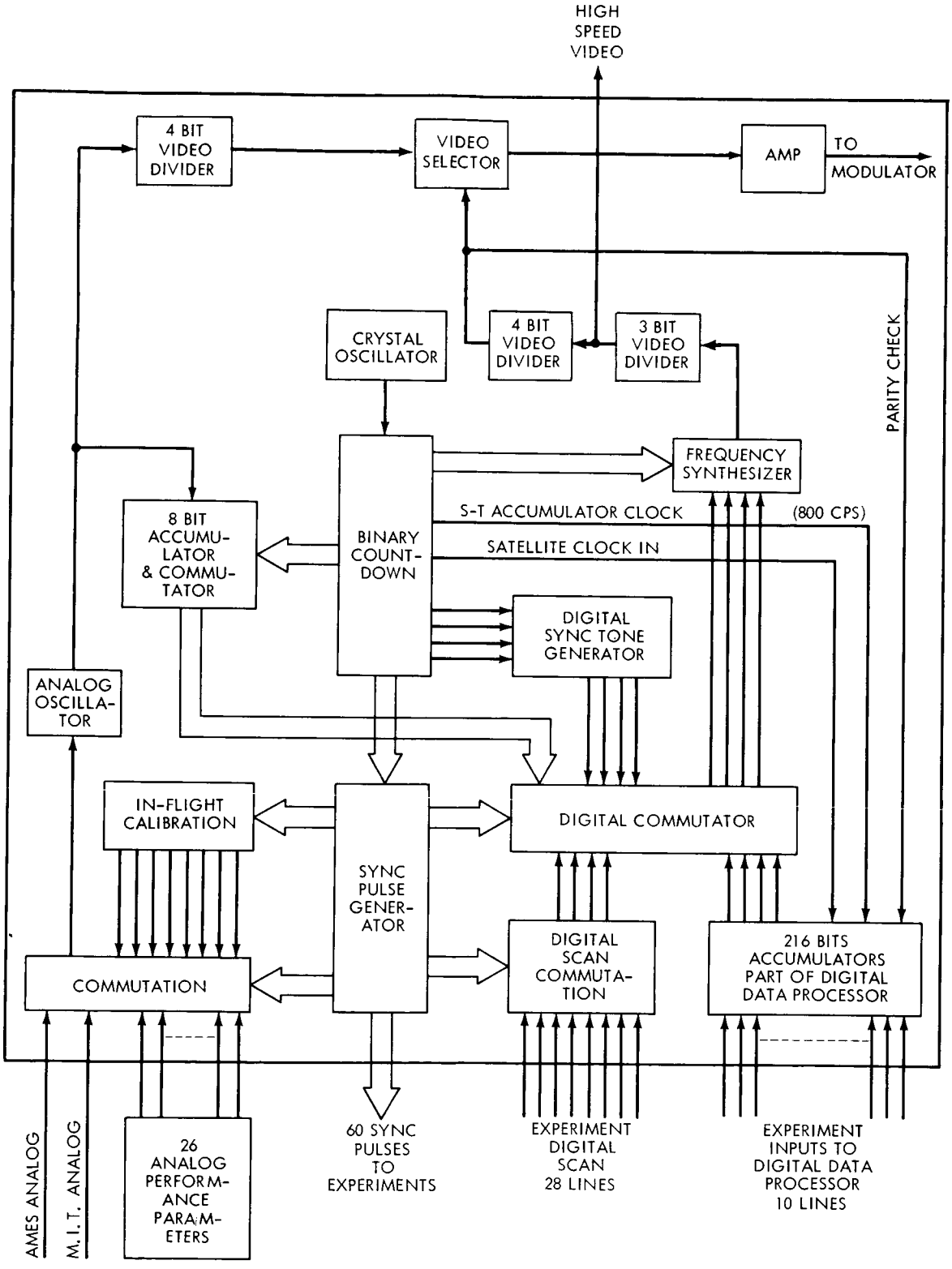

Figure 29–Encoder Operation

- Encodes time-multiplexed data from various instruments and experiments into a form suitable for the transmitter modulator.
- Provides sync signals for data sampling and/or reference frequencies.
- Provides accumulators for storage of University of Iowa and University of California data.
- Provides A/D conversion and commutation of performance parameter data.
- Provides parity check for optical aspect data.
- Provides a spacecraft sequence counter which is needed to identify each sequence of data.
- Provides voltage-to-frequency conversion for Ames magnetometers and MIT experiment.

Encoder Operation — The basic operations of the encoder system are interdependent as can be seen from Figure 29. The selection of the basic frequency for the crystal oscillator was dictated by the need to provide compatibility with ground support equipment, and the proved reliability of the encoder oscillator and hardware from previous flights.

The telemetry format (see Figure 30) consists of 32 channels and 16 frames which make up one sequence of data. Each channel consists of a 160 ms burst of one frequency which has values of from 312.5 cps to 937.5 cps for analog data transmission, 400 cps (equivalent to a binary 1111) to 775 cps (equivalent to a binary 0000) in steps of 25 cps for digital data transmission, and a 275-cps unique sync pulse. The basic time reference for the telemetry is one sequence (81.92 seconds) in which 1320 digital data bits, approximately 975 analog data bits, and 128 synchronization bits are transmitted giving an average bit rate of 29.6 bits per second.

In general, the inputs and outputs of the encoder are isolated via 100K-ohm resistors, so that the encoder system is isolated from spurious signals or experiment failures. In addition, each experiment and instrument has its own output for sync pulses so that failure of an experiment or instrument does not effect the sync pulses to other units.

Encoder read-in from the various experiments and instruments must be frozen after the first 100 microseconds for digital data and 10 ms for analog data so that only one frequency is transmitted during a telemetry data burst. All accumulators are frozen within the encoder, from the time readout starts until the readout is finished, except for two 24-bit University of Iowa accumulators which are frozen within the experiment.

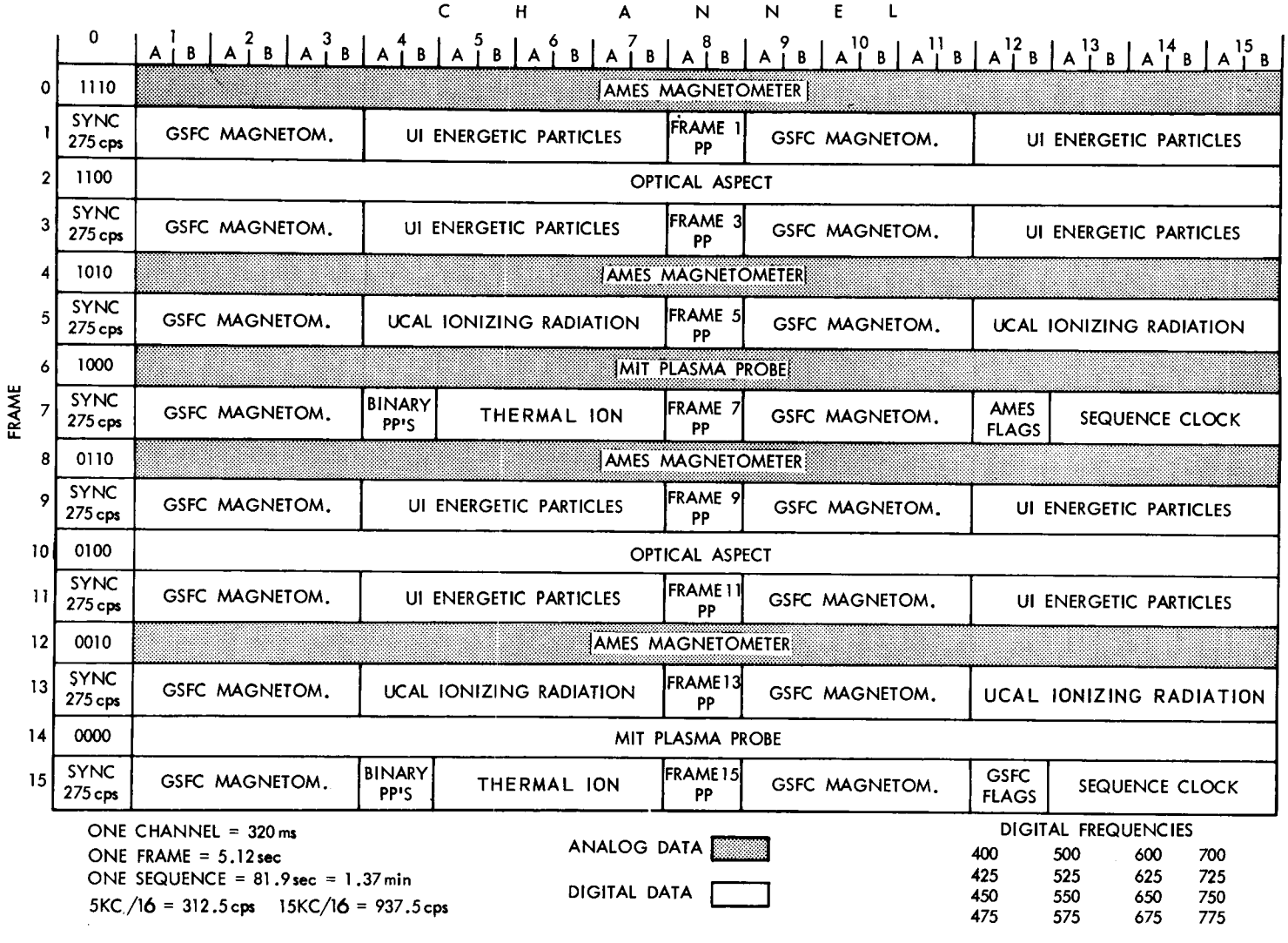

Figure 30–AIMP Encoder Format

Analog Data — Ames and MIT are the only experiments which require telemetered analog data. The experiment input to the encoder is a voltage which varies between 0 and 5 volts. A zero volt input is converted to a frequency of 15 KC by the analog oscillator and a +5 volt input to 5 KC. The output of the oscillator is fed to a 4-bit video divider (divide by 16) which changes the frequency range to 312.5 cps and 937.5 cps. The analog signal is then sent to a video selector that gates either the digital or analog to an amplifier whose output is fed to the transmitter.

There are twenty-six analog performance parameters (see Table 6). Subcommutation of the performance parameters is integral to the encoder system. Four sequences are required to readout the major performance parameters. The encoder performance parameter itself is further sub-commutated and requires 16 sequences to perform in-flight oscillator calibration.

The performance parameter outputs are voltages varying from 0 to +5 volts. During Channel zero of the odd frames, the output voltage from a specific performance parameter is gated to the analog oscillator for 20 ms. The pulses generated by the analog oscillator (200 to 300 cycles for 5 to 15 Kc) are stored in an eight-bit accumulator until readout in Channel 8A and 8B as PFM digital data.

Digital Data — Inputs from the experiments and instruments vary depending on whether the data storage is located in the encoder or in the instrument or experiment. The input to the encoder from experiments with their own storage is four lines (one for each bit in a binary PFM-tone burst) on which a voltage of greater than +3 volts is defined as a "1" and near ground as a "0" state. The voltages on these lines must remain stable for 100 μsec after the start of a readout (tone burst). The experiments and instruments with their own storage perform their own scans of these accumulators, so that only four leads are required to send the data information to the encoder.

The California and Iowa experiments have one lead going to the encoder for each separate accumulator. California has three 16-bit accumulators and one 12-bit accumulator, and Iowa has four 20-bit accumulators and two 24-bit accumulators. The input pulses are counted when they change from ground to a voltage greater than +3 volts. The pulses are 2 μsec or greater in length.

The digital commutator gates the voltages on the digital input lines from an experiment, instrument, or encoder accumulator to a 17-level, crystal-controlled frequency synthesizer which generates frequencies in the range 35.2 Kc to 99.2 Kc. These frequencies are counted down (divided by 128) by seven binary stages (a 3-bit video divider and 4-bit video divider) to give a video output which is

TABLE 6
AIMP-D Performance Parameter Assignments

Channel 8 (8 bits each) — analog input			
Frame No.	Sequence 1	Frame No.	Sequence 3
1	PP1, +12 volts main buss	1	PP1, +12 volts main buss
3	PP2, battery voltage	3	PP2, battery voltage
5	PP3, battery current	5	PP3, battery current
7	PP4, solar-array current	7	PP4, solar-array current
9	PP5, spacecraft current	9	PP5, spacecraft current
11	PP6, +28 volts transmitter	11	PP17, transmitter temperature
13	PP7, +7 volts temperature PP's	13	PP18, battery temperature
15	PP8, UI voltage	15	PP19, prime converter temperature
	Sequence 2		Sequence 4
1	PP9, solar experiment 1	1	PP20, solar-array temperature
3	PP10, solar experiment 2	3	PP21, Ames temperature 1
5	PP11, solar experiment 3	5	PP22, Ames temperature 2
7	PP12, solar experiment 4	7	PP23, GSFC magnetometer temperature
9	PP13, solar experiment temperature	9	PP24, UCAL temperature
11	PP14, fourth-stage bottle temperature/ Temple temperature	11	PP25, MIT temperature
13	PP15, fourth-stage bottle temperature/ fourth-stage firing duration	13	PP26, UI temperature
15	PP16, encoder-oscillator calibration	15	PP16, encoder-oscillator calibration
Bit	Channel 4A	Bit	Channel 4B
2^0	BP1, fourth-stage timer #1, first decade	2^0	BP5, fourth-stage timer #2, first decade
2^1	BP2, fourth-stage timer #1, second decade	2^1	BP6, fourth-stage timer #2, second decade
2^2	BP3, third-stage separation/fourth-stage separation	2^2	BP7, magnetometer booms erection
2^3	BP4, separation armed	2^3	BP8, separation armed

nearly symmetric. Each of the 17 possible frequencies (275 cps, 400 to 775 cps in 25-cps steps) contains an integral number of cycles in the burst time, so that the digital data video output is coherent to a useful accuracy. The output of the 4-bit video divider is fed to the video selector and then to the output amplifier. A test point at the output of the 3-bit video divider where the frequency range is 4.4 to 12.4 Kc is used to feed the "high speed video" to the encoder ground support test equipment. At present, all PFM encoders built for the IMP or AIMP series use the same test equipment, and a test output with frequency range of 4 to 15 Kc is made available in the design of each encoder.

Crystal Oscillator, Binary, Countdown, and Sync Pulse Generator — The heart of the encoder is its 409.6 Kc crystal-controlled oscillator in which two crystals slightly displaced in frequency are used. In the event the primary crystal fractures, the secondary crystal controls the oscillation, and only a minor shift in frequency occurs while stability remains essentially unaltered. Should both crystals fracture, the circuit acts as a free running multi-vibrator and both the frequency and stability are greatly affected.

In the countdown chain, the 409.6 Kc is counted down to 186.0 ncps. The input at various stages of the countdown is used to construct sync pulses. The sync pulses required are generally different for each experimenter. The various outputs are fed to other sections of the encoder where they are combined to obtain the frequencies or pulses required.

Most pulses have standard output impedances as follows: Off condition, approximately +6.5V at 200 K ohm, and On condition, approximately -3V at 100 K ohms. All experiment and instrument sync pulses are isolated from one another.

Satellite Clock (Sequence Counter) — The encoder system contains a sequence counter which is commonly termed the "satellite clock." It consists of a 16-bit accumulator. The counter receives one count every sequence (81.92 seconds), and therefore it takes 60 days before repetition of clock readout occurs unless encoder power is interrupted. Once the sequence counter is referenced to a time standard, the time recorded by the telemetry station on the data tapes can be compared to the sequence clock for time correlation. The sequence counter starts in an arbitrary state when power is turned on.

In-Flight Calibration — The analog oscillator output varies slightly with temperature and age; therefore, an onboard calibration system has been included to check the oscillator output. A special four-volt standard is carried in the encoder converter as part of this function. Ground, 2.5 volts, 4 volts, 4 volt standard, and 5 volts are commutated into the analog oscillator and treated in

the same manner as any other analog performance parameter. All of the encoder calibration voltages, with the exception of the standard, are obtained through precision resistor divider networks from the main +7.5V supply line to the encoder. The system accuracy of the analog data is at least ±1% over a 0°C to +40°C temperature range.

Encoder Accumulation — The encoder system has two types of accumulators, an "S" and "S-T." The "S" type is a straight binary counter. The "S-T" type is a straight binary counter until 1/2 the total count is reached, at which time the counter is reset and 800 cps clock pulses are counted until readout. Thus the time to accumulate 1/2 the total count can be determined.

Optical Aspect Parity Check — The output of the video selector is monitored for the first 14 half channels (1A to 7B) and last 16 half channels (8A to 15b) of each optical aspect system data output. For each of the two monitors the least four significant bits of the sum of the sexadecimal zeros complement of each channel are stored until readout in Channels 13A and 13B of Frames 7 and 15, and each separate reading provides a check of the previous optical reading. If a burst is processed by the ground data processing line improperly due to noise or bad sync, the parity check calculation will not agree with the parity check readout.

Use of Metal Oxide Silicon Field Effect Transistors (MOS) — The primary design restraint on the encoder system was power. The increased complexity of the encoding system required a change in construction in order to maintain a reasonable size and to facilitate the construction of the modules. A type of integrated circuit was required. Metal Oxide Silicon Field Effect Transistors (MOS) circuits were found to have the best electrical properties for this specific system.

MOS devices are susceptible to radiation damage, and in near-earth orbits shielding is required. In the lunar orbit or in alternate mission orbits (perigee 30 to 40 K Km) the effects of radiation are negligible. This will be the first use of MOS circuits in a spacecraft.

Performance Parameters — The performance parameter card to be flown on AIMP D&E will transform all the essential currents, voltages and temperatures on the spacecraft into a voltage input to the encoder (see Figure 31).

The method employed to monitor currents is a magnetic amplifier. This method affords a wide dynamic range with very good linearity.

The voltage sensor employs a simple voltage dividing technique.

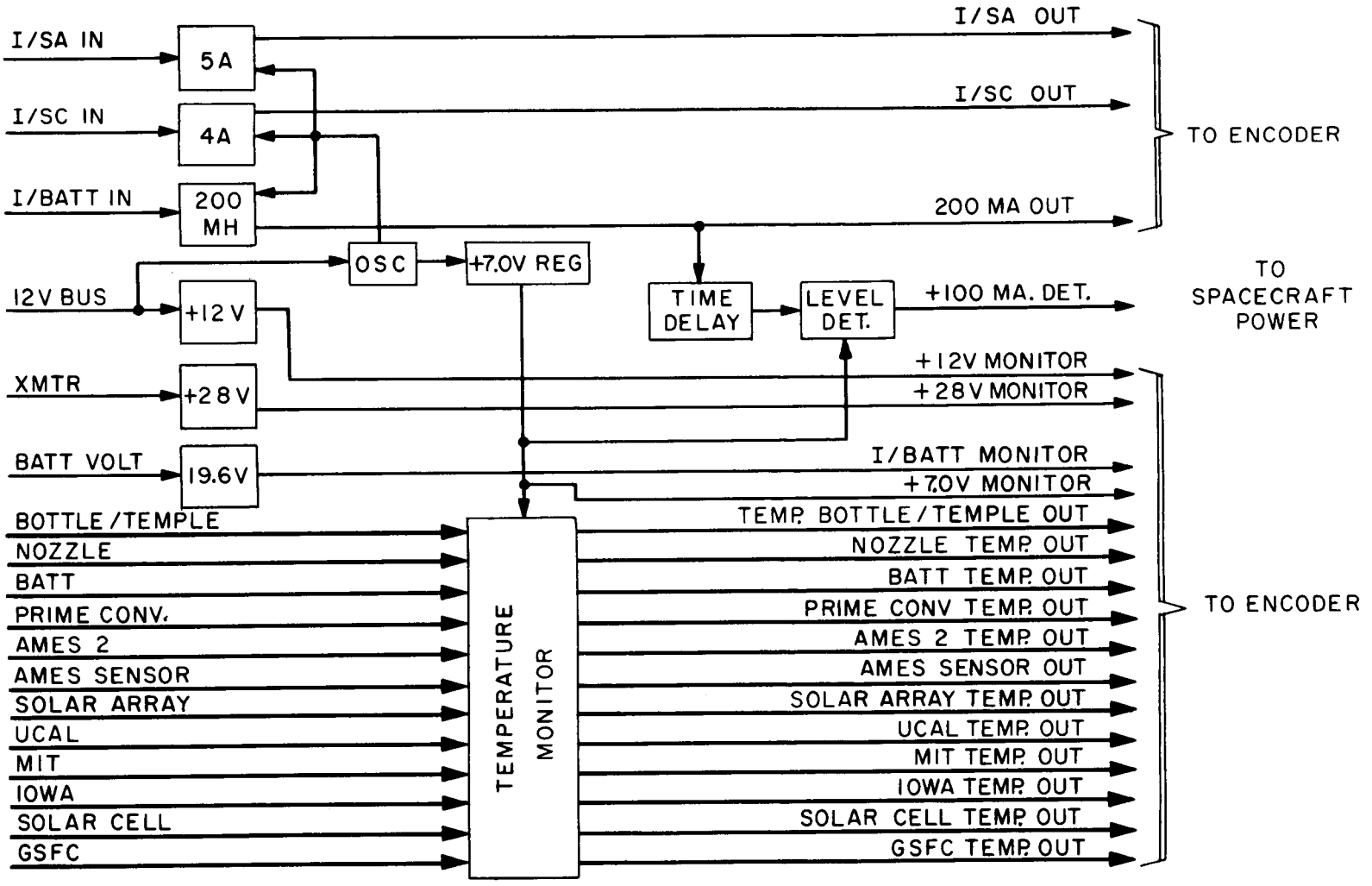

Figure 31–Performance Parameter Block Diagram

The temperature sensor used on this spacecraft employs a thermistor-resistor network combination. The wide resistance-to-temperature variation eliminates the need for an amplifier circuit. This method is also capable of good linearity over the entire temperature range.

The currents to be monitored vary from a small trickle charge of a few milliamperes to the solar array current of some five amperes. To monitor these currents, a self-saturating magnetic amplifier is used. The gain of this amplifier is adjusted according to the magnitude of the input signal. The output voltage from the magnetic amplifier is adjusted according to the telemetry, 0 to +5 volts.

The 200-milliampere current sensor has a 100-milliampere detector associated with it. This detector will transmit a signal when the input current exceeds 100 milliamperes. This information, along with information from the power supply, will allow the voltage to be switched to a more favorable mode of operation and hopefully increase the life of the batteries of the spacecraft.

The voltages that are of interest on board this spacecraft are (1) +12v main buss; (2) battery voltage; (3) +28v transmitter. Simple voltage-divider networks are employed to monitor these voltages. The output to the telemetry under normal operation conditions should not receive a signal any greater than 6 volts. Therefore, a Zener diode is placed across the output of each voltage divider to clip any signal in excess of 5.5 volts.

There are fourteen temperatures that will be monitored on AIMP D&E. These temperatures cover a range from -150°C to +130°C. Each sensor consists of a thermistor-resistor network combination. Excellent linearity can be obtained in well-designed temperature sensors using this type of circuity. The 7-volt power source necessary for the temperature sensors is located in the performance parameter card, and the regulation of this power supply is better than one percent. Standard thermistor-resistor networks were used so that only one calibration curve was required.

The performance parameter card consumes less than 100 milliwatts and has good linearity over the entire temperature range of -60°C to 80°C.

Spacecraft RF System

The RF system includes the transmitter, the range and range rate system, command receiver, command decoder, antenna, and antenna hybrid.

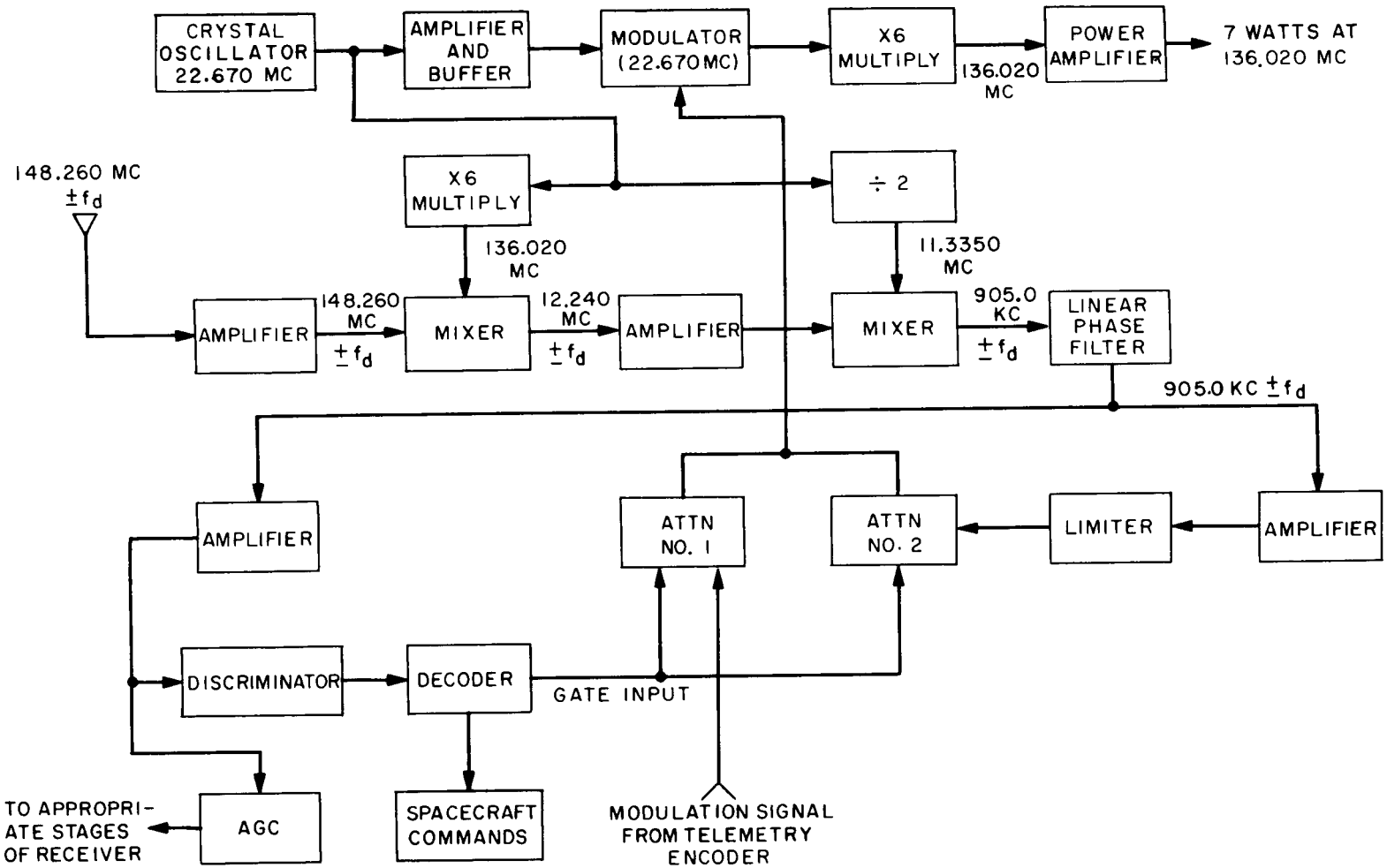

Figure 32–Simplified Block Diagram - Range and Range Rate System

The AIMP-D RF system (see Figure 32) was designed to provide a means for transmitting telemetry information, receiving and decoding commands, and transponding range and rate signals originated by a ground station. A redundant command system is used to provide a back-up in the event of a failure of the prime command system. The receiving systems are connected to the spacecraft antenna system in an orthogonal manner to eliminate losses due to power splitting and to provide a limited degree of polarization diversity. The general principles of operation are described in the following paragraphs.

Telemetry Transmitter — The telemetry transmitter has a power output of 7 watts and operates with a carrier frequency of 136.020 megacycles. The carrier frequency remains within 3.0 kilocycles of the assigned frequency under all spacecraft environmental conditions. The carrier is phase-modulated by a square wave from the telemetry encoder and has a peak phase deviation of one radian. This provides 30% of the transmitter power in the carrier and 70% in the sidebands. The transmitter signal is designed to be compatible with ground station phase-lock receiving systems.

Command Subsystem — Commands are received by the spacecraft on a frequency of 148.260 megacycles, which is phase-modulated by command codes. The sensitivity of the receiver system is -115 dbm. The peak phase deviation of the command signal is one radian. The detected command signal is fed to a command decoder which determines when any of the possible commands have been received. Each of the commands must be preceded by a standard address tone. Nine of the commands are formed by a standard GSFC sequential tone command sequence. Each of these commands is composed of four tones (see Figure 33), the first of which is the address tone, followed by three execute tones. The length of each tone is one second, and all tones are separated by one-half second blanks. In addition to the integrating time delay of the tone detectors, the command decoders have three timing circuits. The first determines the "time on" for a normal command, the second arms the command output circuit at the proper time for the last execute tone to occur, and the third disarms the decoder if the execute tones arrive too rapidly or if a failure occurs in the first or second level memories.

The tenth command is used to command the ranging function and is different from the other nine. The ranging command consists of the address tone followed by the ranging signal. If the ranging signal appears within 5 seconds after the disappearance of the address tone, the ranging function will be initiated and the spacecraft will remain latched in this mode of operation until approximately two seconds after termination of the ranging signal. The four-kilocycle component of the ranging signal is used to detect the ranging mode. One of the standard commands is used as an emergency "cut-off" of the decoder ranging

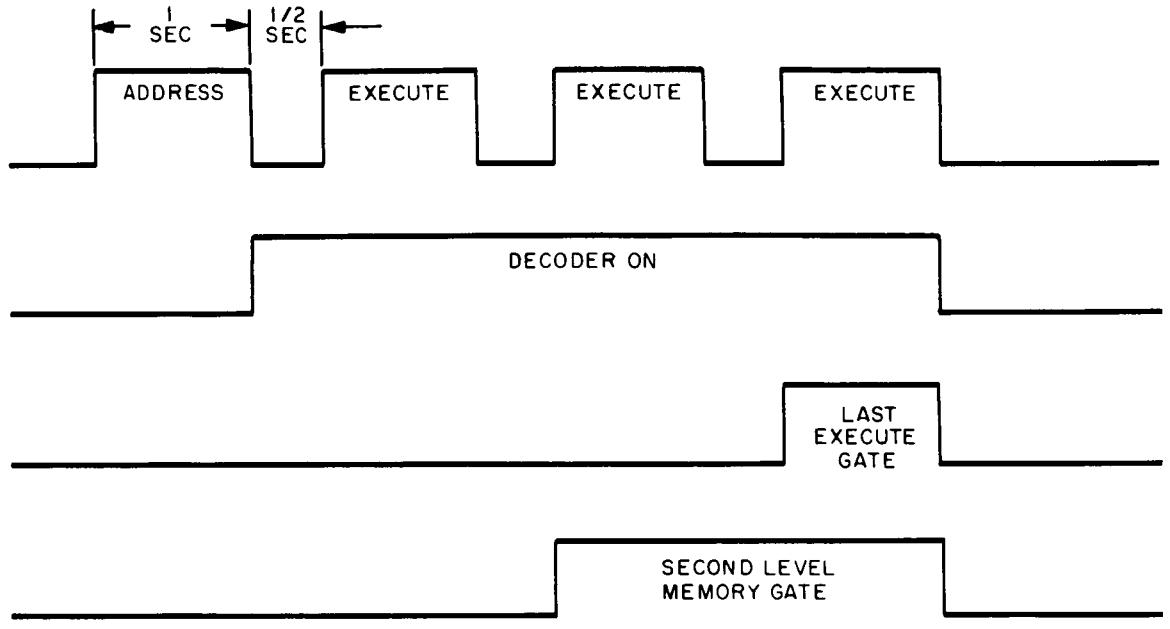

AIMP-D COMMANDS

1. START FOURTH-STAGE TIMERS (TWO-HOUR TIMERS)
2. STOP FOURTH-STAGE TIMERS
3. DIRECT FIRE FOURTH STAGE (INTERLOCKED WITH COMMAND NO. 1)
4. ARM SEPARATION (INTERLOCKED WITH COMMAND NO. 1)
5. DIRECT SEPARATION (INTERLOCKED WITH COMMANDS NO. 1 AND 4)
6. TRANSMITTER ON
7. TRANSMITTER OFF
8. INITIATE UNDER VOLTAGE CYCLE (LOCKED OUT UNTIL FOURTH-STAGE SEPARATION)
9. RANGE AND RANGE RATE RESET
10. RANGE AND RANGE RATE ON

Figure 33–Command Sequence

circuit, in the event a failure occurs and the decoder remains latched in the Range and Range Rate (R&RR) mode without a ranging signal.

Range – When it is desired to obtain range or range rate of the satellite, the ranging function is initiated by the 148.260 megacycle signal as described previously. The ranging modulation is composed of a group of sub-carriers which are 20 Kc, 4 Kc, 4.8 Kc, 4.16 Kc, 4.032 Kc, and 4.008 Kc. The modulation index is 0.35 radians peak for the 20-Kc and 4-Kc modulating frequencies, and 0.1 radians peak for all others. The system is also compatible with pseudorandom ranging codes, provided a suitable 4 Kc signal component is available in the code for proper decoder operation. As can be seen from Figure 32, the 148.260 MC signal is amplified and then fed into a mixer. The other input to the mixer comes from a times-six multiplier which is fed from the 22.670 MC master oscillator in the transmitter. The output of the mixer is

tuned to the difference frequency which is 12.240 MC ± the doppler frequency (fd) and fed into an amplifier. The output of the amplifier is mixed with 1/2 the crystal oscillator frequency giving an output of 905.0 KC ± fd, which is fed into a linear-phase filter. The linear-phase filter is of prime importance in the R&RR System since it provides an output which has a constant delay for all signal components over all expected values of fd. The output from the linear-phase filter carries all of the sidebands resulting from the modulating frequencies introduced at the ground station and is divided into two paths. In one path the output is amplified, limited, and fed into an attenuator. In the other path the output is amplified, fed into a discriminator and then to a decoder. Upon the reception of a R&RR interrogation, the decoder generates a gate which causes attenuator No. 1 to attenuate the telemetry encoder modulation and causes attenuator No. 2 to provide zero attenuation for the 905 KC R&RR signal. The system remains in the R&RR mode until the R&RR signal disappears. The outputs of attenuators 1 and 2 are fed to the modulator of the telemetry transmitter; therefore, when in the R&RR mode, the transmitter output is modulated by 905.0 KC ± fd. (See Figure 34.) The 905.0 KC signal is in turn modulated by the frequencies indicated at the beginning of this paragraph, so that effectively a PM/PM signal is generated. When not in the R&RR mode, the decoder provides

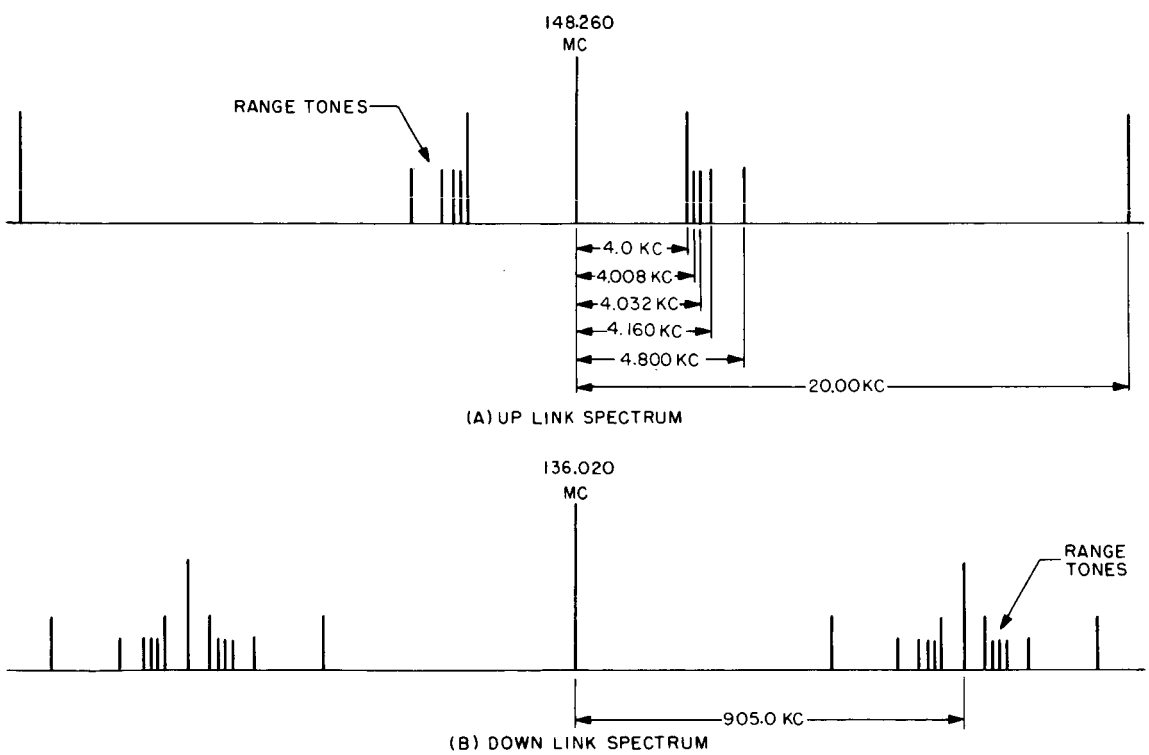

Figure 34–Range and Range Rate Transmitter Modulation

for zero attenuation through attenuator No. 1 and a high attenuation through attenuator No. 2, so that the transmitter output is modulated only by the telemetry encoder modulating signal. Figure 34A illustrates the spectrum of the signal transmitted from the ground tracking station. Figure 34B illustrates the spectrum of the signal transmitted from the satellite during the R&RR mode. The actual range of the spacecraft is determined by the use of basic sidetone ranging techniques applied to the signal received from the satellite and the original signal transmitted from the tracking station.

Range Rate — The range rate of the satellite is determined through the use of the doppler principle as applied to the signal transmitted and received from the satellite. As shown in Figure 32, the frequency of the command signal received by the spacecraft is equal to 148.260 MC ± fd. The frequency shift due to the one-way doppler effect is given by:

$$fd = \pm f_0 \quad \frac{v}{v + c}$$

where

f_0 = frequency of ground station transmitter

v = velocity of satellite relative to the earth

c = velocity of light

The sign preceding the right hand side of the equation is determined by whether the range of the satellite is increasing or decreasing. A decreasing range would imply a positive sign.

Following the received signal through the R&RR system aboard the satellite, it can be seen that during the time the system is in the R&RR mode the transmitter output will be a 136.020 MC signal modulated by 905.0 KC ± fd. Range rate is then determined at the ground station by measuring the received spacecraft carrier frequency, translated R&RR carrier frequency, and the ground station transmitted frequency, and performing the required calculations.

AIMP Antenna System — The AIMP antenna feed system consists of two major parts plus the interconnecting cables. The first of these is the diplexer/coupler assembly. This is a stripline unit about 4" × 6" × 1/4" consisting of a 90° 3 db coupler and a stripline diplexer attached to one coupler input. The

telemetry transmitter and the backup command receiver are fed into the diplexer. The prime receiver is fed from the other coupler port. The transmitter input is divided by the coupler into two equal signals phased 90° apart. These are fed to the antenna.

The second part consists of four antennas fed as a tilted-turnstile system. The antennas make an angle of 15° to the top surface of the spacecraft. Each antenna consists of a radiating element approximately one-quarter wavelength long with a chamber at its base for impedance matching components. The antennas are matched to an impedance of 100 + jo ohms at the telemetry frequency, and are fed into two pairs of opposite elements. These are connected by a one-half wavelength cable. Since the inputs to the two pairs are phased 90° apart, this results in the antennas being fed in phase-quadrature. The pattern polarization characteristics show left-hand circular off the top of the spacecraft, linear near the equator and right-hand circular off the tail. Antenna gain is approximately +2db off-nose and -3db off-tail. (See Figure 35 and 36.)

Power Systems

This section contains a description of the AIMP power system, which consists of:

- Solar Array
- Solar Array Regulator
- Battery
- Prime Converter
- Optical Aspect Converter
- Encoder Converter

The AIMP-D spacecraft normal load is 2.2 amps at 18.3 volts.

AIMP Solar Array — The primary source of power for the AIMP spacecraft is the solar array which provides power for the spacecraft and recharges the storage batteries during the sunlit portion of the orbit. In the design of the array, primary consideration was given to obtaining maximum power, reliability, and stability at a minimum cost in weight.

The solar array consists of four identical solar paddles mounted so that, in the orbital configuration, the spars, which run through the centerline of the paddles, extend radially outward from the spacecraft. The paddles are positioned around the spacecraft at angles 90° apart and, in order to provide power

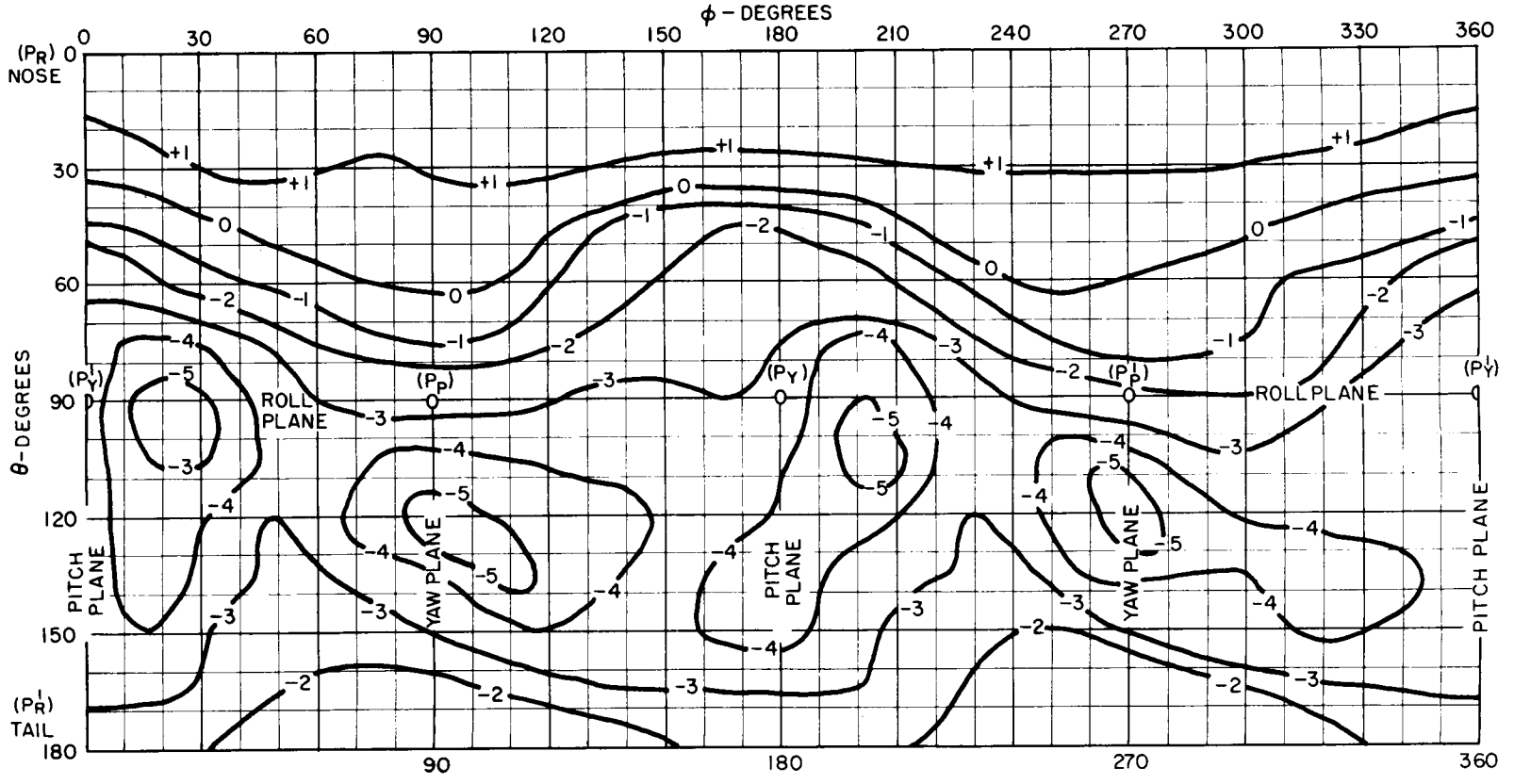

Figure 35–Antenna Pattern

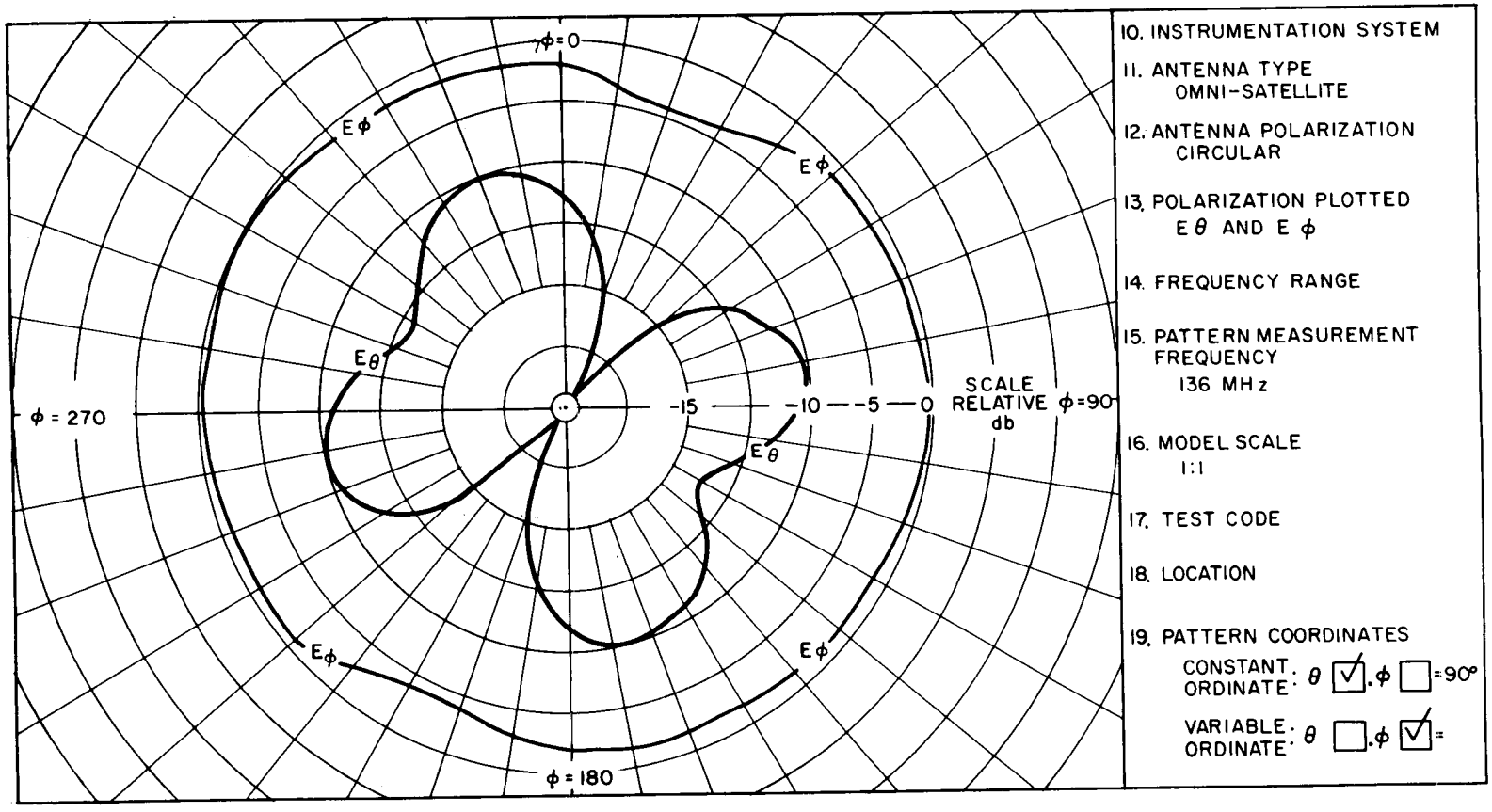

Figure 36–Antenna Pattern (0 =90°)

at any arbitrary sunline-to-spin axis angle, they are pitched to an angle of 25° between the plane of the paddle and the spacecraft spin axis.

Each solar paddle is basically rectangular in area with a length of 27.60 inches and a width of 25.25 inches. A square (1-inch on a side) aluminum spar tube runs through the length of the paddle at the centerline providing a means for attachment to the spacecraft at the inboard end and a means for tie-down, during launch, at the outboard end. Construction of the solar paddle substrate utilizes an 0.7-mil aluminum honeycomb core upon which is mounted a skin consisting of a double layer of 1.5-mil epoxy-impregnated Fiberglas, a silver, expanded-metal conductor, and another layer of 1.5-mil Fiberglas. (See Figure 37.) In this construction the Fiberglas provides the necessary insulating characteristics between the solar cells, the expanded-metal conductor and the core. The expanded metal, which is laid down directly beneath the solar cell modules, provides a path for a sheet current return which, by retracing the current in the solar cells, causes cancellation of the stray magnetic field generated by that current. The complete sandwich unit eliminates the need for a separate substrate skin while still providing the structural strength necessary for the launch conditions. For stability, silicone adhesives are used for bonding of the solar cells

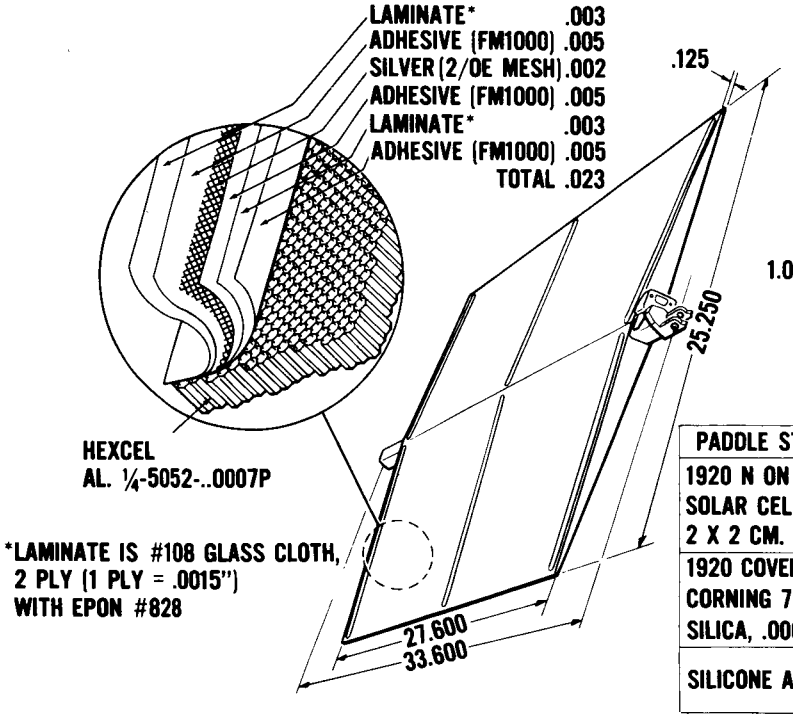

WEIGHT BREAKDOWN

PADDLE STRUCTURE		2.72 LB.
1920 N ON P SILICON SOLAR CELLS, 2 X 2 CM.	30g / 100 CELLS	1.27 LB.
1920 COVERSLIDES CORNING 7940 FUSED SILICA, .006 THICK	15g / 100 CELLS	0.64 LB.
SILICONE ADHESIVE	15g / 100 CELLS	0.63 LB.
	TOTAL	5.26 LB.

Figure 37–Solar Paddle Construction

and their glass shields. The solar cells are bonded to the substrate with RTV-40 and the shields are bonded to the solar cells with RTV-602.

Power is generated by the conversion of solar energy to electrical energy by means of a total of 7680 2 cm × 2 cm solar cells divided equally among the four paddles, with 960 cells bonded on each paddle face. The cells on each paddle are further divided into four groups which are each isolated electrically from the others by means of a parallel pair of UT-262 diodes. With each group the cells are multiply interconnected, with gold-plated molybdenum bus bars, into a series-parallel arrangement of 48 cells in series by 5 cells in parallel to provide redundancy and reliability.

Shallow-diffused, N/P, gridded, silicon solar cells are used to provide both high-conversion efficiency (10% minimum) under air mass zero solar illumination and also stability in the space radiation environment. In addition, a lightweight assembly is achieved by the use of cells which are only 12.5-mils in nominal thickness and which incorporate solderless titanium-silver contacts. Problems with these cells were noted after the AIMP-D Launch. Cells on spare paddles deteriorated. The cause was linked partially to moisture and rework.

The solar cells are each protected individually by a 6-mil thick, fused silica cover glass with a 410-millimicron cut-off, ultraviolet filter on the cell side and an anti-reflecting coating on the exposed side. This arrangement provides for maximum conversion efficiency by maintaining the light transmission characteristics of the cover glass-adhesive combination in an ultraviolet and hard particle radiation environment, by protecting the solar cells against micrometeorite damage and by reducing the cell operating temperature.

The weight of each complete solar paddle assembly is nominally 2400 grams. This gives an array weight of 9600 grams, or 21.1 pounds.

The power-producing capability of each solar paddle face, prior to degradation, is 42.8 watts at 19.8 volts if operated at 40°C* and oriented for maximum illumination toward the sun in space. At the end of a lifetime of one year, the maximum degradation anticipated is 15 percent. Since the power capability of the complete solar array varies with aspect, time voltage, and temperature, complete details cannot be given here. However, capabilities under various conditions of interest are shown in the following table.

*A thermistor package is mounted within the spar of each solar paddle for the monitoring of temperatures during both pre-launch testing and flight (only one sensor being monitored during flight).

Solar Array Power Output
(Watts)

	Normal Operation (19.6V)		Shadow Emergency (15.5V)	
	Average Power at Minimum Aspect	Minimum Instantaneous Power	Average Power at Minimum Aspect	Minimum Instantaneous Power
Initial	66.1	54.4	57.9	47.6
End of Life	56.2	46.3	49.2	40.5

AIMP Solar Array Regulator — The solar array regulator functions to prevent excessive voltage generated by the solar cells from damaging the spacecraft experiments and its battery.

The regulator will operate in either of two stable states depending upon the state of charge of the battery. A current sensor in the battery charge circuit determines the state of charge. When the battery requires charge currents in excess of 100 ma, an appropriate signal to the regulator will set the regulation at 19.6 volts. When the battery charge current diminishes to less than 100 ma, the regulation will be at 18.3 volts to eliminate the possibility of cell unbalance which would occur at the higher potential.

The "dump" circuit is composed of 8 emitter-followers which are isolated from each other by an isolation module. This eliminates cross-talk, in the event of a failure of any of the dump transistors, and permits normal operation of the remaining circuits. Figure 38 is a block diagram of the regulator system.

AIMP Prime Converter — Power from the solar-array-battery-shunt regulator is regulated, converted, and supplied to the spacecraft load at three different voltage levels by the prime converter. This is accomplished by the combination of three separate subsystems working together, as shown in the block diagram, Figure 39.

To accommodate the large operating voltage swing on the input, a switching-mode regulator is used to perform the task of the pre-regulator. Basically a switch, it is turned on and off at a 9.8-Kc rate and has a duty cycle determined by a closed-loop servo system. The switch is connected between an LC-filter on the input and an LC-filter on the output and is stimulated by two power transistors which are alternately driven into and out of saturation as a result of the combined action of a small power oscillator and saturable reactors. The

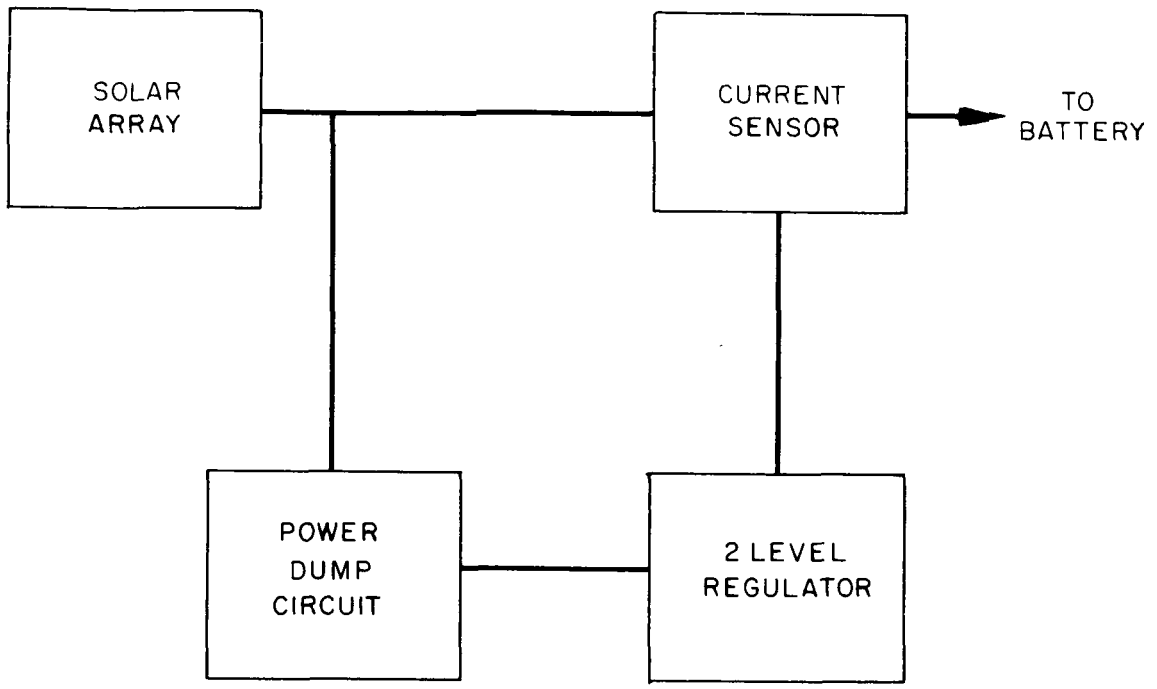

Figure 38–Solar Array Regulator Block Diagram

output voltage level is less than the minimum input voltage, and in this case is approximately 11.7 volts.

A DC-to-DC converter operating on the output of the pre-regulator provides three separate isolated voltages. Each voltage is then regulated to within ±1 percent by independent series-type voltage regulators. The regulators, all

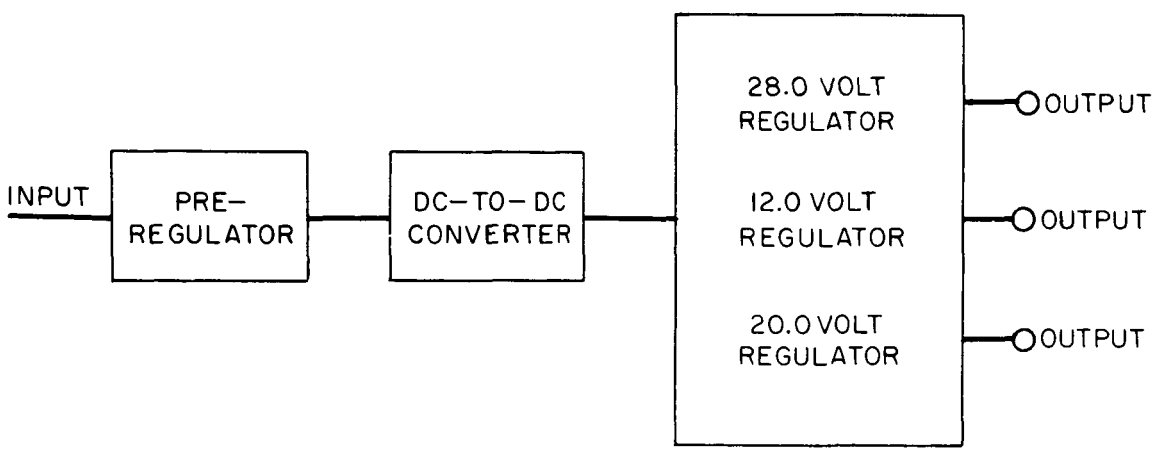

Figure 39–Voltage Regulator

TABLE 7
AIMP Power Allotment

	Initial (Nominal) Watts	End of Life (Worse Condition) Watts
Solar Array Output	66.1	49.2
	Peak (Watts)	Average (Watts)
System Voltage (12-9.6) Breakdown		
Undervoltage detector	.240	.240
Solar array regulator	.196	.196
GSFC or Ames magnetometer flipper	4.000	.028
Total	4.436	.464
Regulator Converter Breakdown		
Experiments		
Ames magnetometer (+12v)	.800	.800
GSFC magnetometer (+12v)	1.000	1.000
University of California (+12v)	.200	.200
Temple University (+12v)	.500	.500
University of Iowa	.700	.700
MIT (+20v)	3.500	1.100
Total	6.700	4.300
Telemetry		
Encoder and DDP system (+12v)	2.380	2.150
Transmitter (+28v)	16.500	16.500
Range and range rate and command (+12v)	1.610	1.610
Total	20.490	20.260
Instruments		
Optical aspect system (+20v)	1.500	.950
Performance parameters (+12v)	.137	.137
Fourth-stage electronics (+12v)	.420	.000
Fourth-stage parameter (+12v)	.240	.240
Total	2.297	1.327
Total prime converter load	29.480	25.887
Input to prime converter at 74% efficiency	39.897	34.982
Load on 12-19.6v bus	4.436	.464
Regulator-converter input	39.897	34.982
Battery charging	8.000*	8.000
Total power allotment	52.333**	43.446

*Battery charge not an actual peak demand load-nominal figure only.
**True peak demand load 44.333w.

similar in design, inherently have self-protection for short circuits. For this reason a bypass is incorporated on the 20.0-volt and 12.0-volt line to supply a short circuit current pre-determined by the fuse rating on the line. Power allotments are shown in Table 7.

AIMP Encoder Converter — The encoder converter converts the +12.0 vdc ±1 percent output of the prime converter to five d.c. voltage levels (listed in Table 8) required to power the PFM encoder and digital data processor (DDP). A transformer-coupled multivibrator is used to chop the +12-volt d.c. input at a 4 Kc rate. The resulting square wave is then transformed to five a.c. voltages which after being rectified and filtered provide the desired d.c. levels. As indicated in the block diagram (Figure 40), three voltage regulators are used. The regulator for the +7.5-volt line is required to meet the close tolerance imposed on this output voltage. The other two regulators, in addition to maintaining the required regulation, provide a requested lower a.c. output impedance than obtainable with a capacitive filter. The block diagram also shows a +4.0-volt d.c. reference. This reference is included in the converter module but is not part of the converter circuit.

TABLE 8
Output Voltages of Encoder Converter

Output Voltage (volts)	Regulation	Output Current (ma)	Temperature Limits (°C)
+7.5	±.25	1 to 5	0 to +40
	±.5%	1 to 5	-10 to 0
	±1%	1 to 5	-60 to -10 & +40 to +80
+6.5	±1%	50 to 70	0 to +40
	±5%	50 to 70	-60 to 0 & +40 to +80
-3.0	±1%	1 to 11	0 to +40
	±5%	1 to 11	-60 to 0 & +40 to +80
-4.0	±5%	40 to 60	-60 to +80
-9.0	±10%	.5 to 1	-60 to +80

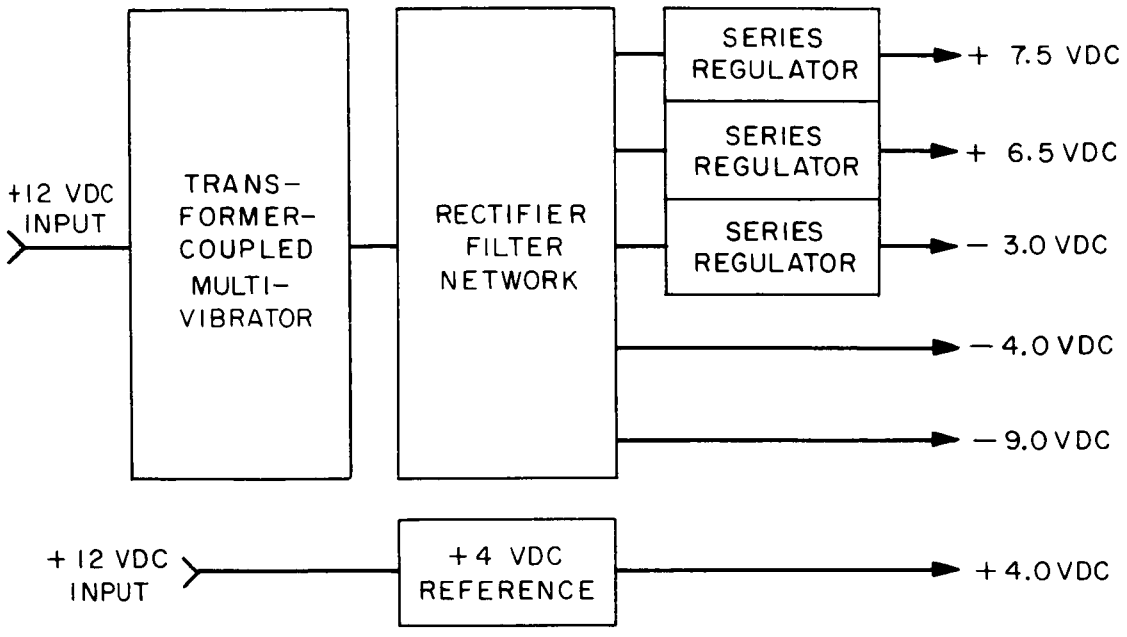

Figure 40–Encoder Converter Block Diagram

AIMP-D Optical Aspect Converter — The purpose of the optical aspect converter is to supply power to the optical aspect computer and sensor.

The input to the converter is +20-volts ±1% from the prime converter. The outputs of the optical aspect converter are as follows:

	Voltage	Tolerance	Load
(1)	+12V	±5%	12 ma (constant)
(2)	+3.5V	±10%	110 ma (Minimum)
			540 ma (Maximum)

The +12V output has a ±5% tolerance for changes in the nominal voltage due to temperature, drift, and input voltage variation. A series regulator was used on this line to provide the required source impedance of less than 5 ohms for a step change in load of 1 ma (around the nominal load) from d.c. to 1 Kc.

The +3.5V output has a ±10% tolerance for changes in the nominal voltage due to temperature, drift, load, and input voltage variation.

The optical aspect converter supplies the voltages specified above over a temperature range from -30°C to +60°C. In addition, the converter will start at -65°C with a 12-ma load on the +12V line and a 470-ma load on the +3.5V line.

A block diagram of the optical aspect converter is given in Figure 41.

AIMP Battery — An 11-amp hour battery was chosen for the AIMP (D&E) mission to ensure that sufficient power would be available to fire the fourth stage igniters and separation bolts and that the spacecraft would operate at least three hours in the shadow condition. The battery sustains spacecraft operation down to a temperature of -20°C.

The silver-cadmium cell is characterized by a positive electrode consisting of six sintered silver plates and a negative electrode consisting of seven

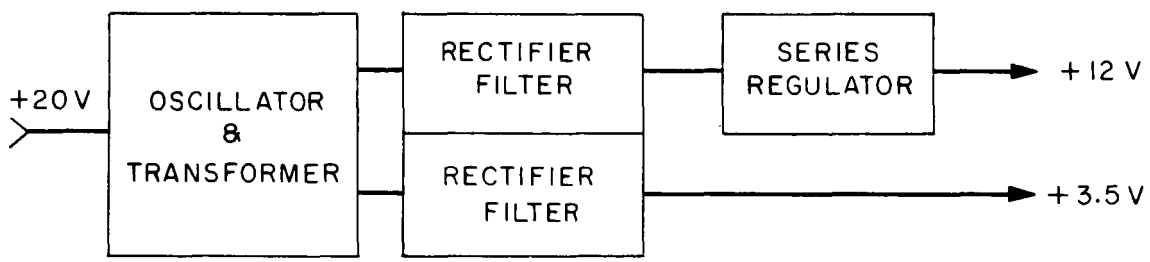

Figure 41–Optical Aspect Converter Block Diagram

pasted cadmium plates separated by a composite separator system of four layers of silver-treated cellophane and two layers of non-woven nylon coupled with a 40 percent potassium hydroxide electrolyte solution. It is the only suitable rechargeable sealed battery for this spacecraft because of its inherent magnetic-free properties.

The battery consists of 13 11-amp-hour cells connected in series and encapsulated in epoxy with an outer case of magnesium giving a total weight of 10.0 pounds. The battery also contains a magnetic compensation loop which is an extension of the negative wire that is re-routed along the top and side of the cells to cancel out stray magnetic fields that are generated by current flowing in the intercell connectors, terminals, and the electro-chemical cells. The battery has a nominal operating voltage range of 19.8-volts on charge and 13.0-volts on discharge over a temperature range of 0°C to 50°C.

The epoxy used to encapsulate the battery was chosen so that its expansion and contraction rate are almost identical to the cell cases. An encapsulated battery has been cycled from -65°C to 50°C without cracks or separation occurring.

The discharge characteristics for the 11-amp hour battery for various temperatures and the nominal spacecraft load of 3 amps is shown in Figure 42. The battery during discharge is exothermal; therefore, in shadow conditions the battery temperature initially rises slightly and then starts a gradual cooling which even in a 6.8 shadow case does not drop below -20°C. The spacecraft is turned off when the battery voltage reaches 12 volts ±.1 volt. When the load is removed, the battery voltage rises to an open-circuit voltage of 14.8 volts.

A silver-cadmium battery exhibits two distinct charge levels that are represented chemically by a silver monoxide ($Ag_2 0$) and a silver-peroxide (Ag0) charge sequence (see Figure 43). At room temperature the transition from the $Ag_2 0$ to the Ag0 levels occurs from 18 to 40 percent recharge depending on the rate of charge. As can be seen from Figure 43, the change from one level to

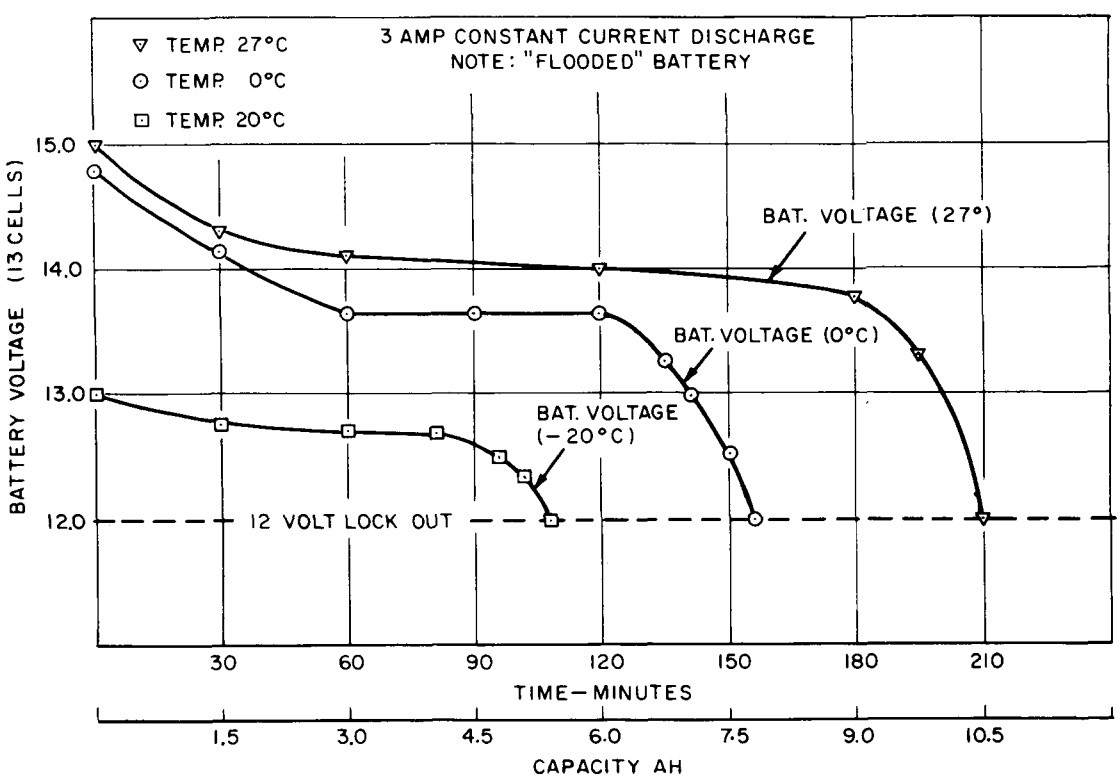

Figure 42–Battery Discharge Characteristics

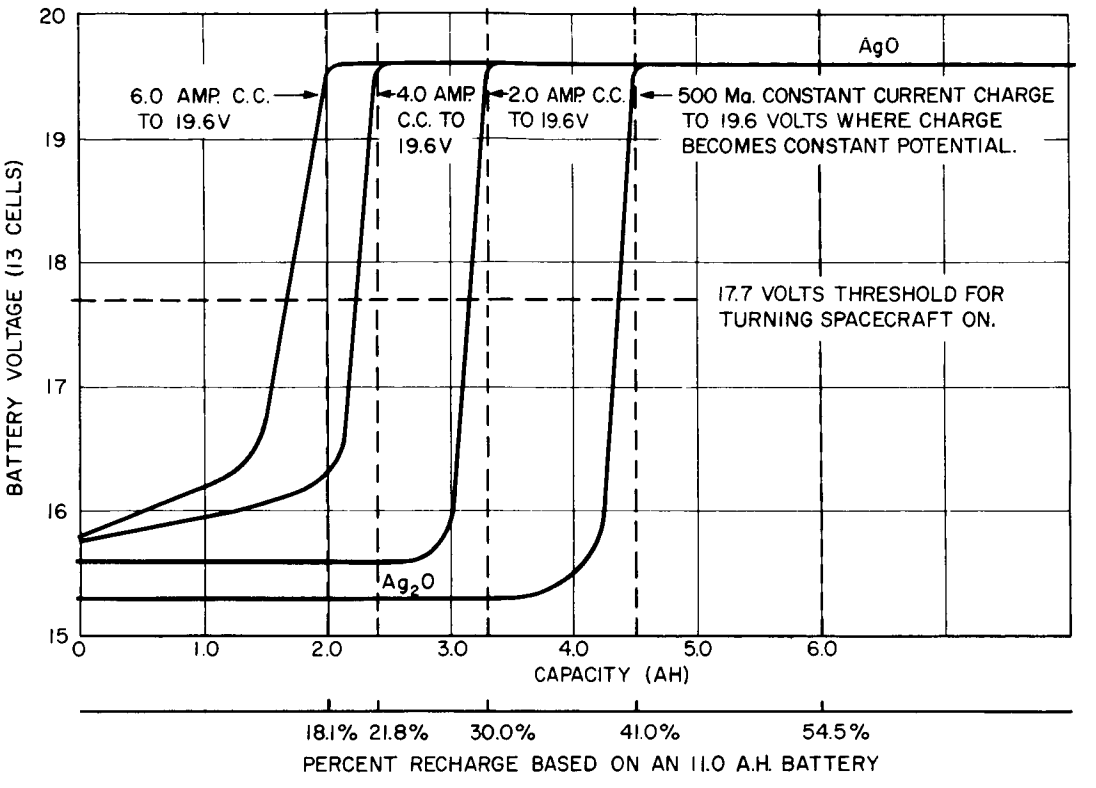

Figure 43–Battery Charge Sequence

the other is rapid. It has been decided to use the change in charge voltage (15.6 to 19.6) to turn the spacecraft on when a voltage of 17.7 volts is exceeded.

The total output of the solar array (approximately five amps) is used to charge the battery when the spacecraft is in the undervoltage state. An excess current of approximately two amps is available to charge the battery when the spacecraft is on. The amount of current the battery can accept diminishes as the battery becomes charged, and when the battery accepts less than 100 ma, the charging voltage is changed from 19.6 to 18.3. In the event the battery accepts more than a 100-ma charge, the voltage is switched back to 19.6 from 18.3. The purpose of the two-step voltage regulator is to prevent serious cell unbalance and resultant high internal pressures which would occur if the battery was charged at 19.6 volts for a prolonged period of time even though the charging current drops to a few milliamps.

The battery has a short circuit current of 120 amperes.

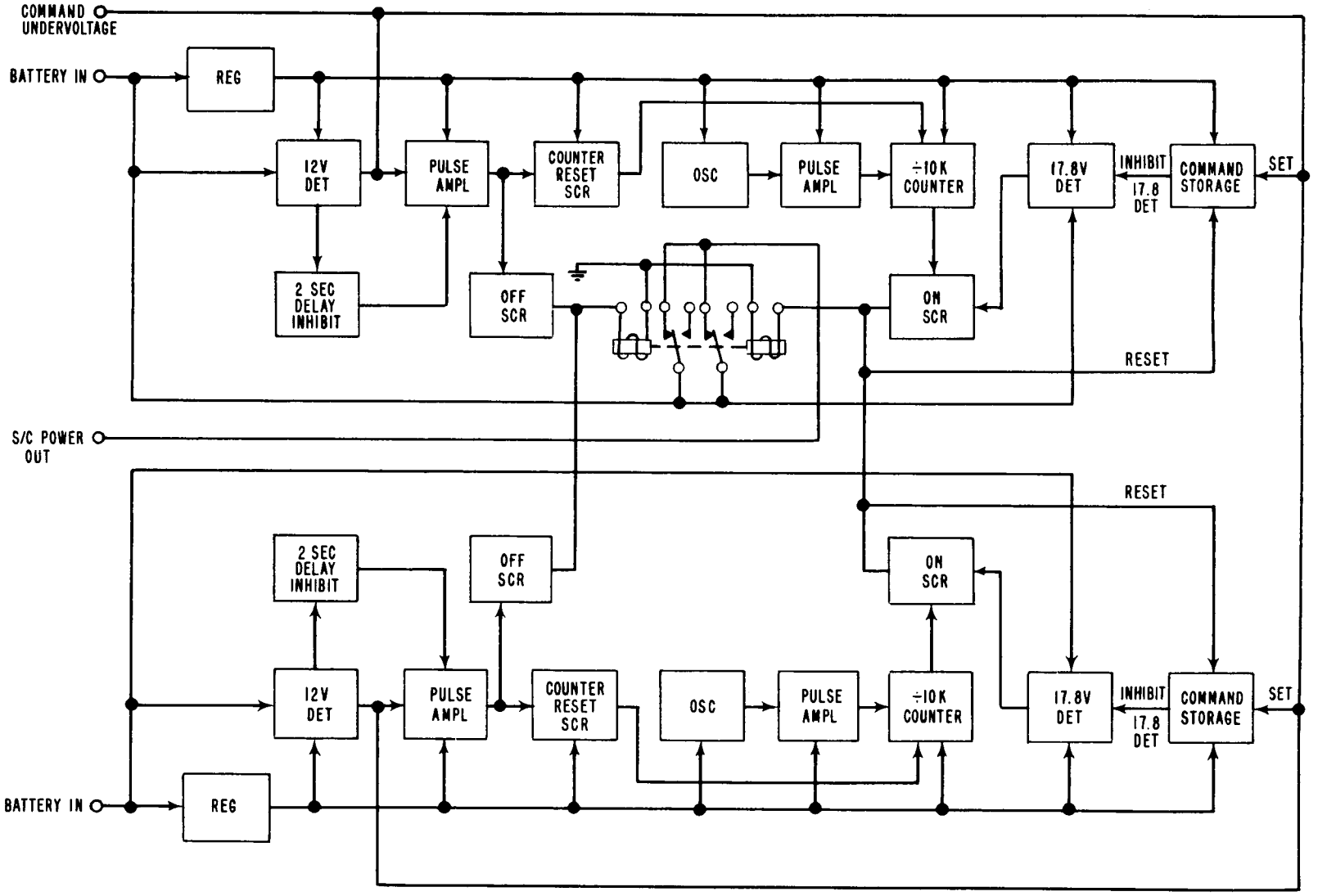

Figure 44–Undervoltage Block Diagram

Spacecraft Programmer

The undervoltage system, fourth-stage ignition and separation system, flipper control, and fourth-stage performance parameter are covered in this section.

Undervoltage System — The prime consideration in designing the undervoltage system was to keep the spacecraft on in the presence of transients while assuring adequate protection for the battery. The fact that the battery is not required to assist the solar array outputs for peak spacecraft loads and that the battery has the capability of delivering a 120-ampere short circuit current (sufficient to burn out most shorts before battery is damaged) makes this philosophy feasible for this spacecraft.

The undervoltage system, shown in Figure 44, is completely redundant, with each of the redundant circuits having only the payload relay in common. Each of these circuits contains a 12-volt level detector, a 17.7-volt level detector, an active two-second delay, and a command circuit. When the spacecraft batteries drop to 12 volts, a two-second delay begins. The two-second delay time was chosen so that the spacecraft would remain on in the event of a solar array partial failure which might cause the battery voltage to drop below 12 volts due to peak load requirements during part of a spacecraft revolution. If the voltage rises again before the end of the delay, the payload will remain on. If, however, the voltage does not recover the payload will be turned off. The batteries, now unloaded, will rise in voltage. If this voltage exceeds 17.7 volts, the payload will be turned on. If the battery voltage does not exceed 17.7 volts in this condition, the most probable reason for the original 12-volt condition to exist is the excessive spacecraft power drain. If this overload condition still exists when the spacecraft is turned back on, the off-on cycle will repeat itself once and remain on in an attempt to burn out the cause of the overload (battery delivers 120 amps when short circuited), because as long as the overload condition existed, turnoff would continue to occur, rendering the payload useless. This burnout mode does not affect the other system function, that is, a protection of the payload when the batteries are in a discharge state because of a shadow or a poor solar aspect. If the batteries reach a 12-volt level owing to either of the above causes, the voltage will never exceed 17.7 volts when the load is removed, and the spacecraft will remain off until that level is reached or until the 4-hour clock turns it on. To bring the battery to full charge, there is a command mode of operation whereby the spacecraft will remain off for four hours regardless of system voltage. This mode of operation is initiated via an RF command.

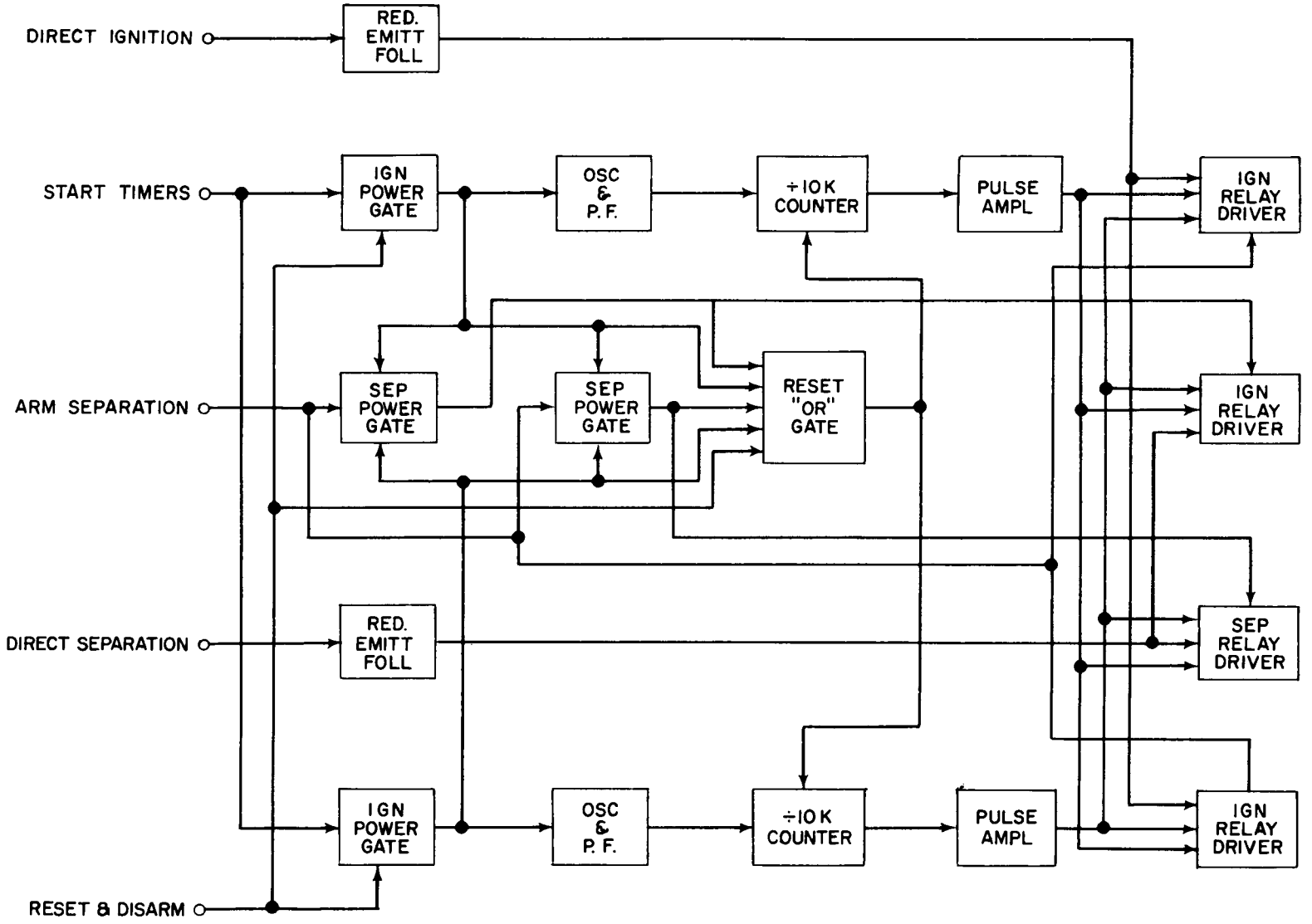

Figure 45–Fourth Stage Ignition and Separation Timer

After undervoltage has been reached because of a long shadow and the spacecraft turned off, the normal mode of turn-on is the 17.7-volt level detector. Upon emerging from a shadow, the solar array will initially charge the battery to approximately 15.5 volts. When the battery chemical state changes due to receipt of approximately 40-percent charge, the voltage rises toward the upper fully charged voltage of 18.3-volts. When the 17.7-volt threshold is reached, the spacecraft is turned on and the solar array then supplies the spacecraft power as well as recharging the battery, which will only accept the low charge current.

Fourth Stage Ignition and Separation Timer — This system was designed for internal high reliability and to lessen the probability that a spurious signal or faulty station command would prematurely fire the fourth stage. This system functions only in connection with the fourth-stage firing and separation; therefore, at fourth-stage separation the prime power to the system is removed.

The fourth-stage timer (see Figure 45) is a redundant control circuit for the retromotor ignition and the separation mechanisms. The timer is controlled by RF command via the command decoder. Basically, it contains four latching power gates: two 2-hour timers, a master reset circuit and four relay drivers. The five normal modes of operation are:

- Timed ignition and timed separation
- Timed ignition and direct separation
- Direct ignition and timed separation
- Direct ignition and direct separation
- No ignition and direct separation

NOTE: The non-ignition and timed-separation mode is a catastrophic failure on the part of ground control. In this case ignition and separation occur simultaneously.

These modes of operation are controlled by the following commands:

- Start timers
- Reset and disarm
- Direct ignition
- Arm separation
- Direct separation

The sequence of commands required to place the system in each of the five modes of operation is:

Mode	Command Sequence
1	1
2	1, 5
3	1, 3
4	1, 3, 5
5	1, 4, 5

Command No. 2 resets the counters and disarms all relay drivers. In this state the system is ready to accept any of the above command sequences.

Prior to Command No. 1, all relay drivers are disarmed and cannot be fired. The status of the system is telemetered at all times prior to separation.

Flipper Control and Fourth State Performance Parameter — The flipper control and fourth stage performance parameter are located on a half-card module and for this reason are treated together.

Flipper Control — The flipper control consists of three encoder-driven power switches which are used to supply current to the flipping mechanism of the Ames and GSFC Experiments. Two switches are associated with the Ames experiment with power from one switch causing the flipper to flip in one direction and power from the other switch causing the flipper to flip in the reverse direction. The one power switch associated with the GSFC flipper causes it to flip to its opposite state. Each flipper is activated once a day but staggered by 12 hours. GSFC and Ames switches are isolated from each other and each set of electronics is separately fused.

Fourth Stage Performance Parameter — The fourth-stage performance parameter electronics are designed to measure the burn time of the fourth stage. Third-stage separation resets the circuit as a precaution, since third-stage burn may have activated the "g" switch sensor. Upon fourth-stage ignition a "g" switch gates the output of a pulse amplifier which is driven by a relaxation oscillator into a 10-bit scaler which generates a 1024-step, 0-5-volt staircase input to the encoder. The scaler contains 10 complimentary flip-flops interconnected to count in a binary manner. The maximum counting time is 30 seconds.

Optical Aspect System

The AIMP optical aspect system incorporates two types of optical systems; a sun-sensor system composed of two digital solar aspect sensors and a moon/earth sensing system which consists of three pencil-beam telescopes. The optical aspect telemetry data is processed on the ground to determine spacecraft orientation, spin rate, and shadow or sunlight condition. On board the spacecraft the optical aspect system furnishes a see-sun pulse to the various instruments and experiments requiring this input for sectoring or other purposes.

The optical aspect system has two modes of operation. In the first mode, called the transfer trajectory mode, three optical aspect readings are read out for every one moon/earth scan readout (M, A, A, A,). When the fourth stage is separated, a microswitch changes the optical aspect system to the orbit mode in which seven moon/earth scan readouts for every one aspect readout (M, M, M, M, M, M, M, A) are made.

The optical aspect system has two complete data frames (2 and 10) in each sequence. The aspect and moon data is taken in Frame 0 or 8. The time to sun is measured from Frame 0 or 8, Channel 0.

The following is the data telemetered during an aspect readout:

Channel	Data
0	Telemetry data sync signal
1A	Lower order bit is the I.D. bit, which is a 1 for aspect readout. Other three bits meaningless.
1B	Highest order bit is part of sun angle gray code readout. Lower order three bits meaningless.
2A-2B	Sun angle gray code.
3A, 3B, 4A	Sun time readout Number 800 cps count from Frame 0 or 8, Channel 0 to see-sun pulse from sun sensor command module.
4A, 5A, 5B	Moon width #1 — number of 800 cps from horizon or terminator to horizon or terminator of moon or earth as seen by telescope number.
6A, 6B, 7A	Moon width #2 (same as #1 except measured by telescope #2).

Channel	Data
7B, 8A, 8B	Moon width #3 (see above).
9A, 9B, 10A	Spin period is number of 800 cps pulses between successive see-sun pulses.
10B, 11A, 11B	Moon time #1 — number of 800 cps from see-sun pulse to sighting of the moon's horizon or edge of terminator as sensed from the moon/earth telescope 1.
12A, 12B, 13A	Moon time #2 same as above except for use of telescope #2.
13B, 14A, 14B	Moon time #3 same as above except for use of telescope #3.
15A, 15B	Meaningless

The following is the data transmitted during a moon scan:

Channel	Data
0	Telemetry data sync signal.
1A, 1B	Least order bit of 1A is an I.D. bit which is "0" for moon/earth scan readout. Next bit is an "0" if spacecraft is in sunlight and a 1 if spacecraft is in shadow. Highest two bits of 1A and least three bits of 1B measure brightness of last element of scan readout. Highest bit of 1B is meaningless.
2A to 15B	All data consists of two-bit brightness measurements. In the 2-bit measurement, a 00 means element i is more than 2 brightness levels brighter than element i-1. 01 means element i is less than 2 brightness levels brighter than element i-1. 10 means element i is less than 2 brightness levels darker than element i-1. 11 means element i is more than 2 brightness levels darker than element i-1.

Digital Sensors and Their Functions — Each of the two digital sensors cover approximately a 90° field of view and is exactly the same in construction except that one photocell in one sensor is not connected so that no ambiguity exists at the 90° spacecraft spin axis sun orientation when both sensors are illuminated. In each sensor, the incident sunlight passes through a slit on the top of a quartz

block and is screened by a gray-coded pattern on the bottom of the block to either illuminate or not illuminate each of nine photocells. The angle of incidence determines which photocells are illuminated. (See Figure 46.) Outputs from each photocell are amplified and the presence of signal is translated as a binary "1" and the absence as a "0." This data is stored in the optical aspect accumulator until readout by the encoder.

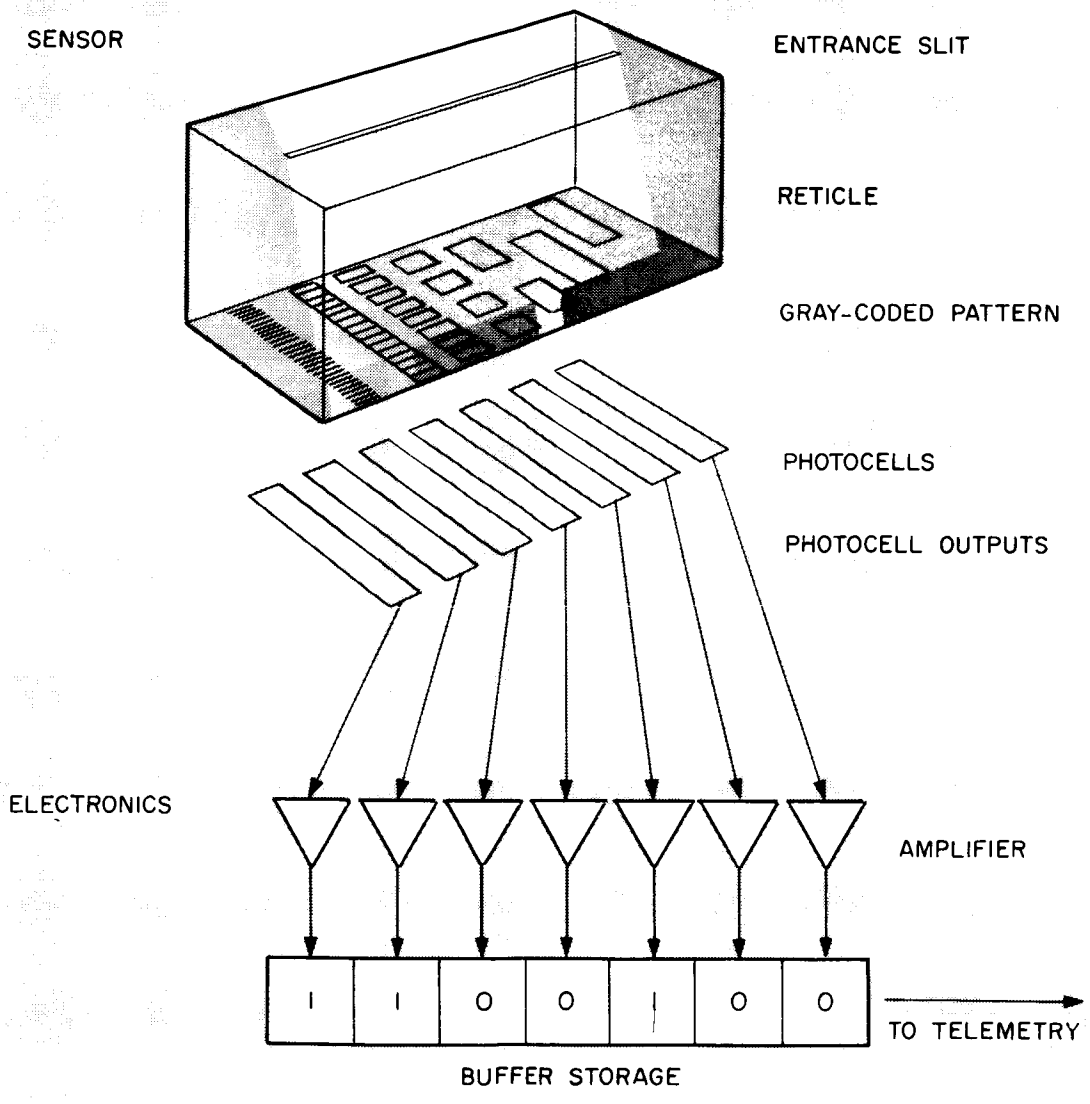

Figure 46–Solar Aspect Sensor

The digital sensors require no in-flight calibration and are insensitive to earthshine or moonshine. The sensors have a resolution of .5 degrees over a 128° field of view with an accuracy of ±.25°.

Associated with each digital sensor is a command reticle that is a trigger for the optical sensor permitting the angle to be readout only when the sun is contained in a plane at a right angle to the slit in the gray coded digital sensor reticle. The command reticle has slits on the top and bottom surfaces mounted over a photocell. The slits are oriented 90° to the slit in the gray-coded reticle digital sensors.

The output of the command reticle is also used as the source to start and stop the spin rate counters and as a signal to stop the see-sun time clock. The see-sun onboard pulse has a rise time of less than 10^{-4} from zero to +3.0 volts, an impedance of 10K and a duration of from seven to 18 milliseconds. The spin period is a count of the number of 800-cps clock counts between successive sun pulses. The sun time is the number of 800-cps clock counts from the start of Channel 0, Frame 8 to the telemetry format to the first sun pulse.

The operation of the command reticle is affected by spacecraft spin axis/ sun orientation. The sun pulse occurs at the same spacecraft sun orientation (sun in a plane 90° to digital sensor) from approximately 5 to 175 degrees. Outside these limits the sun pulse is either late or early to normal spacecraft orientation but its occurrence remains consistent, giving a true spin rate but a false sun time, until approximately 1 degree or 189 degree spin axis sun orientation is reached. Below 1 degree or above 189° the command reticle is continuously illuminated.

Moon-Earth Sensing System — Each of the three earth-horizon telescopes is made of a single lens of five square centimeters aperture and 3.7 inches focal length placed one focal length in front of a 0.012" diameter pin hole. (See Figure 47.) A Texas Instruments LS453 photo-diode is mounted behind the pin hole. This configuration provides a pencil-beam field of vision with 0.2° resolution. These three telescopes are mounted so that they point at angles of 45°, 90°, and 135° respectively from the spacecraft spin axis in the same plane as the command slit of the digital sun sensor.

The output from each telescope is amplified by a preamplifier and sent to the amplifier card. Here each preamplifier output is fed into a high-gain saturating amplifier which saturates on at one-tenth the light expected from the moon. Thus, each sensor and amplifier produces a saturated output signal which indicates when the telescope is sweeping across a lighted portion of the moon's or earth's surface. The duration of these outputs from each telescope and their

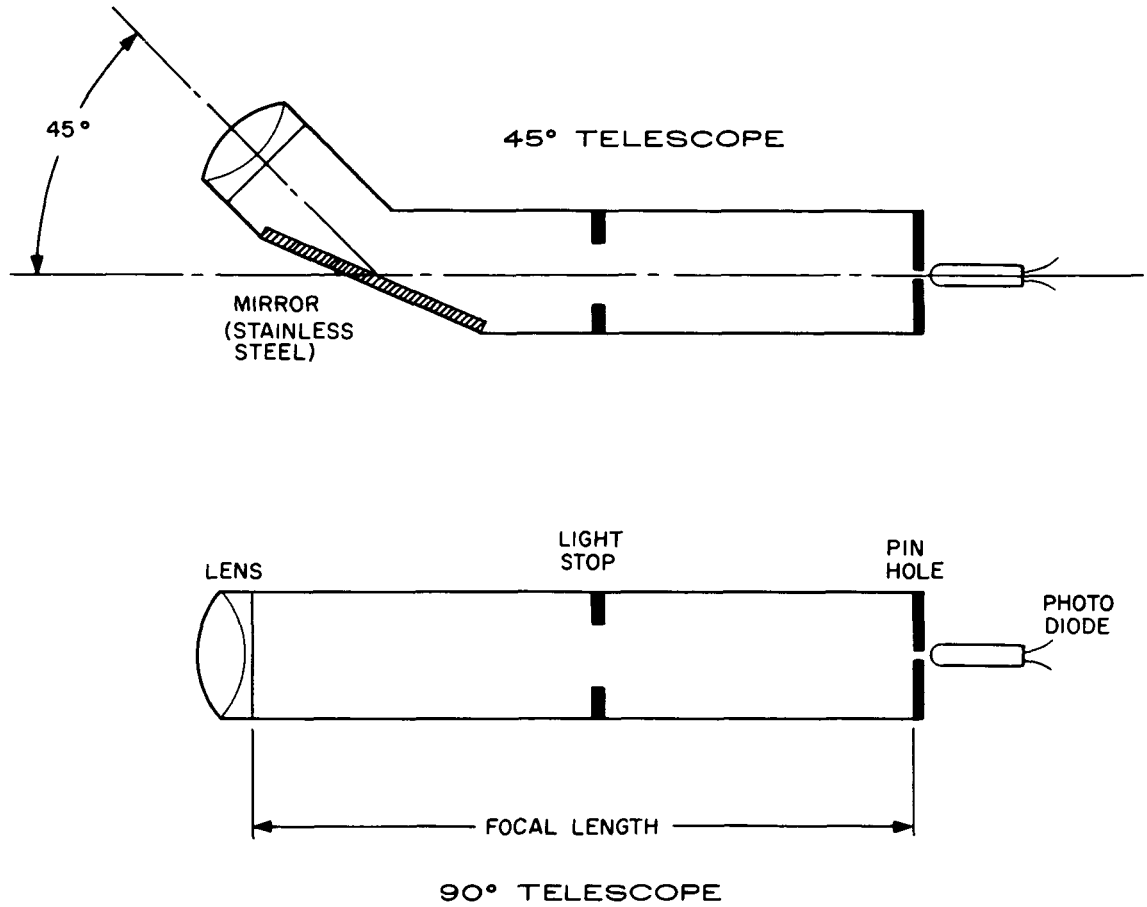

Figure 47–Moon-Earth Telescope

timing relative to the sun slit command provide the information necessary to uniquely determine the position of the spacecraft spin axis.

In addition to the horizon position and width information measured by these telescopes, a system has been devised to use their rather good (0.2°) resolution capabilities for the transmission of video information. One of the telescopes is selected by a system of priority logic to be transmitted as a video scanner. The signal from the selected telescope is routed to a video amplifier in addition to its high-gain saturating amplifier. The video amplifier has self-adjusting brightness and contrast controls which expand the video signal to full-scale unsaturated output. This output is then sent to an analog-to-digital converter where it is prepared for transmission as a digital signal. This digital output information is then sent to the Aspect Computer Card where it is stored in a shift register until the appropriate telemetry readout time.

In order to operate within the allotted bit transmission rate, only selected parts of the video scanning are processed for transmission. One line is processed each readout (which occurs every 40 seconds). Only the center 10-degree segment of each video line is processed and transmitted. The selection of the center 10-degree line segments to be processed is done in a scan position computer.

Miscellaneous

This section will cover minor electrical devices used in the AIMP spacecraft.

Fuses — All non-line instruments and all experiments on AIMP must be fused. Buss GLN 4/10 amp and GLX 6/10 amp TRON pigtail fuses were used. The main purpose of the fuses is to protect the prime converter from major overloads. Each fuse used is derated by a factor of two or greater. The fuses are heavily epoxied onto the electronics circuit board or to a metal heat sink to ensure proper heat dissipation in a vacuum.

Four-Volt Standard — A 799-AT-38 Evenvolt Reference Unit is used in the AIMP for a reference voltage in the encoder calibration. This unit has the following characteristics:

Input:	12 volts d.c. ±1%
Output:	4.0 volts d.c.
Output regulation and Temperature Coefficient:	Output within 0.1% from -10°C to +40°C input changes of ±1%
Stability:	0.01% per year

The standard is inherently short and/or open circuit-proof. The output is not isolated from the input. The 700-Series Evenvolt Reference Unit consists of special, simple circuitry comprising resistors, Zenor diodes, and in some cases, transistors with proper compensations where required.

Accelerometer — A miniature accelerometer switch is flown on AIMP to measure the time interval of fourth-stage burn. It is a unidirectional single-axis switch, closing or opening an electrical circuit at a preset value of acceleration. The accelerometer is of simple, rugged construction and the spring mass system is gas damped. The following are the characteristics of this device as published by Mason Electronics for their model 174.

Acceleration range = close H T 2 g's

Accuracy Range = ±5%

Repeatability = 0.25 g

Temperature Range = -65 to 250°F

Contact Rating = 100 MA continuous

Weight = 3/4 ounce